DISSERTATION

Studies on the regulation of flowering and senescence in response to carbon/nitrogen nutrient availability in Arabidopsis

（シロイヌナズナにおける **C/N** 栄養条件に応じた花成・老化制御機構に関する研究）

Submitted to the Graduate School of Life Science, Hokkaido University

In partial fulfillment of the Requirements for the Degree of Doctor of Philosophy in Life Science

Shoki Aoyama

Biosystems Science Course

Graduate School of Life Science

Hokkaido University, Sapporo, Japan

Submitted on March 2018

TABLES OF CONTENTS

ACKNOWLEDGEMENTS

I would like to express my deepest gratitude to Prof. Junji Yamaguchi and Dr. Takeo Sato for valuable advice and encouragement throughout my study and works.

I also express special gratitude to Dr. Juntaro Negi (Kyushu University) for CO_2 manipulation system, Drs. Takushi Hachiya (Nagoya University), and Junpei Takano (Osaka Prefecture University) for technical advice on the hydroponic culture, Drs. Takato Imaizumi (University of Washington), Mitsutomo Abe (University of Tokyo), Shogo Ito (Kyoto University) for valuable advice regarding flowering analysis and providing the related materials, Drs. Hirofumi Nakagami and Yuko Nomura (RIKEN CSRS) for experimental collaboration regarding phosphoproteome analysis, and Drs. Tsuyoshi Nakagawa (Shimane University) and Shoji Mano (NIBB) for providing the gateway destination vectors.

I am also very grateful Drs. Yukako Chiba, Shugo Maekawa, Sun Huihui, Yosuke Maruyama, Shigetaka Yasuda, Yuya Suzuki, Lorenzo Guglielminetti, Thais Huarancca Reyes, and Yu Lu for technical advice and significant discussion.

Finally, I greatly thank all members in my laboratory for their assistance, help, and friendliness. I also express my heartfelt gratitude to my family for supporting my life.

This work was supported by the Japan Society for the Promotion of Science (JSPS) Research Fellowship for Young Scientists (2015-2018), by JSPS Grant-in-Aid for Scientific Research on Innovative Areas: Comprehensive Studies of Plant Responses to High CO_2 World by An Innovative Consortium of Ecologists and Molecular Biologists of (2011-2014), and by the Plant Global Education Project from the Nara Institute of Science and Technology (2013)

PREFACE

To optimize growth and metabolism, Plants sense and respond to environmental factors with their sophisticated mechanisms. Nutrient availability, in particular the availability of carbon (C) and nitrogen (N), is important in the regulation of plant metabolism and development. In addition to their independent utilization, the ratio of C to N metabolites in the cell, referred to as the C/N balance, is also important for the regulation of plant growth and primary metabolism (Coruzzi and Zhou, 2001; Martin et al., 2002). To elucidate the molecular mechanism of plant C/N response, our laboratory isolated Arabidopsis Tóxicos en Levadura 31 (ATL31) as a novel C/N regulator (Sato et al., 2009). ATL31 functions as ubiquitin ligase (E3) and negatively regulates C/N response via the degradation of 14-3-3 proteins (Sato et al., 2011; Yasuda et al., 2014).

To clarify the molecular mechanism of plant C/N response, most of previous study including our laboratory had evaluated the early post-germinative growth stage of Arabidopsis grown on the sugar containing medium (Coruzzi and Zhou, 2001; Lu et al., 2015; Martin et al., 2002; Sato et al., 2009; Yasuda et al., 2017). The post-germinative growth is notably arrested with hyper-accumulation of anthocyanin on the medium including a lot of sugar and limited nitrogen (high C/low N). Owing to the clear phenotype, this method is useful for genetic or molecular biological analysis but remains some problems. At first, besides the post-germinative growth, the later growth stage such as flowering and senescence must be affected by cellular C/N status. In addition, C source for plants is not supplied from sugar in the medium but synthesized from atmospheric CO_2 in natural environment. Therefore, the cellular C/N status must be affected by the balance between atmospheric CO_2 and the available N amount taken up

from soil (CO_2/N) in practice.

In Chapter I, I carried out CO_2/N response analysis using the combined methods of CO_2 manipulation and hydroponic culture for N regulation to elucidate further physiological plant C/N response and the role of ATL31. This study revealed that the combination of elevated atmospheric CO_2 concentration with limited N availability (high CO_2/low N) causes disrupted cellular C/N balance, that is, the hyper-accumulation of sugars and induced nitrogen starvation, which induces leaf senescence progression. Moreover, I also demonstrated that ATL31 plays an important role in the regulation of the senescence.

In Chapter II, I focus on the relationship between C/N nutrient availability and flowering. Flowering is important event for plant as the transition from vegetative to reproductive phase and the molecular mechanisms have largely studied. However, the relationship between nutrients such as C and N availability and flowering was poorly understood even though its importance has been indicated from long ago. In this study, I reconsidered the hydroponic culture method and established the condition that early flowering was induced by high CO_2/low N or merely low N conditions in Arabidopsis. Moreover, I investigated its molecular mechanism, and demonstrated that the phosphorylation level of FLOWERING BHLH 4 (FBH4) is increased and the down-stream genes *CONSTANSE (CO)* and *FLOWERING LOCUS T (FT)* are transcriptionally up-regulated by low N condition. These factors are essential in photoperiod pathway, and which activation might be important for N-responsive early flowering.

ATLs are plant specific E3s that identified 91 isoforms in Arabidopsis genome (Aguilar-Henonin et al., 2006; Guzmán, 2014). Besides ATL31, to investigate the other

ATL member, particularly sugar and/or nitrogen responsive one is important to elucidate the whole aspects of the plant C/N response. In Chapter 3, I reported about ATL15 which is a novel sugar responsive ATL. I demonstrated that ATL15 protein plays a significant role as a membrane-localized ubiquitin ligase that controls sugar-responsive plant growth in Arabidopsis.

Aguilar-Henonin, L., Bravo, J., and Guzmán, P. (2006) Genetic interactions of a putative Arabidopsis thaliana ubiquitin-ligase with components of the Saccharomyces cerevisiae ubiquitination machinery. *Curr Genet*. 50: 257–268.

Coruzzi, G.M., and Zhou, L. (2001) Carbon and nitrogen sensing and signaling in plants: emerging 'matrix effects'. *Curr Opin Plant Biol*. 4: 247–53.

Guzmán, P. (2014) ATLs and BTLs, plant-specific and general eukaryotic structurally-related E3 ubiquitin ligases. *Plant Sci*. 215–216: 69–75.

Lu, Y., Sasaki, Y., Li, X., Mori, I.C., Matsuura, T., Hirayama, T., et al. (2015) ABI1 regulates carbon/nitrogen-nutrient signal transduction independent of ABA biosynthesis and canonical ABA signalling pathways in Arabidopsis. *J Exp Bot*. 66: 2763–2771.

Martin, T., Oswald, O., and Graham, I.A. (2002) Arabidopsis seedling growth, storage lipid mobilization, and photosynthetic gene expression are regulated by carbon:nitrogen availability. *Plant Physiol*. 128: 472–81.

Sato, T., Maekawa, S., Yasuda, S., Domeki, Y., Sueyoshi, K., Fujiwara, M., et al. (2011) Identification of 14-3-3 proteins as a target of ATL31 ubiquitin ligase, a regulator of the C/N response in Arabidopsis. *Plant J*. 68: 137–46.

Sato, T., Maekawa, S., Yasuda, S., Sonoda, Y., Katoh, E., Ichikawa, T., et al. (2009)

CNI1/ATL31, a RING-type ubiquitin ligase that functions in the carbon/nitrogen response for growth phase transition in Arabidopsis seedlings. *Plant J*. 60: 852–64.

Yasuda, S., Aoyama, S., Hasegawa, Y., Sato, T., and Yamaguchi, J. (2017) Arabidopsis CBL-Interacting Protein Kinases Regulate Carbon/Nitrogen-Nutrient Response by Phosphorylating Ubiquitin Ligase ATL31. *Mol Plant*. 10: 605–618.

Yasuda, S., Sato, T., Maekawa, S., Aoyama, S., Fukao, Y., and Yamaguchi, J. (2014) Phosphorylation of Arabidopsis Ubiquitin Ligase ATL31 Is Critical for Plant Carbon/Nitrogen Nutrient Balance Response and Controls the Stability of 14-3-3 Proteins. *J Biol Chem*. 289: 15179–15193.

Chapter I

Ubiquitin ligase ATL31 functions in leaf senescence in response to the balance between atmospheric CO_2 and nitrogen availability in Arabidopsis

Summary

Carbon (C) and nitrogen (N) are essential elements for metabolism, and their availability, called C/N balance, must be tightly coordinated for optimal growth in plants. Previously, we have identified the ubiquitin ligase CNI1/ATL31 as a novel C/N regulator by screening plants grown on C/N stress medium containing excess sugar and limited N. To further elucidate the effect of C/N balance on plant growth and to determine the physiological function of ATL31, we performed C/N response analysis using an atmospheric CO_2 manipulation system. Under conditions of elevated CO_2 and sufficient N, plant biomass and total sugar and starch dramatically increased. In contrast, elevated CO_2 with limited N did not increase plant biomass but promoted leaf chlorosis with anthocyanin accumulation and increased senescence-associated gene expression. Similar results were obtained with plants grown in medium containing excess sugar and limited N, suggesting that disruption of C/N balance affects senescence progression. In *ATL31* overexpressing plants, promotion of senescence under disrupted CO_2/N conditions was repressed, whereas in the loss-of-function mutant it was enhanced. The *ATL31* gene was transcriptionally upregulated under N deficiency and in senescent leaves and *ATL31* expression highly correlated with *WRKY53* expression, a key regulator of senescence. Furthermore, transient protoplast analysis implicated the direct activation of *ATL31* expression by WRKY53, which was in accordance with the results of *WRKY53* overexpression experiments. Together, these results demonstrate the

importance of C/N balance in leaf senescence and the involvement of ubiquitin ligase ATL31 in the process of senescence in Arabidopsis.

Introduction

Plant growth and development are controlled by the concerted actions of signaling pathways that are triggered by various environmental conditions and developmental cues. Nutrient availability, in particular that of carbon (C) and nitrogen (N), is one of the most important factors for the regulation of plant metabolism and development. In addition to independent utilization, the ratio of C to N metabolites in the cell is also important for the regulation of plant growth, and is referred to as the ‘‘C/N balance’’ (Coruzzi and Zhou 2001; Martin et al. 2002). In nature, C and N availability changes in response to environmental conditions, such as atmospheric CO_2, light availability, diurnal cycles, seasonal effects, rain fall, and factors influencing microbial activity (Gibon et al. 2004; Kiba et al. 2011; Miller et al. 2007; Smith and Stitt 2007). Cold and biotic stress can also affect carbohydrate partitioning and metabolism (Klotke et al. 2004; Roitsch and Gonzalez 2004). Plants sense and adapt to changing C/N conditions via precise partitioning of C and N sources and fine-tuning of complex cellular metabolic activity (Sato et al. 2011b; Sulpice et al. 2013). C/N balance clearly affects the plant phenotype in the early post-germinative growth stage. Arabidopsis seedlings grown in medium containing high levels of sugar (100 mM glucose or sucrose) and limited N (0.1 mM N) showed purple pigmentation in cotyledons and severely inhibited post-germinative growth (Martin et al. 2002; Sato et al. 2009). The expression of genes related to photosynthesis, such as *rubisco small subunit 1A* and *chlorophyll binding protein 2*, or the anthocyanin biosynthetic enzyme *chalcone synthase*, is regulated by

the C/N balance rather than by C or N individually. The Arabidopsis PII-like protein AtGLB1 and the glutamate receptor AtGLR1.1, which are able to directly bind 2-oxoglutarate and glutamate, respectively, are important factors in the coordinated regulation of C and N metabolism (Ferrario-Mery et al. 2005; Hsieh et al. 1998; Kang and Turano 2003). However, little is known about the molecular mechanisms responsible for the regulation of C/N sensing and signaling.

Our laboratory previously isolated the ubiquitin ligase ATL31 as a novel C/N regulatory protein in Arabidopsis plants (Sato et al. 2009). ATL31 is a member of the plant-specific ubiquitin ligase ATL family, which comprises proteins that contain a transmembrane-like hydrophobic region at the N-terminus, a basic amino acid-rich region, a RING-H2 type zinc finger domain, and a non-conserved C-terminal region (Aguilar-Hernandez et al. 2011; Serrano et al. 2006). In the early post-germinative growth stage, ATL31 overexpression caused a C/N insensitive phenotype in *carbon/nitrogen insensitive 1-dominant (cni1-D*) plants and resulted in the expansion of green-colored cotyledons under conditions of excess sugar and N depletion (high C/low N medium), whereas the *atl31* loss-of-function mutant showed a hypersensitive phenotype. Subsequent proteomic analyses identified 14-3-3 proteins as interactors of ATL31 (Sato et al. 2011a). 14-3-3 proteins bind to phosphorylated motifs and function in multiple developmental processes by regulating the activity of a wide variety of target proteins (Bachmann et al. 1996; Chevalier et al. 2009; Mackintosh 2004; Roberts 2003). In particular, 14-3-3 proteins have been reported to regulate primary C and N metabolism by directly interacting with essential enzymes (Comparot et al. 2003; Shin et al. 2011). Further biochemical and genetic analyses demonstrated that ATL31 targets 14-3-3 proteins for ubiquitination to regulate C/N response in Arabidopsis plants (Sato

et al. 2011a). These results revealed the plant-specific regulatory mechanism of C/N nutrient signaling via the ubiquitin-proteasome system.

Supplementing exogenous sugar into the medium is a conventional and useful method for analyzing the sugar and C/N response and has revealed essential signaling factors. However, since sugar is not naturally found in soil, it is necessary to further evaluate the physiological function of each signaling factor under improved experimental conditions. The physiological C source for higher plants is sugar produced from atmospheric CO_2. The increasing atmospheric CO_2 concentration is a serious environmental problem as it causes elevated temperatures that could lead to major ecological consequences, such as changes in plant growth, worldwide (Hikosaka et al. 2011; Knohl and Veldkamp 2011; Long et al. 2004). Most studies have evaluated the sugar and C/N response phenotype in the early post-germinative growth stage using sugar-supplemented medium because it is a short assay and it is easy to identify differences by counting seedlings with green or purple cotyledons. However, sugar and C/N are thought to affect plant growth throughout its life cycle, including during vegetative and reproductive growth as well as during senescence (Rolland et al. 2006; Watanabe et al. 2013; Wingler et al. 2006). Here, we carried out C/N response analysis with manipulation of atmospheric CO_2 concentrations. The combined methods of CO_2 manipulation and hydroponic culture to regulate N levels enabled a more physiological analysis of the C/N response and the role of ATL31 in plant growth and development. Our study demonstrates that the balance between CO_2 and N availability greatly affected not only plant biomass and carbon metabolism, but also senescence progression in rosette leaves. Both the use of sugar-supplemented medium and the manipulation of atmospheric CO_2 levels showed that ATL31 plays a role in senescence together with the

WRKY53 transcription factor. These results demonstrate the close relationship between C and N availability and the fundamental importance of the C/N balance in plant metabolism and development.

Materials and Methods

Plant materials and growth conditions

Wild-type Arabidopsis Columbia-0 (Col-0) plants were used in this study. *atl31 KO* and *ATL31 OX* plants were prepared as previously described (Sato et al. 2009). Sterilized seeds were sown on rock wool with 1/5×MS liquid medium containing 1 mM NH_4NO_3 and 1 mM KNO_3 (3 mM N). Plants were grown under 280 ppm of atmospheric CO_2 concentration and 12-h light/12-h dark cycles at 22°C in a plant growth chamber for 2 weeks. Then, plants were transferred to each CO_2/N condition; namely, 280 or 780 ppm CO_2 and 0.3 mM or 3 mM N. Rosette leaves for qRT-PCR analysis were harvested 2.5 weeks after CO_2/N treatment. Rosette leaves and stem tissues for fresh weight, sugar, starch, anthocyanin and chlorophyll measurements were harvested 4 weeks after CO_2/N treatment.

Transient C/N response assay

Wild-type Col-0, *atl31KO*, and *ATL31 OX* plants were grown on modified MS medium containing 100 mM glucose and 30 mM N for 2 weeks after germination and then transferred to C/N medium containing 100 or 200 mM glucose and 0.3 or 30 mM N. Plants were harvested 24 or 72 hours after C/N treatment for quantitative analysis of transcript levels or anthocyanin measurements, respectively.

qRT-PCR analysis of transcript levels

Total RNA was isolated using the RNeasy Mini Kit (Qiagen) with On-Column DNase Digestion according to the manufacturer's protocol. Purified RNA (400 ng) was used for the reverse transcription reaction with Super Script II (Invitrogen). cDNA was diluted 1:2 with distilled water for qRT-PCR (1:100 dilution only for *18s rRNA*). qRT-PCR analysis was performed using SYBR *premix EX Taq* (Takara) on a Mx3000P QPCR System (Agilent Technologies) according to the manufacturer's protocol. *18s rRNA* was used as internal control for calculating ⊿⊿ Ct. Specific primer sets used for qRT-PCR analysis are listed in Table 1.

Starch quantification

Leaves (0.1 g FW) were rapidly frozen in liquid nitrogen, ground to a powder and extracted twice in 0.5 ml of 80% boiling ethanol for 5 min. Samples were then centrifuged at 12,000*xg* for 15 min at 15°C. The combined supernatants were used for soluble carbohydrate (glucose, fructose, sucrose) quantification. Pellets were resuspended in 0.5 ml of 20 mM KOH and boiled for 15 min. Samples were then centrifuged at 8000*xg* for 15 min at 15°C. Supernatants were utilized for starch digestion. Samples (100 µl) were combined with 100 µl of 100 mM Na-acetate (pH 5.2) containing 10 U alpha-amylase (Sigma) and incubated at 37°C for 1 hour. After boiling for 2 min, samples were cooled and treated with 100 µl of 100 mM Na-acetate (pH 4.6) containing 10 U amyloglucosidase (Sigma) at 55°C for 1 hour. After additional boiling for 2 min, samples were cooled and centrifuged for 10 min at 15,000*xg*. Aliquots of the supernatant were used for analysis of glucose content.

Soluble carbohydrate quantification

Samples were assayed for glucose, fructose, and sucrose content using coupled enzymatic assay methods, as described by Pompeiano *et al.* (Pompeiano et al. 2013). The efficiency of the methods was tested by using known amounts of carbohydrates. Recovery experiments determined the losses that took place during extraction procedures. Two experiments were performed for each metabolite by adding known amounts of authentic standards to the sample prior to extraction. The concentrations of standards added were similar to those estimated to be present in the tissues in preliminary experiments. The recovery ranged between 96 and 106%.

Anthocyanin measurement

Total anthocyanin was extracted from frozen homogenized leaves by overnight incubation in 300 µl of methanol acidified with 1% HCl. Next, 200 µl distilled water and 500 µl chloroform were added, and the top layer was collected after centrifugation at 20,000*xg* for 5 min and mixing with 400 µl 60% methanol acidified with 1% HCl. The amount of anthocyanin was determined by measuring absorbance at 532 nm (A_{532}) and 657 nm (A_{657}) using a spectrophotometer. Results were calculated by subtracting A_{657} from A_{532} nm.

Chlorophyll measurement

Chlorophyll was extracted from frozen homogenized leaves with 100% acetone. The supernatant was collected after centrifugation at 20,000*xg* for 5 min and mixed with 1/4 amount of distilled water. Chlorophyll content was determined by measuring

absorbance at 646.6 nm ($A_{646.6}$) and 663.6 nm ($A_{663.6}$) as well as absorbance at 750 nm (A_{750}) (to be used as blank) using a spectrophotometer. Results were calculated by subtracting the blank from each absorbance. Chlorophyll a (μg/ml) was determined using the following formula (12.25 x $A_{663.6}$ – 2.85 x $A_{646.6}$). Chlorophyll b (μg/ml) was determined using the following formula (20.31 x $A_{663.6}$ – 4.91 x $A_{646.6}$).

Plasmid construction and transgenic plant generation

To generate plasmids for transient protoplast analysis, the relevant *ATL31* promoter was amplified by PCR and introduced into the *Hind*III-*Bam*HI sites of pBI221 (Jefferson et al. 1987). The full-length *WRKY53* (*At4g23810*) coding region was amplified by PCR and introduced into the pENTR/D-TOPO vector (Life Technologies) to generate the plasmid pENTRWRKY53. Then, pENTRWRKY53 was recombined into the pUGW2 vector or pGWB5 binary vector (Nakagawa et al. 2007) to make an effector plasmid or GFP-fused WRKY53 plasmid, respectively, according to the Gateway instruction manual (Life Technologies), with the *WRKY53* gene under the control of the CaMV 35S promoter. Primers used for PCR amplification of promoters and effector are shown in Table 1. The WRKY53-GFP fusion plasmid was transformed into *Agrobacterium tumefaciens* pGV3101 (pMP90) by electroporation and then transformed into *Arabidopsis thaliana* Col-0 as described previously (Sato et al. 2009).

Protoplast transfection experiments

Protoplasts were prepared from *Arabidopsis* T87 suspension cells 4 days after subculture (Axelos et al. 1992) as previously described (Iwata et al. 2011). Before transfection, protoplasts were washed, centrifuged at 100*xg* for 5 min at room

temperature and resuspended to a density of 5 x 10^6 protoplasts mL^{-1} in MaMg solution. Approximately 0.75 x 10^6 protoplasts (150 µL suspension) were added to a mixture of 5 µg effector and 20 µg reporter plasmids, after which 65 µL PEG solution (40% PEG (MW 8000; Sigma), 0.1 M $Ca(NO_3)_2$, 0.4 M mannitol) was immediately added and carefully mixed by hand. Following incubation on ice for 20 min and at room temperature for 5 min, the transfection mixture was carefully diluted with 5 mL wash solution. Protoplasts were pelleted by centrifugation at 100*xg* for 5 min and resuspended in 1 mL protoplast culture medium (0.4 M mannitol, 2% sucrose supplemented with 4.3 g L^{-1} MS basal salt mixture, 0.5 mg L^{-1} nicotinic acid, 0.5 mg L^{-1} pyridoxine hydrochloride, 0.1 mg L^{-1} thiamine hydrochloride, 2 mg L^{-1} glycine, 10 mg L^{-1} inositol, pH 5.6).

Transfected protoplasts were transferred to 3.5 cm petri dishes, incubated under a dim light at 22°C for 15 hours and lysed. The soluble extracts were divided; one half was used for analysis of reporter-GUS activity, while the other half was used for normalization. GUS activity was normalized against the relative transformed reporter-GUS plasmid amount. Protoplasts transfected with reporter construct alone were used as control. Data are shown as the mean of three biological replicates ± standard deviation (SD). Predicted cis elements in the ATL31 promoter were searched for using the PLACE database (http://www.dna.affrc.go.jp/PLACE/index.html) (Higo et al. 1999).

Results

High C and low N stress induces leaf senescence

In order to examine the effects of changes in the C/N ratio and *ATL31* expression in

mature plants, plants were grown under different C/N conditions. Wild-type (WT) Arabidopsis plants were grown in normal C/N medium containing 100 mM glucose (G) and 30 mM nitrogen (N) (low C/high N) for 2 weeks and then transferred to each modified C/N medium containing 100 mM G and 0.3 mM N (low C/low N), 200 mM G and 30 mM N (high C/high N) or 200 mM G and 0.3 mM N (high C/low N). Three days after transfer, WT plants grown under high C/low N conditions showed slight chlorosis and increased purple pigmentation of true leaves (Figure 1A). Anthocyanin accumulated more than 7-fold in high C/low N medium compared to low C/high N control medium (Figure 1B). Plants grown under low C/low N and high C/high N conditions exhibited similar purple pigmentation (Figure 1A), and anthocyanin accumulation increased approximately 3.2- and 2.7-fold, respectively, compared to plants grown in normal C/N medium (Figure 1B). Gene expression of *rubisco small subunit 1A* (*RBCS1A*), a photosynthetic marker, decreased 0.5-fold in low C/low N and high C/high N conditions and 0.3-fold in high C/low N stress conditions compared to low C/high N medium (Figure 2A). The expression of *chlorophyll binding protein 2* (*CAB2*) also decreased 0.6-fold in high C/low N medium (Figure 2B). On the other hand, expression of *chalcone synthase* (*CHS*) and *PRODUCTION OF ANTHOCYANIN PIGMENT 1* (*PAP1*)/*MYB75*, a key enzyme and a transcription factor that regulate anthocyanin biosynthesis, dramatically increased by more than 7- and 60-fold in high C/low N conditions, respectively (Figure 2C, D).

Since decreased photosynthetic activity and anthocyanin accumulation are typical phenotypes of leaf senescence, expression of the senescence marker gene *WRKY53*, an essential senescence-related transcription factor (Lim et al. 2007; Miao et al. 2004), was also evaluated. *WRKY53* transcripts increased approximately 4-fold in low C/low N

medium and 10-fold in high C/low N medium compared to control medium (Figure 2E). These results suggest that C/N affects plant growth in the vegetative growth stage, and that high C/low N conditions may induce leaf senescence.

In addition, the physiological function of C/N response regulator ATL31 was also evaluated in the mature developmental stage. Gene expression of *ATL31* was affected by C/N and increased approximately 2-fold in low C/low N medium and 6-fold in high C/low N stress conditions (Figure 2F). Transient C/N treatments for the loss-of-function mutant (*atl31 KO*) demonstrated that accumulation of anthocyanin was enhanced in *atl31 KO* plants compared to WT plants grown under high C/low N conditions (Figure 1A, B), suggesting that ATL31 is involved in C/N response at the mature growth stage. An anthocyanin accumulation was also observed in *atl31 KO* plants in response to low C/low N and high C/low N. However, there was no statistically significant difference compared to WT (Figure 1A, B). On the other hand, anthocyanin accumulation was not significantly repressed in *ATL31* over-expressor (*ATL31 OX*) plants compared to WT plants, although it was partially repressed in each C/N medium condition (Figure 1A, B).

CO_2/N balance regulates plant growth and carbon metabolism

To further understand the physiological importance of the C/N balance in plants, an improved analysis of C/N response was performed using manipulated atmospheric CO_2 concentrations as a C source. In these experiments, Arabidopsis WT plants were grown in a hydroponic culture system under differing atmospheric CO_2 concentrations (280 or 780 ppm) and N concentrations in the medium (0.3 or 3 mM).

Prior to treatment, all plants were grown under 280 ppm CO_2 and 3 mM N (low

CO_2/high N as a control) condition for 2 weeks to avoid developmental differences between plants. Then, the plants were transferred to each CO_2/N condition. After 4 weeks under each CO_2/N condition, Arabidopsis plants showed apparent differences among conditions. When plants were grown under elevated CO_2 and sufficient N (high CO_2/high N), plant growth was dramatically promoted and leaves were enlarged (Figures 3A, B and 8). The fresh weight of above-ground tissues increased more than 3-fold compared to plants grown under low CO_2/high N conditions (Figure 4A). However, even with abundant CO_2, plants grown under high CO_2/low N conditions did not grow as much as plants grown under high CO_2/high N conditions (Figures 3A, B and 4A). In addition, they showed a senescence phenotype, such as purple pigmentation and chlorosis (Figure 3B). Indeed, anthocyanin dramatically accumulated, approximately 20-fold, while chlorophyll content decreased to less than half in plants grown under high CO_2/low N conditions compared to those grown under low CO_2/high N conditions (Figure 6C, D). Since there was no visible senescence-promoting effect under either low CO_2/low N or high CO_2/high N condition at the same growth stage (Figure 3A, B), it became apparent that the senescence phenotype was not due to limited levels of N or elevated CO_2, but was dependent upon the CO_2/N balance.

To evaluate the effect of CO_2/N on the biosynthesis and metabolism of C metabolites, the amounts of sugar and starch in rosette leaves were quantified. Glucose, fructose, sucrose, and starch concentration (amount per fresh weight) significantly increased in plants grown under high CO_2/low N conditions (Figure 4B). Accumulation of sugars was also observed in low CO_2/low N conditions compared with that in low CO_2/high N, but was not largely extended rather than that in high CO_2/low N condition (Figure 4B). The total amount of sugars in rosette leaves in single plants was estimated by measuring

fresh weight and sugar concentration (Figure 4C). The total glucose amount was about 3-fold higher in plants grown under high CO_2 conditions compared to those grown under low CO_2, indicating that the endogenous total glucose level is affected by CO_2 but not by N conditions (Figure 4C). On the other hand, the amount of fructose, sucrose, and starch significantly increased in plants grown under low N conditions, especially when combined with exposure to high atmospheric CO_2 levels (Figure 4C). These results indicate that the balance between CO_2 and N availability has a great effect on plant biomass and carbohydrate metabolism, which may affect senescence progression in plants.

Elevated CO_2 and limited N transcriptionally down-regulates the photosynthesis genes and up-regulates senescence-related genes

Plants grown under high CO_2/low N conditions exhibited a senescence phenotype, indicated by color changes, such as chlorosis and purple pigmentation in rosette leaves (Figure 3B), similar to those observed in plants grown in high C/low N medium (Figure 1A). The transcript levels of genes involved in the C/N response were examined in plants grown under each CO_2/N condition before they showed an apparent senescence phenotype (2.5 weeks after transfer). A decrease in *RBCS1A* transcripts and an increase in *CHS* transcripts were observed in plants grown under high CO_2/low N conditions (Figure 5A, B) as well as in plants grown in high C/low N medium (Figure 2A, C). These results are consistent with promotion of senescence progression. In addition, the senescence-regulator gene *WRKY53* and the downstream marker *SAG12* were transcriptionally activated under high CO_2/low N conditions (Figure 5C, D), which is also indicative of senescence promotion.

Interestingly, the expression of cytosolic *glutamine synthase 1.4* (*GLN1.4*) and high-affinity *NITRATE TRANSPORTER 2.4* (*NRT2.4*), both of which are transcriptional markers induced by N deficiency (Ishiyama et al. 2004; Kiba et al. 2012), was also highly promoted under high CO_2/low N conditions, although expression was not affected under low N conditions when coupled with low CO_2 (Figure 5E, F). These results suggest that CO_2 and N levels affect each other and trigger senescence progression when N is depleted in plants exposed to elevated atmospheric CO_2.

ATL31 functions in leaf senescence under high CO_2/low N condition

The physiological function of ATL31 in mature leaves was investigated under different CO_2 and N conditions. Interestingly, it has been predicted that *ATL31* is transcriptionally induced in an age-dependent manner, which is highly correlated with *WRKY53* expression based on analysis of a publicly accessible microarray database (Figures 6A and 9). Promotion of *ATL31* expression in senescent leaves was also confirmed in our previous study (Maekawa et al. 2012). Quantitative RT-PCR (qRT-PCR) analysis showed that *ATL31* transcript levels increased under high CO_2/low N conditions (Figure 6B), which is similar to the increase seen in plants grown in high C/low N medium (Figure 2F), suggesting an involvement of ATL31 in the progression of a senescence phenotype under high CO_2/low N conditions.

The senescence phenotype was suppressed in *ATL31 OX* plants, whereas it was accelerated in *atl31 KO* mutants (Figure 3B). Anthocyanin accumulation was significantly enhanced in *atl31 KO* mutants compared to WT plants grown under high CO_2/low N conditions, whereas it was repressed in *ATL31 OX* plants (Figure 6C). In contrast, the decrease in chlorophyll content was suppressed in *ATL31 OX* plants as

compared with WT plants and *atl31 KO* mutants (Figure 6D). A similar accelerated senescence phenotype to the one seen in the *atl31 KO* was also observed when plants were grown under normal CO_2 and soil conditions, whereas the *ATL31 OX* showed a slight delay in senescence progression (Figure 10), suggesting that ATL31 plays an essential role in leaf senescence, even under normal growth conditions. Taken together, these results demonstrate that ATL31 is transcriptionally induced in maturely developed leaves under high CO_2/low N conditions and associated with leaf senescence progression.

ATL31 is the potential target of the senescence-related transcription factor WRKY53

As aforementioned, *ATL31* transcription was induced during senescence, and *ATL31* expression highly correlated with the expression of *WRKY53* (Figures 5C and 6A, B). On the other hand, senescence regulator WRKY53 was also transcriptionally induced in response to different C/N stress conditions (Figure 2E). Together, these results suggest a physiologically close relationship between ATL31 and WRKY53 function. In addition, several W-box-like sequences, which are recognized as cis-elements by the WRKY transcription factor, were detected 5'-upstream of the *ATL31* coding region (Figure 7A) using the cis-element database PLACE (http://www.dna.affrc.go.jp/PLACE/). To explore the possibility that WRKY53 directly regulates *ATL31* transcription, a reporter assay was performed using Arabidopsis protoplast cells. The *ATL31* promoter was fused to the GUS reporter gene (pATL31:GUS). Then, the reporter plasmid and a CaMV p35S:WRKY53 effector plasmid were co-transfected into Arabidopsis protoplast cells, followed by quantification of GUS activity. Co-transfection of WRKY53 with the

ATL31 promoter containing 7 W-box-like sequences (-1,178 bp to -1) led to a 25-fold increase in GUS activity (Figure 7A). To identify the region necessary for transcriptional activation, various deletion constructs of the *ATL31* promoter were made. Reporter analysis demonstrated that the construct containing W-boxes 1 to 5 (-648 to-1) was sufficient for *ATL31* transcriptional activation by WRKY53 (Figure 7A). Additional experiments narrowed down this region even further and showed that W-box 1 (-109 to -1) was enough for *ATL31* induction by WRKY53 in Arabidopsis protoplast cells. It should be noted that there were significant differences in GUS activity in the absence or presence of W-boxes 6 and 7 in addition to W-boxes 1 to 5 (Figure 7A), indicating that W-boxes 6 and 7 may also have some physiological effect on efficient *ATL31* induction in plants. In addition, *ATL31* transcript levels in Arabidopsis plants overexpressing *WRKY53* (*WRKY53 OX*) were analyzed. Isolation of the *WRKY53 OX* plant was confirmed by PCR with genome DNA and by transcript analysis (Figure 7B, C). GFP fluorescence and immunoblot analysis confirmed the successful expression of WRKY53-GFP protein (Figure 11A, B). In *WRKY53 OX* plants, *ATL31* mRNA expression was increased compared to WT plants (Figure 7D). These results suggest that the *ATL31* gene could be a direct transcriptional target of WRKY53 in plants.

Discussion

CO_2/N affects leaf senescence progression in plants

In this study, we analyzed the C/N response upon atmospheric CO_2 manipulation with hydroponic culturing, which revealed the effect of the C/N balance on plant growth and the close relationship between C and N metabolism. Elevated CO_2 levels and the degree of N availability affected both plant biomass and senescence progression (Figures 3-6).

Under conditions of elevated CO_2 and sufficient N, plants could produce more carbohydrates via photosynthesis and convert them into organic compounds such as proteins for plant growth. In contrast, under elevated CO_2 conditions with limited N availability, plants could not grow well and instead responded with senescence progression, indicated by phenotypical changes, such as chlorosis and anthocyanin accumulation (Figures 3B and 6C, D).

Senescence progression correlated with the increased expression of genes encoding enzymes and transporters involved in adaptation to N starvation, such as GLN1.4 and NRT2.4 (Fuentes et al. 2001; Ishiyama et al. 2004; Kiba et al. 2012) under elevated CO_2 and limited N conditions (Figure 5E, F). Interestingly, *GLN1.4* and *NRT2.4* expression was not upregulated in plants grown under low CO_2 conditions with limited N. It has been reported that plants grown under elevated atmospheric CO_2 typically decrease cellular concentrations of nitrogen compared with plants grown under ambient CO_2 (Coleman et al. 1993; Long et al. 2004). These results suggest that excess sugar produced under elevated CO_2 conditions alters cellular nitrogen availability and partitioning, which disturbs the plant's ability to coordinate N-metabolism and plant growth under limited nitrogen conditions. On the other hand, N availability also affects sugar metabolism. Under limited N conditions, but not upon exposure to elevated CO_2, the concentration of soluble sugars and starch in plants increased (Figure 4). ADP-glucose pyro-phosphorylase (AGPase), a key enzyme for starch biosynthesis, is transcriptionally upregulated by N starvation (Scheible et al. 1997), which is also consistent with the increased accumulation of starch under elevated CO_2 and limited N conditions observed in this study (Figure 4B, C). In contrast, protein amounts in rosette leaves decreased approximately 0.3-fold under elevated CO_2 and limited N compared to

sufficient N conditions (Figure 12), together suggesting that carbon flux is regulated by nitrogen availability. Based on these results, we concluded that elevated CO_2 and limited N availability mutually affect each other and thereby severely disrupt the cellular C/N balance, which leads to promotion of leaf senescence. A recent study demonstrated that a sugar metabolite, trehalose 6-phosphate (T6P), is an essential signaling molecule for the initiation of senescence in plants grown in high sugar medium (Wingler et al. 2012). Furthermore, T6P was also reported as a regulatory molecule functioning in flowering transition in Arabidopsis (Wahl et al. 2013). Thus, the role of T6P in the C/N signaling cascade should be examined in future studies.

ATL31 functions in leaf senescence

The physiological function of the C/N-related ubiquitin ligase ATL31 was evaluated using growth media with various C/N ratios as well as combined manipulation of atmospheric CO_2 and N availability in the medium. Gene expression of *ATL31* was induced in response to N deficiency in the C/N medium (Figure 2F). In addition, *ATL31* expression was promoted during senescence in response to high CO_2/low N conditions (Figure 6B). It has been reported that the amounts of several sugars increase in the senescent leaf, whereas the amounts of nitrogen compounds decrease (Pourtau et al. 2004; Watanabe et al. 2013; Wingler et al. 2012; Wingler et al. 2006), suggesting a physiological function for ATL31 in senescence progression in response to C/N status. Actually, *atl31 KO* mutants showed a more severe senescence phenotype under elevated CO_2 and limited N conditions, whereas *ATl31 OX* plants showed repressed senescence progression (Figures 3 and 6C, D). Similar results were also observed in the *KO* and *OX* plants grown under ambient CO_2 and normal soil conditions (Figure 10). From these

results, we concluded that ATL31 may be involved in senescence progression via C/N signaling and/or metabolism in plants.

It should be noted that *ATL31 OX* plants showed a different phenotype depending on whether they underwent C/N or CO_2/N treatment. In particular, under high CO_2/low N conditions, *ATL31 OX* plants showed a decrease in anthocyanin compared to WT (Figure 6C), whereas after high C/low N stress treatment *ATL31 OX* plants did not show a significant difference compared with WT plants (Figure 1B). Previously, we have reported that *ATL31 OX* plants exhibited stress resistance and expanded green-colored cotyledons when seedlings were grown in high C/low N stress medium (300 mM glucose/0.3 mM N), whereas WT plants showed a severe growth defect with strong purple pigmentation (Sato et al. 2009). Therefore, the resistance seen in *ATL31 OX* plants may change depending on what type of C/N stress the plants are exposed to. ATL31 is expected to contribute to the adaptation of plants to long-term limited N conditions, for instance by remobilizing nitrogen metabolites or by improving nitrogen-use efficiency in mature plants.

ATL31 gene expression is highly correlated with *WRKY53* expression. WRKY53 is a member of the large WRKY transcription factor family and positively regulates senescence-related gene expression (Miao et al. 2004; Miao and Zentgraf 2007). WRKY transcription factors are involved in diverse physiological processes, including development and secondary metabolism as well as biotic and/or abiotic stress response (Ishihama and Yoshioka 2012; Rushton et al. 2010). WRKY proteins contain either one or two DNA-binding domains, harboring the conserved amino acid sequence WRKY, which directly binds to the W-box motif (T/CTGACC/T) in target gene promoters. Since *WRKY* genes usually contain some W-box motifs in their promoters, they can be

transcriptionally autoregulated or crossregulated by other WRKY factors. Although pull-down analysis identified several senescence-associated genes (SAG) and other WRKY transcription factors as direct targets of WRKY53 (Miao et al. 2004), little is known about the targets, especially in regard to which targets are involved in nutrient stress-induced senescence. Results from our reporter assay in protoplasts and qRT-PCR analyses of *WRKY53 OX* plants (Figure 7) demonstrate that WRKY53 can activate *ATL31* expression via direct binding to the W-box in the *ATL31* promoter. *WRKY53* expression was promoted not only at senescence stage, but also in response to high C/low N conditions similar to *ATL31* expression, implicating that WRKY53 protein physiologically controls ATL31 levels in response to the cellular C/N status in plants. Taken together, these results demonstrate that ATL31 is transcriptionally induced under high C/low N conditions and involved in senescence progression in plants. The activity of WRKY53 and other WRKY family proteins is regulated via phosphorylation by MAP kinases as a part of pathogen signaling (Ishihama and Yoshioka 2012; Rushton et al. 2010). Further studies are needed to elucidate the mechanism underlying WRKY53 activation in response to C/N status, to further characterize the relationship between WRKY53 and ATL31 and to understand the upstream signaling components that regulate C/N-induced leaf senescence.

ATL31 functions as a RING-type ubiquitin ligase and regulates post-germinative growth via fine-tuning the stability of 14-3-3 proteins in response to changes in C/N status (Sato et al. 2011a). 14-3-3 proteins recognize specific amino acid motifs, including phosphorylated Ser/Thr residues, and regulate many cellular signaling cascades. In particular, 14-3-3 proteins regulate C/N metabolism by directly binding to essential enzymes involved in carbohydrate and nitrogen metabolism, such as nitrate

reductase, sucrose phosphate synthase, ADP-glucose pyrophosphorylase, glutamine synthetase, or H^+-ATPase (Chevalier et al. 2009; Comparot et al. 2003). To further understand the molecular mechanism underlying the regulation of primary metabolism and senescence progression in plants, we should clarify the function of 14-3-3 proteins in senescence regulation and the upstream signaling cascade modulating ATL31 activity under disrupted CO_2/N conditions.

References

Aguilar-Hernandez, V., Aguilar-Henonin, L. and Guzman, P. (2011) Diversity in the Architecture of ATLs, a Family of Plant Ubiquitin-Ligases, Leads to Recognition and Targeting of Substrates in Different Cellular Environments. *Plos One* 6.

Axelos, M., Curie, C., Mazzolini, L., Bardet, C. and Lescure, B. (1992) A protocol for transient gene expression in Arabidopsis thaliana protoplasts isolated from cell suspension cultures. *Plant physiology and biochemistry* 30: 123-128.

Bachmann, M., Huber, J.L., Liao, P.C., Gage, D.A. and Huber, S.C. (1996) The inhibitor protein of phosphorylated nitrate reductase from spinach (Spinacia oleracea) leaves is a 14-3-3 protein. *FEBS Lett* 387: 127-131.

Chevalier, D., Morris, E.R. and Walker, J.C. (2009) 14-3-3 and FHA domains mediate phosphoprotein interactions. *Annu Rev Plant Biol* 60: 67-91.

Coleman, J.S., Mcconnaughay, K.D.M. and Bazzaz, F.A. (1993) Elevated Co2 and Plant Nitrogen-Use - Is Reduced Tissue Nitrogen Concentration Size-Dependent. *Oecologia* 93: 195-200.

Comparot, S., Lingiah, G. and Martin, T. (2003) Function and specificity of 14-3-3 proteins in the regulation of carbohydrate and nitrogen metabolism. *J Exp Bot* 54:

595-604.

Coruzzi, G.M. and Zhou, L. (2001) Carbon and nitrogen sensing and signaling in plants: emerging 'matrix effects'. *Current opinion in plant biology* 4: 247-253.

Ferrario-Mery, S., Bouvet, M., Leleu, O., Savino, G., Hodges, M. and Meyer, C. (2005) Physiological characterisation of Arabidopsis mutants affected in the expression of the putative regulatory protein PII. *Planta* 223: 28-39.

Fuentes, S.I., Allen, D.J., Ortiz-Lopez, A. and Hernandez, G. (2001) Over-expression of cytosolic glutamine synthetase increases photosynthesis and growth at low nitrogen concentrations. *J Exp Bot* 52: 1071-1081.

Gibon, Y., Blasing, O.E., Palacios-Rojas, N., Pankovic, D., Hendriks, J.H.M., Fisahn, J., et al. (2004) Adjustment of diurnal starch turnover to short days: depletion of sugar during the night leads to a temporary inhibition of carbohydrate utilization, accumulation of sugars and post-translational activation of ADP-glucose pyrophosphorylase in the following light period. *Plant J* 39: 847-862.

Higo, K., Ugawa, Y., Iwamoto, M. and Korenaga, T. (1999) Plant cis-acting regulatory DNA elements (PLACE) database: 1999. *Nucleic Acids Res* 27: 297-300.

Hikosaka, K., Kinugasa, T., Oikawa, S., Onoda, Y. and Hirose, T. (2011) Effects of elevated CO2 concentration on seed production in C-3 annual plants. *J Exp Bot* 62: 1523-1530.

Hsieh, M.H., Lam, H.M., van de Loo, F.J. and Coruzzi, G. (1998) A PII-like protein in Arabidopsis: Putative role in nitrogen sensing. *P Natl Acad Sci USA* 95: 13965-13970.

Ishihama, N. and Yoshioka, H. (2012) Post-translational regulation of WRKY transcription factors in plant immunity. *Current opinion in plant biology* 15:

431-437.

Ishiyama, K., Inoue, E., Watanabe-Takahashi, A., Obara, M., Yamaya, T. and Takahashi, H. (2004) Kinetic properties and ammonium-dependent regulation of cytosolic isoenzymes of glutamine synthetase in Arabidopsis. *J Biol Chem* 279: 16598-16605.

Iwata, Y., Lee, M. and Koizumi, N. (2011) Analysis of a transcription factor using transient assay in Arabidopsis protoplasts. . *Methods in Molecular Biology* 754: 107-117.

Jefferson, R.A., Kavanagh, T.A. and Bevan, M.W. (1987) Gus Fusions - Beta-Glucuronidase as a Sensitive and Versatile Gene Fusion Marker in Higher-Plants. *Embo J* 6: 3901-3907.

Kang, J.M. and Turano, F.J. (2003) The putative glutamate receptor 1.1 (AtGLR1.1) functions as a regulator of carbon and nitrogen metabolism in Arabidopsis thaliana. *P Natl Acad Sci USA* 100: 6872-6877.

Kiba, T., Feria-Bourrellier, A.B., Lafouge, F., Lezhneva, L., Boutet-Mercey, S., Orsel, M., et al. (2012) The Arabidopsis Nitrate Transporter NRT2.4 Plays a Double Role in Roots and Shoots of Nitrogen-Straved Plants. *Plant Cell* 24: 245-258.

Kiba, T., Kudo, T., Kojima, M. and Sakakibara, H. (2011) Hormonal control of nitrogen acquisition: roles of auxin, abscisic acid, and cytokinin. *J Exp Bot* 62: 1399-1409.

Klotke, J., Kopka, J., Gatzke, N. and Heyer, A.G. (2004) Impact of soluble sugar concentrations on the acquisition of freezing tolerance in accessions of Arabidopsis thaliana with contrasting cold adaptation - evidence for a role of raffinose in cold acclimation. *Plant Cell Environ* 27: 1395-1404.

Knohl, A. and Veldkamp, E. (2011) GLOBAL CHANGE Indirect feedbacks to rising

CO2. *Nature* 475: 177-178.

Lim, P.O., Kim, H.J. and Nam, H.G. (2007) Leaf senescence. *Annu Rev Plant Biol* 58: 115-136.

Long, S.P., Ainsworth, E.A., Rogers, A. and Ort, D.R. (2004) Rising atmospheric carbon dioxide: Plants face the future. *Annu Rev Plant Biol* 55: 591-628.

Mackintosh, C. (2004) Dynamic interactions between 14-3-3 proteins and phosphoproteins regulate diverse cellular processes. *Biochem J* 381: 329-342.

Maekawa, S., Sato, T., Asada, Y., Yasuda, S., Yoshida, M., Chiba, Y., et al. (2012) The Arabidopsis ubiquitin ligases ATL31 and ATL6 control the defense response as well as the carbon/nitrogen response. *Plant Mol Biol* 79: 217-227.

Martin, T., Oswald, O. and Graham, I.A. (2002) Arabidopsis seedling growth, storage lipid mobilization, and photosynthetic gene expression are regulated by carbon:nitrogen availability. *Plant Physiol* 128: 472-481.

Miao, Y., Laun, T., Zimmermann, P. and Zentgraf, U. (2004) Targets of the WRKY53 transcription factor and its role during leaf senescence in Arabidopsis. *Plant Mol Biol* 55: 853-867.

Miao, Y. and Zentgraf, U. (2007) The antagonist function of Arabidopsis WRKY53 and ESR/ESP in leaf senescence is modulated by the jasmonic and salicylic acid equilibrium. *Plant Cell* 19: 819-830.

Miller, A.J., Fan, X.R., Orsel, M., Smith, S.J. and Wells, D.M. (2007) Nitrate transport and signalling. *J Exp Bot* 58: 2297-2306.

Nakagawa, T., Kurose, T., Hino, T., Tanaka, K., Kawamukai, M., Niwa, Y., et al. (2007) Development of series of gateway binary vectors, pGWBs, for realizing efficient construction of fusion genes for plant transformation. *J Biosci Bioeng* 104: 34-41.

Pompeiano, A., Volpi, I., Volterrani, M. and Guglielminetti, L. (2013) N source affects freeze tolerance in bermudagrass and zoysiagrass. *Acta Agr Scand B-S P* 63: 341-351.

Pourtau, N., Mares, M., Purdy, S., Quentin, N., Ruel, A. and Wingler, A. (2004) Interactions of abscisic acid and sugar signalling in the regulation of leaf senescence. *Planta* 219: 765-772.

Roberts, M.R. (2003) 14-3-3 proteins find new partners in plant cell signalling. *Trends Plant Sci* 8: 218-223.

Roitsch, T. and Gonzalez, M.C. (2004) Function and regulation of plant invertases: sweet sensations. *Trends Plant Sci* 9: 606-613.

Rolland, F., Baena-Gonzalez, E. and Sheen, J. (2006) Sugar sensing and signaling in plants: Conserved and novel mechanisms. *Annu Rev Plant Biol* 57: 675-709.

Rushton, P.J., Somssich, I.E., Ringler, P. and Shen, Q.X.J. (2010) WRKY transcription factors. *Trends Plant Sci* 15: 247-258.

Sato, T., Maekawa, S., Yasuda, S., Domeki, Y., Sueyoshi, K., Fujiwara, M., et al. (2011a) Identification of 14-3-3 proteins as a target of ATL31 ubiquitin ligase, a regulator of the C/N response in Arabidopsis. *Plant J* 68: 137-146.

Sato, T., Maekawa, S., Yasuda, S., Sonoda, Y., Katoh, E., Ichikawa, T., et al. (2009) CNI1/ATL31, a RING-type ubiquitin ligase that functions in the carbon/nitrogen response for growth phase transition in Arabidopsis seedlings. *Plant J* 60: 852-864.

Sato, T., Maekawa, S., Yasuda, S. and Yamaguchi, J. (2011b) Carbon and nitrogen metabolism regulated by the ubiquitin-proteasome system. *Plant signaling & behavior* 6: 1465-1468.

Scheible, W.R., GonzalezFontes, A., Lauerer, M., MullerRober, B., Caboche, M. and

Stitt, M. (1997) Nitrate acts as a signal to induce organic acid metabolism and repress starch metabolism in tobacco. *Plant Cell* 9: 783-798.

Serrano, M., Parra, S., Alcaraz, L.D. and Guzman, P. (2006) The ATL gene family from Arabidopsis thaliana and Oryza sativa comprises a large number of putative ubiquitin ligases of the RING-H2 type. *Journal of Molecular Evolution* 62: 434-445.

Shin, R., Jez, J.M., Basra, A., Zhang, B. and Schachtman, D.P. (2011) 14-3-3 Proteins fine-tune plant nutrient metabolism. *Febs Letters* 585: 143-147.

Smith, A.M. and Stitt, M. (2007) Coordination of carbon supply and plant growth. *Plant Cell Environ* 30: 1126-1149.

Sulpice, R., Nikoloski, Z., Tschoep, H., Antonio, C., Kleessen, S., Larhlimi, A., et al. (2013) Impact of the Carbon and Nitrogen Supply on Relationships and Connectivity between Metabolism and Biomass in a Broad Panel of Arabidopsis Accessions(1[W][OA]). *Plant Physiol* 162: 347-363.

Wahl, V., Ponnu, J., Schlereth, A., Arrivault, S., Langenecker, T., Franke, A., et al. (2013) Regulation of Flowering by Trehalose-6-Phosphate Signaling in Arabidopsis thaliana. *Science* 339: 704-707.

Watanabe, M., Balazadeh, S., Tohge, T., Erban, A., Giavalisco, P., Kopka, J., et al. (2013) Comprehensive Dissection of Spatiotemporal Metabolic Shifts in Primary, Secondary, and Lipid Metabolism during Developmental Senescence in Arabidopsis. *Plant Physiol* 162: 1290-1310.

Wingler, A., Delatte, T.L., O'Hara, L.E., Primavesi, L.F., Jhurreea, D., Paul, M.J., et al. (2012) Trehalose 6-Phosphate Is Required for the Onset of Leaf Senescence Associated with High Carbon Availability. *Plant Physiol* 158: 1241-1251.

Wingler, A., Purdy, S., MacLean, J.A. and Pourtau, N. (2006) The role of sugars in integrating environmental signals during the regulation of leaf senescence. *J Exp Bot* 57: 391-399.

Table and Figures

Table 1. List of primers used for PCR analysis.

Primers for qRT-PCR

Gene	F or R	Sequence (5'-3')
ATL31	F	ACCGGTGGGCTTTTCTTAG
	R	AACTGACGATGTTCCTTCACC
WRKY53	F	CTGTAGTCCCGGTGGCAAAT
	R	CGTTTATCGATGCCGGAGAT
CHS	F	AAGCGCATGTGCGACAAG
	R	TCCTCCGTCAGATGCATGTG
PAP1	F	CCAAGAGGTAGATATTTTGGTTCC
	R	CTATACGCAAACGCAAACAAATG
RBCS1A	F	CTTCCCTTGTTCGGTTGCA
	R	TGCACTCTTCCACTTCCTTCAA
CAB2	F	GCCTCAACAATGGCTCTCTC
	R	TGGCTTGGCAACAGTCTTC
NRT2.4	F	CCGTCTTCTCCATGTCTTTC
	R	CTGACCATTGAACATTGTGC
GLN1.4	F	CTCGATCTCTCCGATTCCAC
	R	ACTGGTCCAGGCAAAGTCC
SAG12	F	CCGGTTTCTGTTGACTGGAG
	R	CGCTGAAAACGCCCAAC
18SrRNA	F	CGGCTACCACATCCAAGGAA
	R	GCTGGAATTACCGCGGCT

Primers for Plasmid construction

Gene	F or R	Sequence (5'-3')
-1178 pATL31	F	AAAAAAGCTTAAAGTCCTTAGTTTG
	R	TATGGATCCTGGAGTCCCAAAAAGTTAG
-648 pATL31	F	CAGAAGCTTTAATTAAAAAAAAAAAGAAG
	R	TATGGATCCTGGAGTCCCAAAAAGTTAG
-219 pATL31	F	ATTAAGCTTTGTATGACTTTTCACTTCC
	R	TATGGATCCTGGAGTCCCAAAAAGTTAG
-191 pATL31	F	ATCAAGCTTTGGAAACTTCTGACCGTCC
	R	TATGGATCCTGGAGTCCCAAAAAGTTAG
-109 pATL31	F	GCTAAGCTTCCACGACTTTTTCAAACTTT
	R	TATGGATCCTGGAGTCCCAAAAAGTTAG
WRKY53	F	CACCGAAGGAAGAGATAT
	R	ATAATAAATCGACTCGTGTAAAAA

Primers for Reporter Assay

Gene	F or R	Sequence (5'-3')
EF1α	F	GACATGAGGCAGACTGTTGCA
	R	CCGGTTGGGTCCTTCTTGT
GUS	F	GGCTATACGCCATTTGAAGC
	R	TTTTTGTCACGCGCTATCAG

Primers for Genotyping check

Gene	F or R	Sequence (5'-3')
WRKY53:GFP	F	CGGCAGTGTTCCAGAATCTC
	R	AAGTCGATGCCCTTCAGCTC

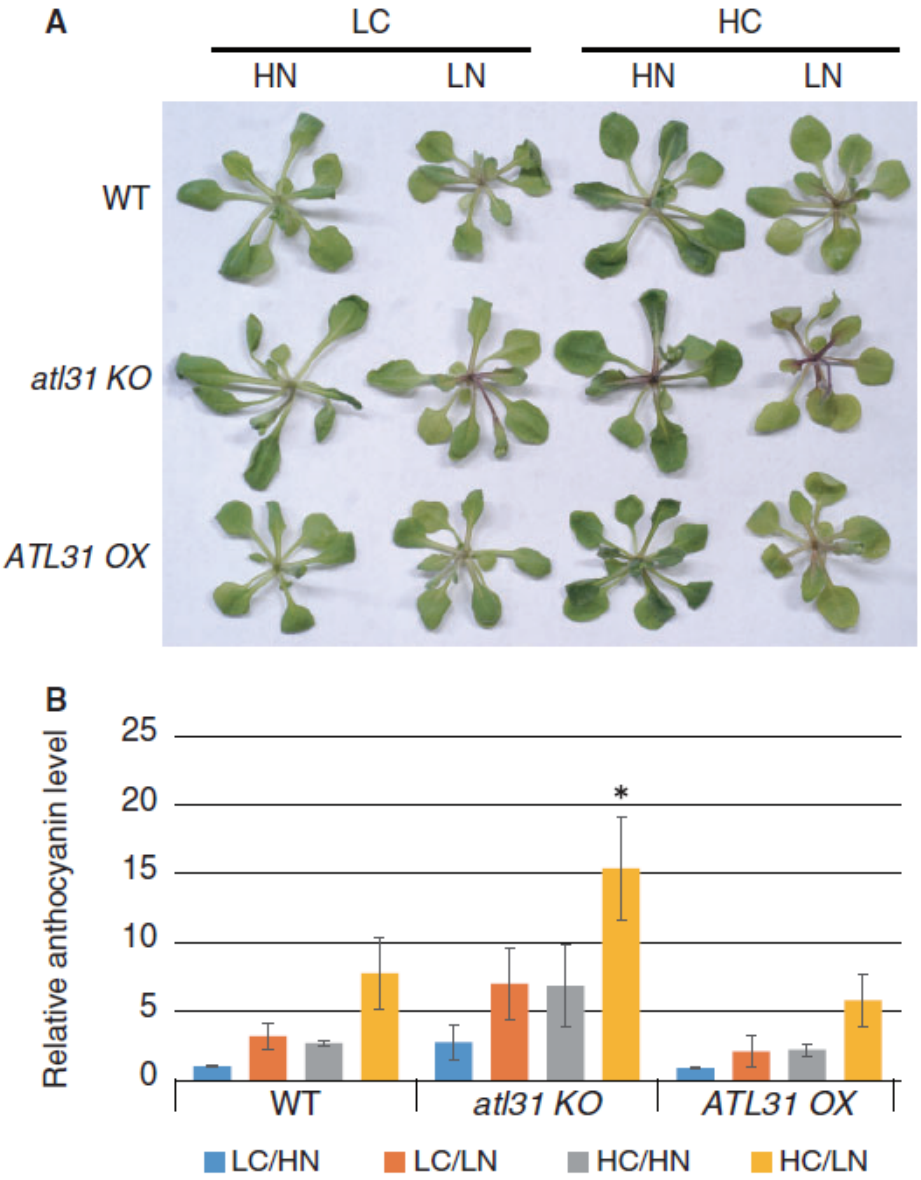

Figure 1. Phenotype of WT, *atl31 KO*, and *ATL31 OX* plants grown in different C/N media.

(A) Growth phenotype of each plant 3 days after transfer from control C/N medium (LC/HN) to modified C/N medium containing 100 mM or 200 mM glucose (LC or HC), and 0.3 mM or 30 mM nitrogen (LN or HN). (B) Anthocyanin accumulation in WT, *atl31 KO*, and *ATL31 OX* plants. Anthocyanin levels in WT plants grown in LC/HN control medium was set to 1 in each condition and genotype. Means ± SD of three independent experiments are shown. Asterisk indicates significant differences compared with WT in each C/N condition as determined by Dunnet analysis ($p<0.05$).

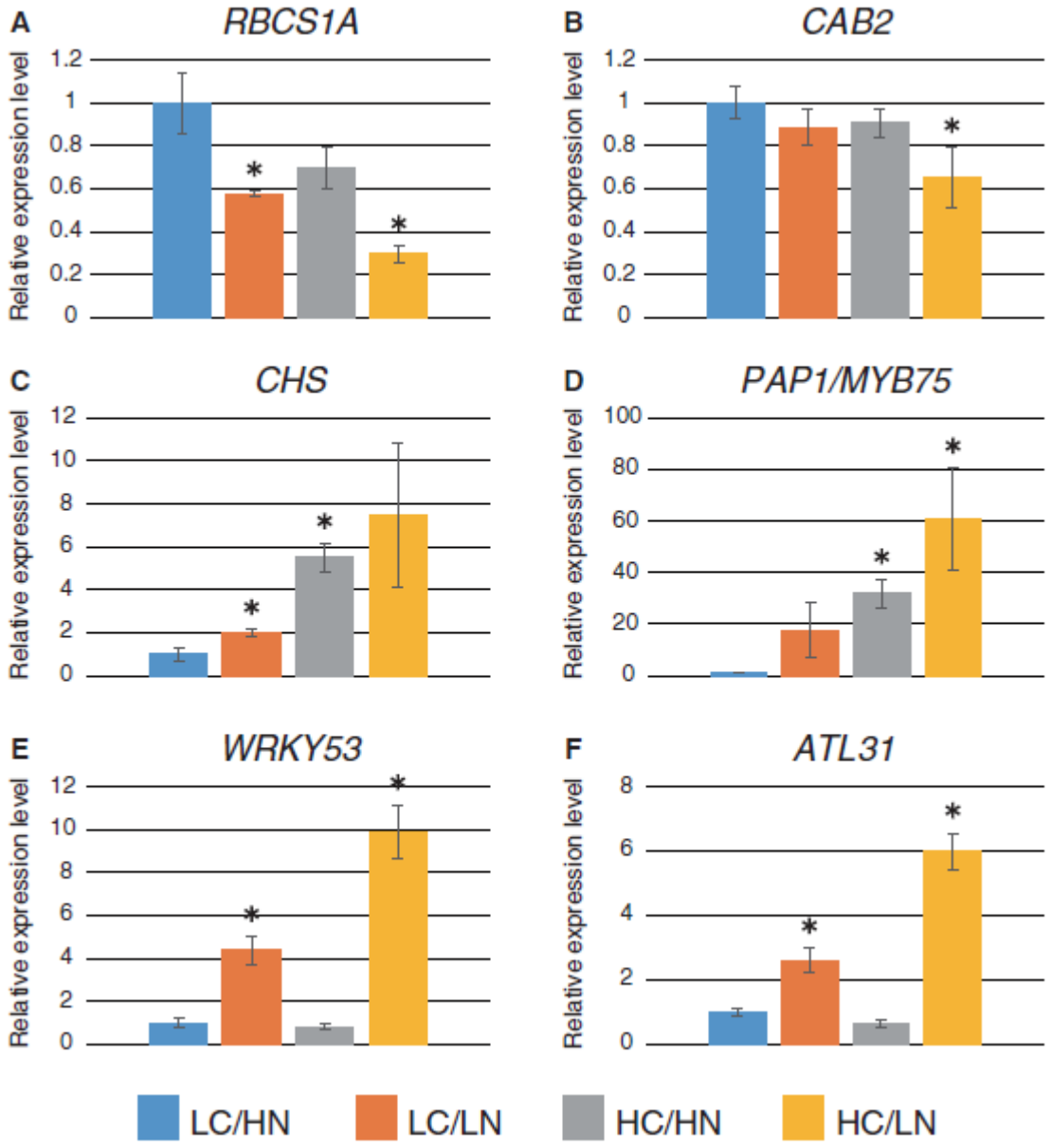

Figure 2. Relative expression levels of C/N- and senescence-related genes.

Expression levels of C/N- and senescence-related genes in WT plants grown in each C/N medium were analyzed by qRT-PCR. Total RNA was purified from WT plants 24 hours after transfer to C/N medium containing 100 mM or 200 mM glucose (LC or HC) and 0.3 mM or 30 mM nitrogen (LN or HN) from control (LC/HN). Relative expression levels were compared with WT plants grown in control C/N medium. Means ± SD of three independent experiments are shown. Asterisk indicates significant differences compared with WT in control C/N condition as determined by Dunnet analysis (p<0.05).

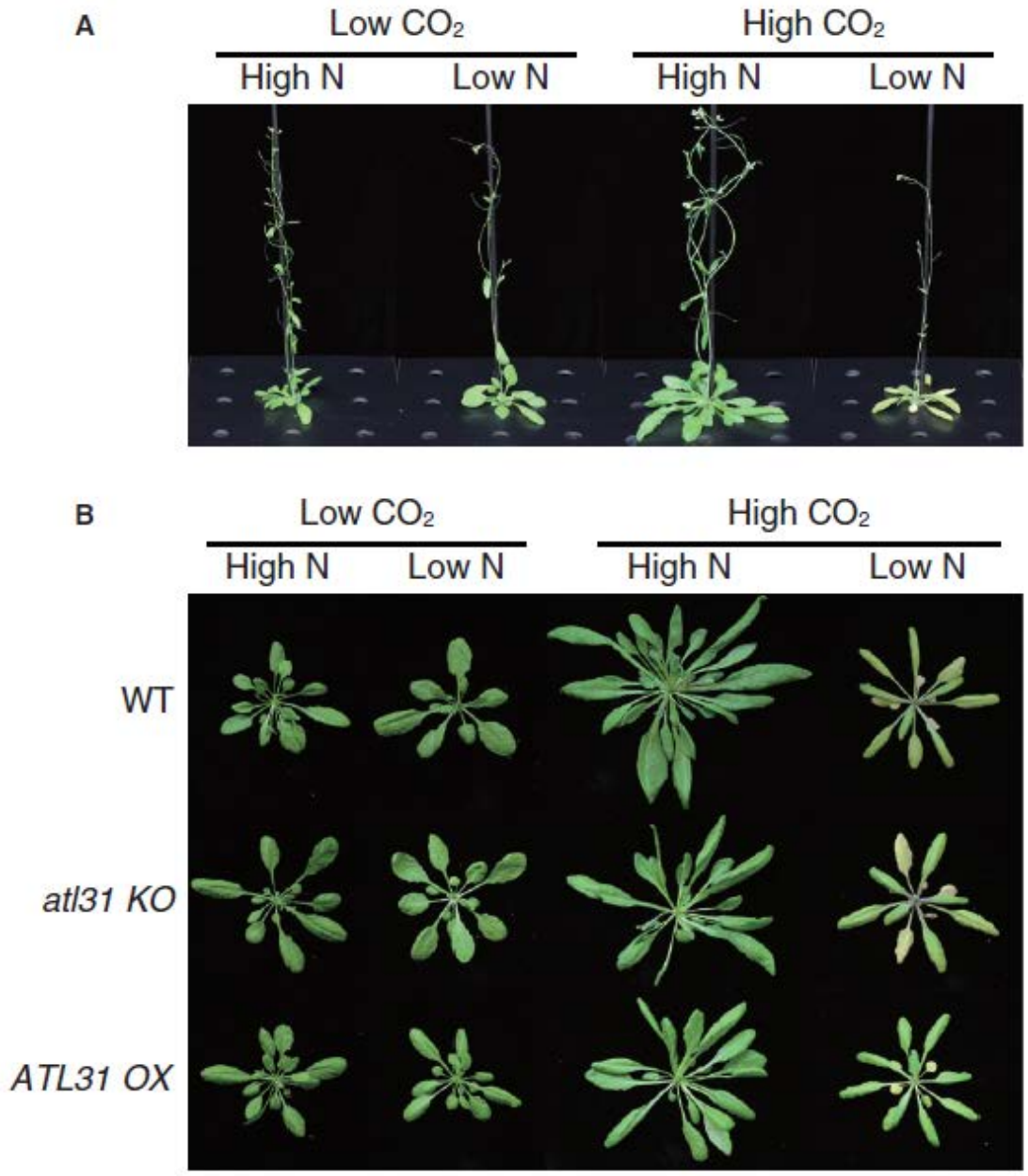

Figure 3. Phenotype of WT, *atl31 KO,* and *ATL31 OX* plants grown under different CO_2/N conditions.

Plants were grown under 280 ppm CO_2 and 3 mM nitrogen (low CO_2/high N) for 2 weeks and then transferred to 280 or 780 ppm CO_2 (low CO_2 or high CO_2) and 0.3 mM or 3 mM nitrogen (low N or high N) conditions and grown for additional 4 weeks. (A) Growth of whole tissue above ground of WT plants. The phenotypes of *atl31 KO* and *ATL31 OX* are shown in Figure 8. (B) Rosette leaves phenotypes of WT, *atl31 KO*, and *ATL31 OX*.

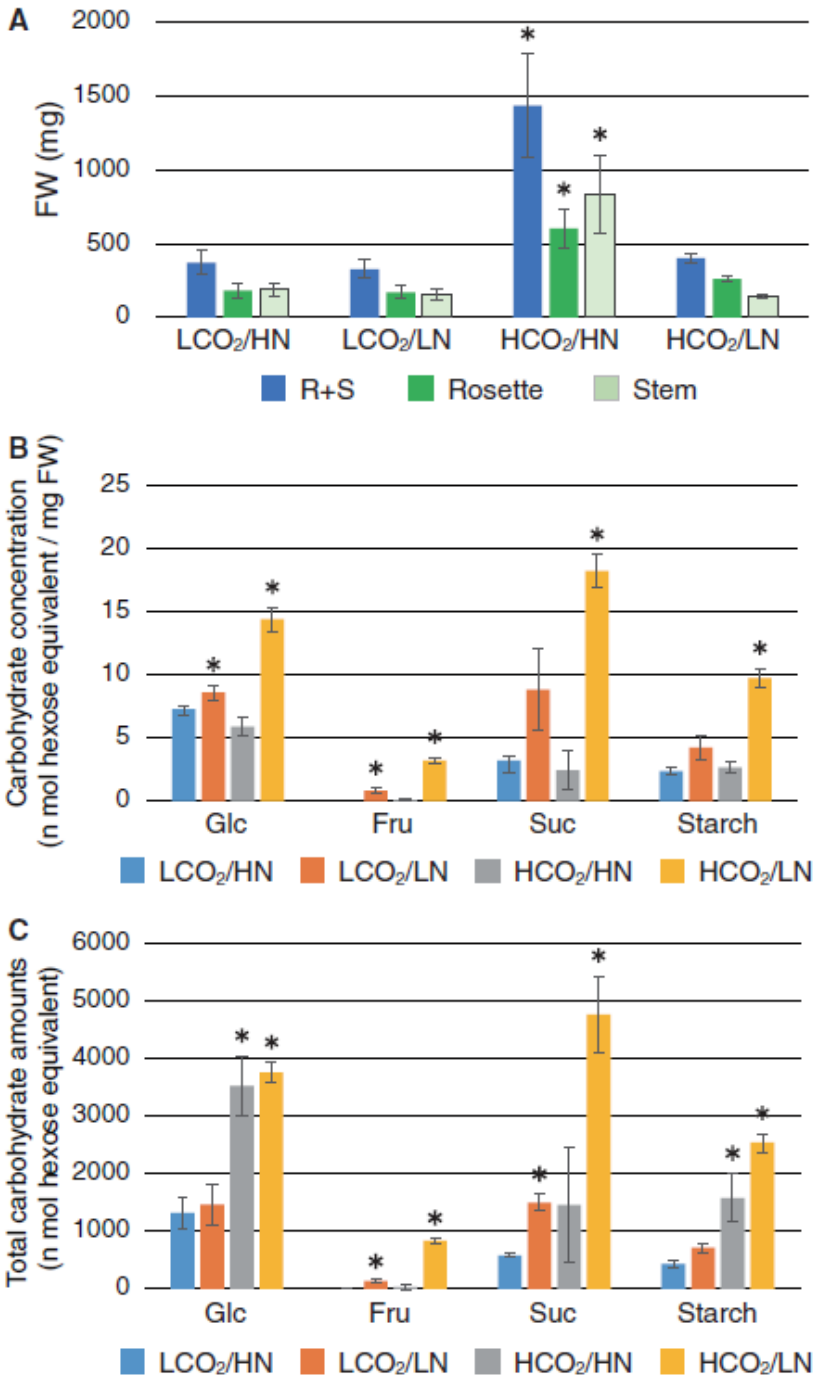

Figure 4. Measurement of biomass, sugar, and starch amounts in response to changes in CO_2/N conditions.

Plants were grown under 280 ppm CO_2 and 3 mM nitrogen (LCO_2/HN) for 2 weeks and then transferred to 280 or 780 ppm CO_2 (LCO_2 or HCO_2) and 0.3 mM or 3 mM nitrogen (LN or HN) conditions and grown for additional 4 weeks. Each plant was harvested at

the middle of the light period. (A) The fresh weight of WT plants grown under each CO_2/N condition was measured. Rosette leaves (R) and stem (S) tissues were measured separately and the average of three independent experiments is shown. (B) Glucose (Glc), fructose (Fru), sucrose (Suc), and starch amounts in rosette leaves were quantified and are shown as concentration (n mol hexose equivalent/mg FW). (C) Total amount of carbohydrate metabolites in rosette leaves were calculated from the carbohydrate concentration and fresh weight. Means ± SD of three independent experiments are shown. Asterisk indicates significant differences compared with WT grown under the control CO_2/N (LCO_2/HN) condition as determined by Dunnet analysis ($p<0.05$).

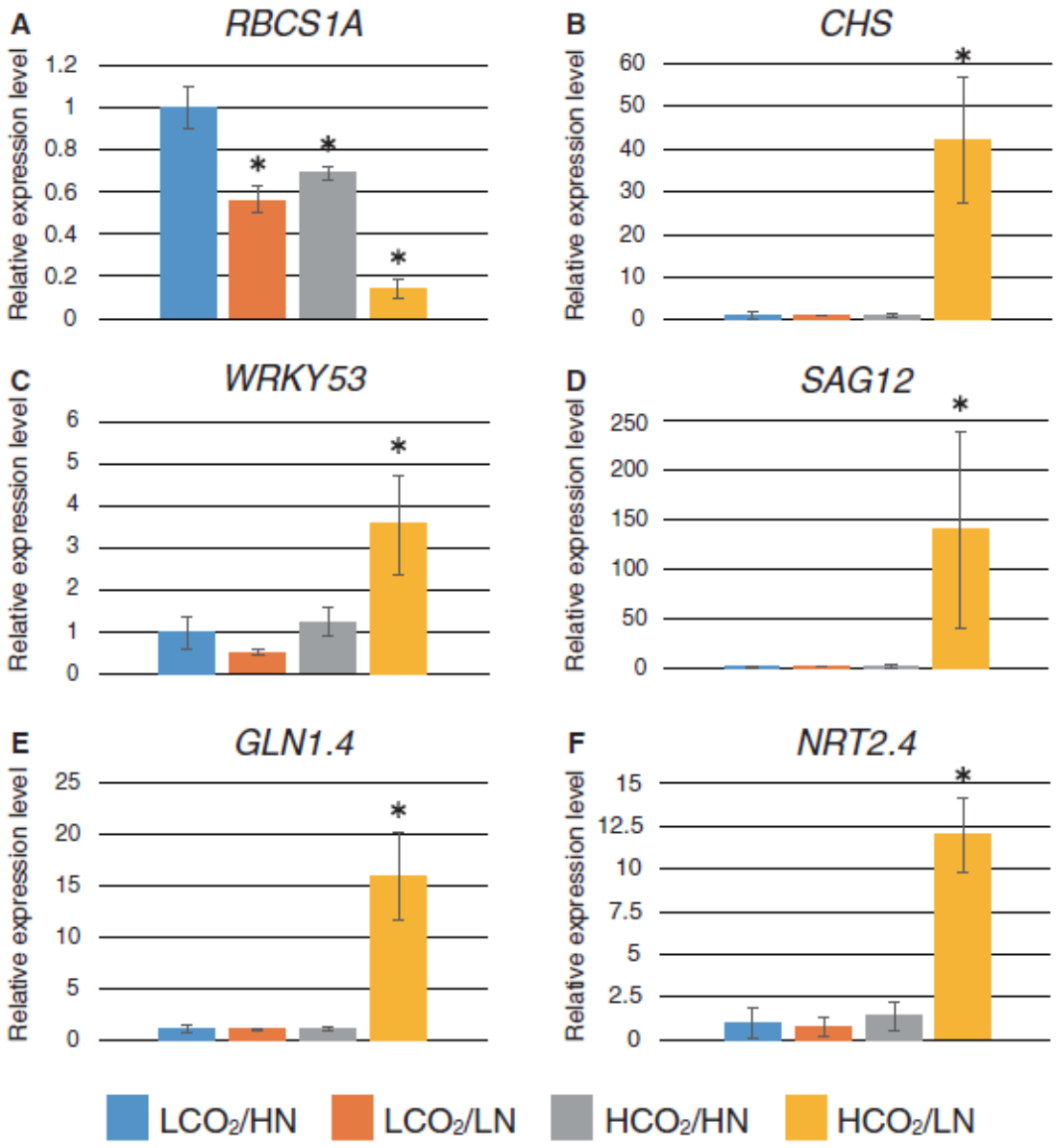

Figure 5. Relative expression levels of C/N- and senescence-related genes.

Expression levels in WT plants grown in each CO_2/N medium were analyzed by qRT-PCR. Total RNA was purified from WT plants grown for 2.5 weeks after transfer to each CO_2/N condition; namely, 280 or 780 ppm CO_2 (LCO_2 or HCO_2) and 0.3 mM or 3 mM nitrogen (LN or HN). Relative expression levels were compared with WT plants grown under control CO_2/N (LCO_2/HN) condition. Means ± SD of three independent experiments with two technical replicates are shown. Asterisk indicates significant differences compared with WT grown under control CO_2/N condition as determined by Dunnet analysis ($p<0.05$).

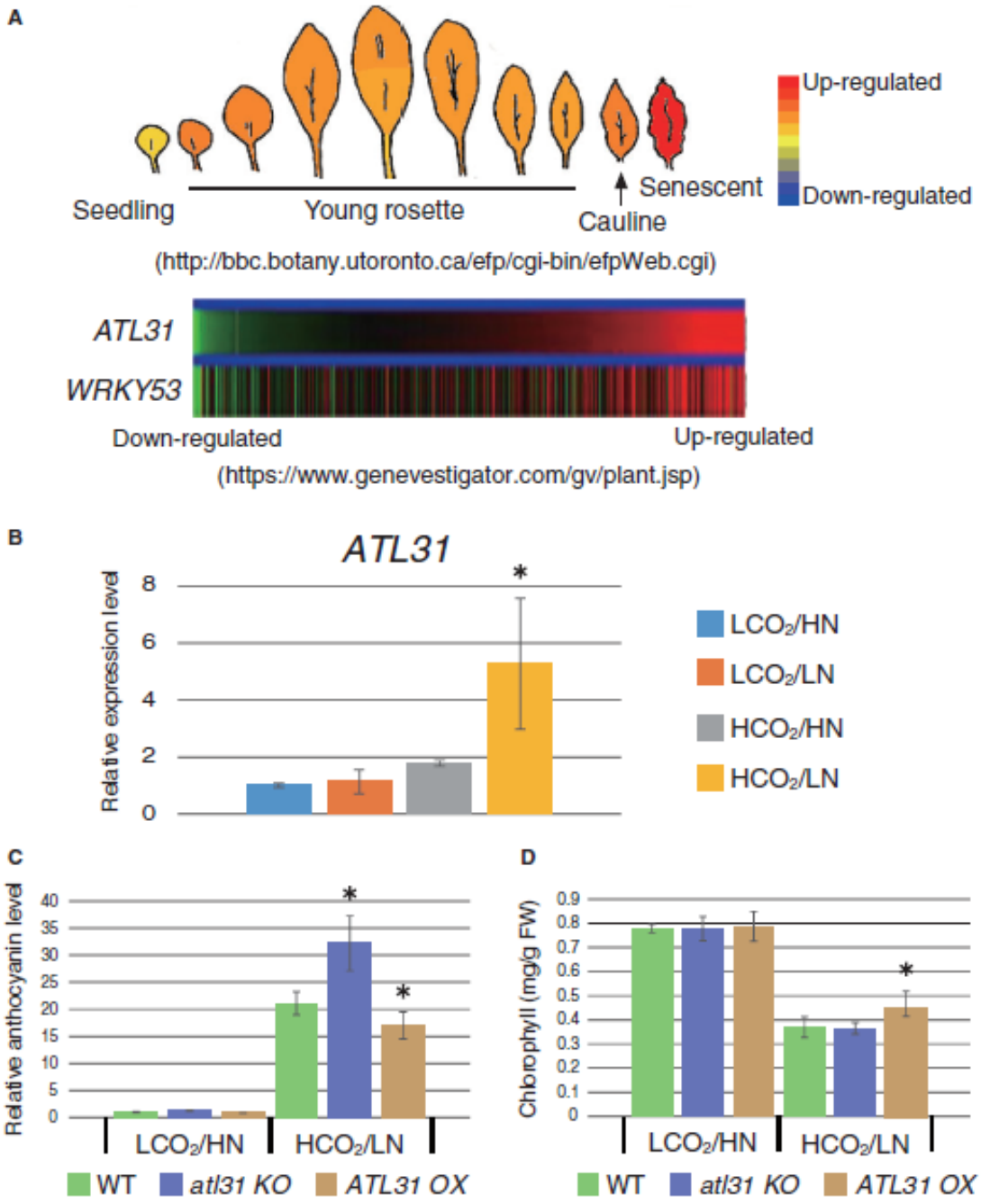

Figure 6. Physiological function of ATL31 in leaf senescence.

(A) Expression pattern of *ATL31* is shown as researched using the publicly accessible microarray database. Age-dependent expression (eFP browser; http://bbc.botany.utoronto.ca/efp/cgi-bin/efpWeb.cgi) (upper panel) and co-expression with WRKY53 (Genevestigator; https://www.genevestigator.com/gv/index.jsp) (lower

panel) were analyzed for the *ATL31* gene. (B) Expression levels of the *ATL31* gene in WT plants grown under each CO_2/N condition were analyzed by qRT-PCR. Relative expression levels were compared with control CO_2/N condition (LCO_2/HN). Means ± SD of three independent experiments with two technical replicates are shown. Asterisk indicates significant differences compared with WT grown under control CO_2/N condition as determined by Dunnet analysis ($p<0.05$). (C-D) Amounts of anthocyanin (C) and chlorophyll (D) were quantified among WT, *atl31 KO,* and *ATL31 OX* plants grown under control 280 ppm CO_2 and 3 mM N (LCO_2/HN) or 780 ppm CO_2 and 0.3 mM N (HCO_2/LN) conditions. Means ± SD of six independent experiments are shown. Asterisk indicates significant differences compared with WT grown under each C/N condition as determined by Dunnet analysis ($p<0.05$).

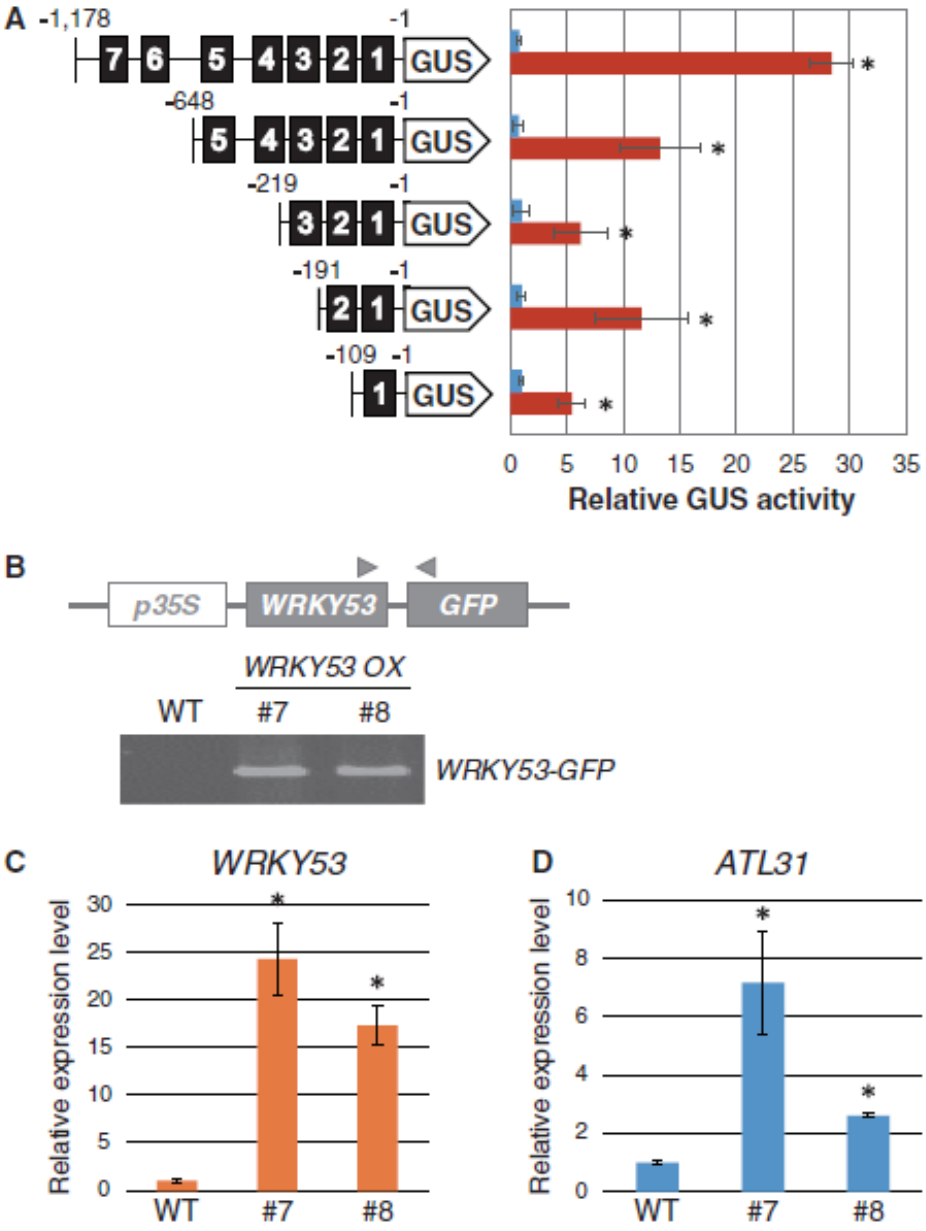

Figure 7. Transcriptional activation of *ATL31* by WRKY53.

(A) Protoplast transient assay. Plasmids containing the promoter sequence of *ATL31* fused to the *GUS* gene and *WRKY53* coding region were co-transfected into protoplast cells, and GUS activity was measured after 15 hours incubation. GUS activity was normalized to transfection efficiency. Means ± SD of relative GUS activity from three independent experiments are shown. Asterisk indicates significant differences compared with negative control cells transfected with *pATL31:GUS* and without *WRKY53* effector as determined by Student's *t*-test (p<0.05). (B) Plasmid construction and primer

(arrowheads) for the isolated *WRKY53* overexpressor (*WRKY53 OX*). PCR analysis with genomic DNA confirmed isolation of *WRKY53 OX* plants. (C-D) Transcript levels of *WRKY53* and *ATL31* as determined by qRT-PCR. mRNA was purified from WT and two independent *WRKY53 OX* plants (line 7 and 8). Relative expression levels of *WRKY53* (C) and *ATL31* (D) genes in *WRKY53 OX* plants were compared with WT. Means ± SD of three independent experiments are shown. Asterisk indicates significant differences compared with WT as determined by Dunnet analysis ($p<0.05$).

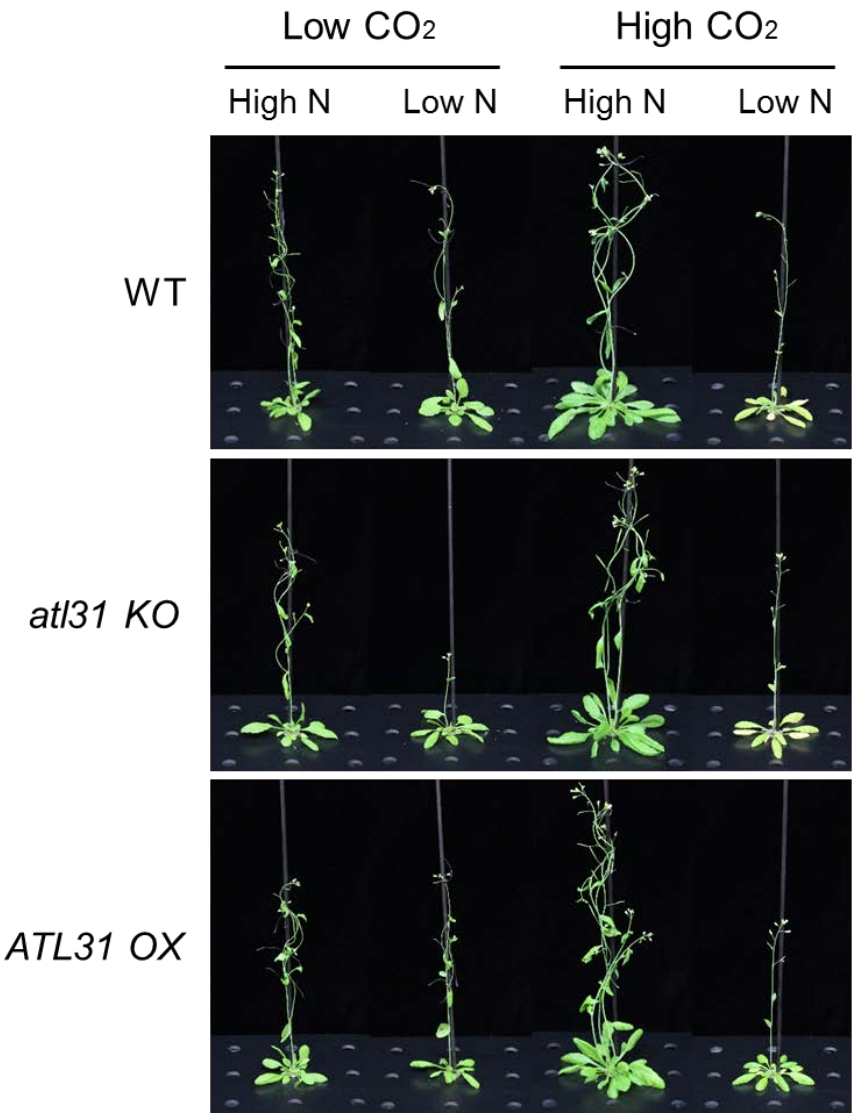

Figure 8. Phenotype of WT, *atl31 KO,* and *ATL31 OX* plants grown under different CO_2/N conditions.

Plants were grown in 280 ppm CO_2 and 3 mM N (low CO_2/high N) for 2 weeks and then transferred to 280 or 780 ppm CO_2 (low CO_2 or high CO_2) and 0.3 mM or 3 mM N (low N or high N) conditions. Growth phenotypes of each plant at 4 weeks after transfer to each CO_2/N condition are shown.

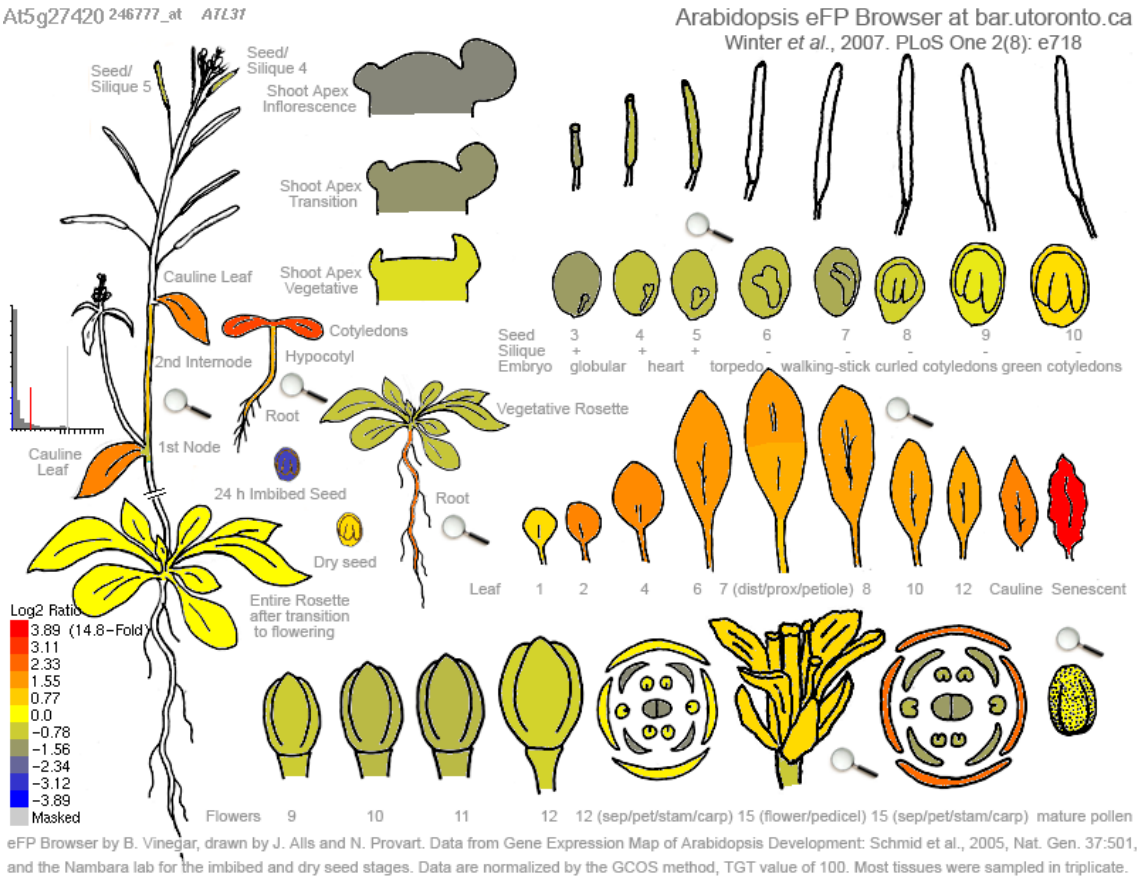

Figure 9. Gene expression pattern of *ATL31* in each tissue and developmental stage.

The expression pattern of *ATL31* was analyzed using the publicly accessible microarray database (eFP browser; http://bbc.botany.utoronto.ca/efp/cgi-bin/efpWeb.cgi). *ATL31* gene expression was strongly induced in the senescent leaf.

Figure 10. Phenotype of WT, *atl31 KO*, and *ATL31 OX* plants.

Plants were grown under ambient CO_2 conditions and in normal soil containing 3 mM N. The image was taken 8 weeks after germination.

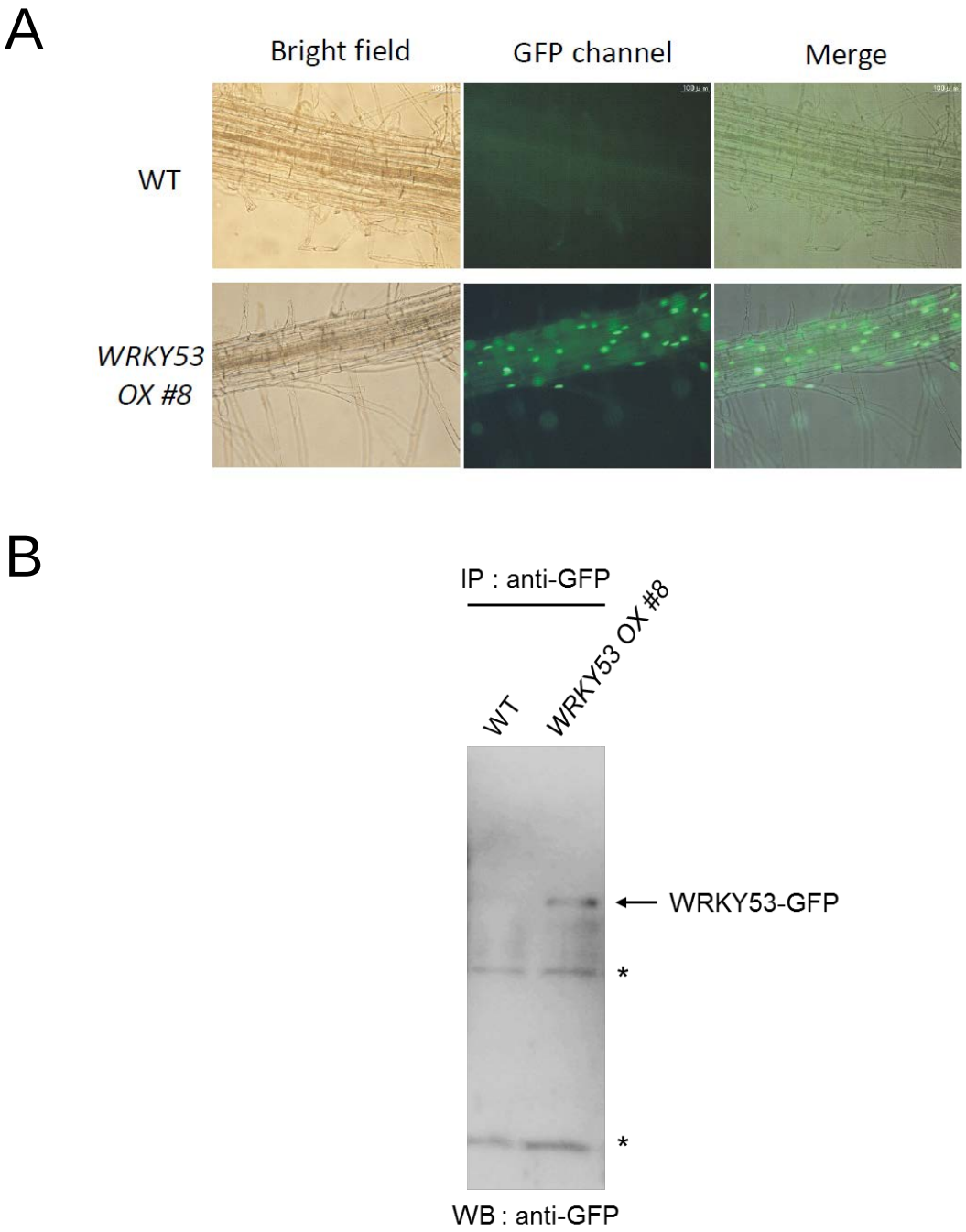

Figure 11. Isolation of transgenic Arabidopsis plants overexpressing WRKY53-GFP.

(A) Observation of GFP fluorescence in the root tissue of wild-type (WT) and *WRKY53-GFP* overexpressing plants (*WRKY53 OX #8*). (B) Immunoprecipitation and immunoblot experiments using anti-GFP in WT and *WRKY53 OX #8* plants.

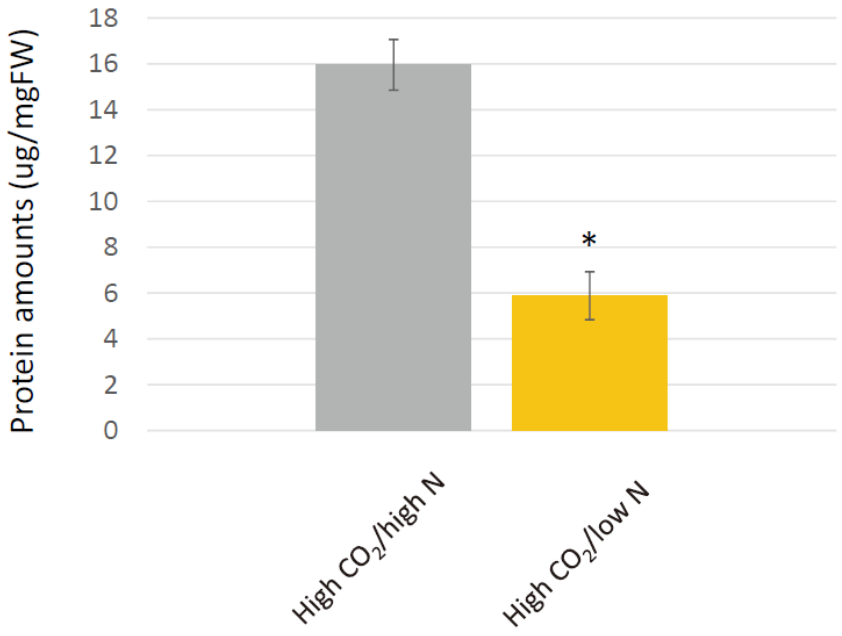

Figure 12. Protein levels in WT Arabidopsis plants.

Protein was extracted from the rosette leaves of WT plants grown in high CO_2/high N or high CO_2/low N condition for 4 weeks after transfer to each condition. Means ± SD of three independent experiments are shown. Asterisk indicates significant differences compared with WT plants grown in high CO_2/high N condition as determined by Student's *t*-test ($p<0.05$).

Chapter II

FLOWRING BHLH 4 functions in flowering regulation in response to limited nitrogen availability in Arabidopsis

Summary

It has been known in agriculture for long time that nitrogen (N) availability affects flowering time. However, the detailed molecular mechanism mediating N-responsive flowering is still unknown. Here, we demonstrate that CONSTANS (CO)-FLOWERING LOCUS T (FT) signaling pathway plays an important role in early flowering induction under limited N condition. We established hydroponic plant culture system and confirmed that Arabidopsis plants showed early flowering phenotype under limited N condition compared to normal N in long days. In this condition, *CO* and *FT* expressions were increased under limited N condition compared to normal N condition. On the other hand, neither early flowering induction nor increase in *FT* expression were observed in a *co* defective mutants under limited N condition. In addition, we found that phosphorylation level of FLOWEING BHLH 4 (FBH4) transcription factor, a direct activator of *CO* expression, was increased in response to limited N treatment. N-responsive early flowering phenotype was partially suppressed in *fbh1/2/3/4* quadruple mutants. Together, our data suggest that N-responsive early flowering is regulated via CO-FT pathway, which might be modulated by phosphorylation of FBH4 in response to N availability.

Introduction

Nitrogen (N) is an essential nutrient to compose major structural component in plants. Therefore, nitrogen availability regulates plant development and affects the amount of crop production (Wang et al., 2012). Phase transition is an important phenomenon in the plant life cycle for own survival and reproduction and largely affected by environmental cues including nitrogen availability (Vidal et al., 2014). Flowering is dynamic phase transition event from vegetative phase to reproductive phase to maximize reproductive success (Castro Marín et al., 2011; Vidal et al., 2014). The importance of relationship between nitrogen availability and flowering time has been known from agricultural aspects. Several studies have reported that flowering time is earlier under limited N condition and later under N-rich condition, and some genes involved in flowering regulation are affected N availability in Arabidopsis (Castro Marín et al., 2011; Kant et al., 2011; Liu et al., 2013; Yuan et al., 2016). However, the molecular signaling pathway mediating flowering in response to N availability is poorly understood.

A large number of factors are involved in flowering regulation. They class as five genetically defined signaling pathways; vernalization, photoperiod, gibberellin, autonomous, and aging pathways and then the pathways are finally integrated into *FLOWERING LOCUS T (FT)*, *SUPPRESSOR OF OVEREXPRESSIION OF CONSTANS1 (SOC1)*, and *LEAFY (LFY)* (Castro Marín et al., 2011; Srikanth and Schmid, 2011; Wellmer and Riechmann, 2010). Castro Marin et al. (2011) demonstrated by mutant analysis that low nitrate signal induces early flowering via a novel signal pathway independent from these known pathways and integrators. However, their study focused on nitrate signal and then did not evaluate nitrogen starvation because glutamine was supplied in all the experimental conditions to avoid influences on amino

acids and protein level (Castro Marín et al., 2011). Another study investigated the expressions of flowering related genes, *FT*, *LFY*, *APETALA1(AP1)*, and *FLOWERING LOCUS C (FLC)* under different nitrogen conditions, and then showed that positive regulators of flowering (*FT, LFY, AP1*) were increased but negative regulator *FLC* was decreased under limited N condition compared to N-rich condition (Kant et al., 2011). Moreover, two studies reported that the expression level of *CONSTANS (CO)*, a key gene of photoperiod pathway, is increased under limited N condition (Liu et al., 2013; Yuan et al., 2016). Yuan et al. (2016) also clarified that *ferredoxin-NADP+-oxidoreductase (FNR1)* and CRY1 played key roles on the up-stream of *CO* expression via changes of NADPH/$NADP^+$ and ATP/AMP ratio and nuclear AMPK activity in flowering regulated by N availability. However, the relation with a further down-stream gene *FT* was not showed, and the molecular mechanism of how *CO* expression is regulated remains unknown.

CO is well known as major positive regulator of *FT* gene expression and then essential in photoperiod pathway (Shim et al., 2017; Song et al., 2013). *CO* gene expression shows diurnal oscillation pattern; lower in morning and early afternoon and higher in evening and night. In the morning to early afternoon, CYCLING DOF FACTOR (CDF) proteins strongly inhibited *CO* expression, and they are degraded by FLAVIN-BINDING, KELCH REPEAT, F-BOX 1 (FKF1)-GIGANTEA (GI) complex in the late afternoon only in long days (Fornara et al., 2009; Imaizumi, 2005; Sawa et al., 2007; Song et al., 2013). In the evening to night, *CO* expression is increased by FLOWERING BHLH transcriptional activators (FBHs) (Ito et al., 2012). Most recently, it was reported that TEOSINTE BRANCHED/CYCLOIDEA/PCF (TCP) transcription factors, in particular TCP4, and PHYTOCHROME AND FLOWERING TIME 1

(PFT1) also activate *CO* expression interacting with FBHs in this time (Kubota et al., 2017; Liu et al., 2017). The repression by CDFs may be strong because the oscillation pattern of *CO* expression was maintained in *FBHs*- or *TCPs*-overexpressing plants (Ito et al., 2012; Kubota et al., 2017; Liu et al., 2017). CO protein is also regulated by several factors (Shim et al., 2017; Song et al., 2013). CO protein only accumulates in the late afternoon in long days. A lot of factors negatively regulate the stability of CO protein in the morning and early afternoon, whereas CO protein is stabilized by FKF1 and phyA in the late afternoon (Lazaro et al., 2015; Shim et al., 2017; Song et al., 2014, 2013, 2012; Valverde, 2004). In the dark, CO protein degraded by COP1-SPA complex, therefore CO function is lower in the dark (Jang et al., 2008; Liu et al., 2008; Sarid-Krebs et al., 2015; Shim et al., 2017). In this study, we examined N-responsive early flowering using hydroponic culture system and transient assay using liquid medium. We then clarified that photoperiod pathway, in particular CO-FT signaling pathway plays an essential role in N-responsive early flowering. Early flowering was observed with promotion of *CO* and *FT* expressions in the evening under low N condition in long days, whereas neither early flowering nor increase in *FT* expression was observed even under low N condition in *co* defective mutant. Moreover, we identified FBH4 as a candidate of novel carbon and/or nitrogen responsive protein by phosphoproteome analysis, and the further analysis revealed that FBH4 was phosphorylated by low N stress treatment. N-responsive early flowering phenotype was partially suppressed in *fbh1/2/3/4* quadruple mutants. In addition, the expression level of *CO* is further increased under low N condition even in *FBH4* overexpressor. Our results demonstrated that N-responsive early flowering is regulated via CO-FT pathway, which might be modulated by phosphorylation of FBH4 in response to N availability.

Materials and Methods

Plant materials and growth conditions

Arabidopsis thaliana ecotype Columbia-0 (Col-0) were regarded as wild-type (WT) in this study. *fbh1/2/3/4 quadruple* mutant (*fbh quadruple*), *co-101*, *ft-2* mutants were prepared as previously described, respectively (Hiraoka et al., 2013; Ito et al., 2012; Takada and Goto, 2003). To generate the *FLAG-FBH4* overexpressing transgenic plant (*FBH4* OX), the full-length *FBH4* cording sequence in Col-0 cDNA was PCR amplified using the primers listed in Table 1. The amplified cDNA was cloned into the pENTR/D-TOPO vector (Invitrogen) and transferred to the pEarleygate202 binary vector (Earley et al., 2006), as described by the manufacturer's protocol (Invitrogen). Constructed vectors were introduced into *Agrobacterium tumefaciens* GV3101 (pMP90) by electroporation, followed by transformation to Arabidopsis using the floral dip method (Clough and Bent, 1998). Sterilized seeds were sown on 10 mM glucose containing MS medium and stratified for 2 days at 4°C. Then, plants were transferred onto rock wool with nitrogen (equal mol/l of NH4NO3 and KNO3) modified liquid 1/5×MS medium (3 mM N or 0.3 mM N) at 10 days after germination for hydroponic culture.

Flowering time experiment

To evaluate of flowering time, plants were grown by hydroponic culture as upper described. Rosette leaf number and the days to flowering were counted when they bolted for 1 cm.

Transient C/N response assay

Plants were grown on modified MS medium (C/N medium) containing 10 mM glucose and 30 mM nitrogen (N) for 2 weeks after germination and then transferred to liquid C/N medium containing 0 or 100 mM glucose and 0.3 or 30 mM N. Plants were harvested 1, 24, or 72 hours after C/N treatment for quantitative RT-PCR analysis.

Phosphoproteome analysis

Col-0 seeds were sown in 1/2×modified MS liquid medium containing 100 mM glucose and 30 mM N in culture flask and grown for 1 week with gently shaking under constant light. Then, they were transferred to control (100 mM glucose and 30 mM N) or stress (200 mM glucose and 0.3 mM N) conditions and grown additional 30 min before collection. Phosphopeptides samples for LC-MS/MS were prepared as follow. Protein extraction from each frozen material, protein digestion with trypsin, and enrichment of phosphopeptides with Ti-HAMMOC were performed in this order, as described previously (Choudhary et al., 2015). LC-MS/MS analysis was performed using An LTQ-Orbitrap XL (Thermo Fisher Scientific) coupled with a Dionex Ultimate3000 pump and an HTC-PAL autosampler (CTC Analytics). Peprides and proteins were identified by database searching using MASCOT server against TAIR10 (http://www.arabidopsis.org/index.jsp). The detailed parameter of LC-MS/MS analysis and calculation of the scores were performed as previously described (Choudhary et al., 2015).

Gene expression analysis

Gene expression was analyzed by qRT-PCR. Total RNA was extracted from

Arabidopsis whole rosette using Trizol-reagent (Invitrogen) and treated with RQ1 RNase-free DNase (Promega), followed by cDNA synthesis using Rever Tra Ace (TOYOBO) and oligo(dT) primer (Promega). qRT-PCR was performed using SYBR premix EX Taq (TaKaRa) with Mx3000P (Agilent Technologies) machine, according to the manufacturer's protocol. *18s rRNA* or *IPP2* was used as internal control for calculating ⊿⊿ Ct. Specific primer sets used for qRT-PCR analysis are listed in Table 1.

FLAG-FBH4 protein enrichment by immunoprecipitation

The crude protein was extracted from 2-week-old *FLAG-FBH4* overexpressing Arabidopsis (400 mg fresh weight) by extraction buffer [50 mM sodium phosphate (pH 7.0), 100 mM NaCl, 10% glycerol, 5 mM EDTA, 0.1% Triton X-100, 0.5% sodium deoxycholate, 10 μM MG132, Complete Protease Inhibitor Cocktail (Roche), and PhosSTOP (Roche)] with homogenization in liquid nitrogen. Extract was mixed with Anti-FLAG M2 Magnetic Beads (Sigma) after elimination of insoluble materials by centrifugation, and then incubated for 1 hour in 4°C with gently mixed using tube rotator. The beads were washed 3 times by wash buffer [50 mM Tris-HCl (pH7.5), 150 mM NaCl, 10% glycerol, 1 mM EDTA, 0.1% Triton X-100]. The beads bound protein was eluted by 150 μg/ml 3×FLAG peptide in wash buffer. The supernatant was mixed with the same amount of 2×SDS sample buffer [62.5 mM Tris, pH 6.8, 2% SDS, 10% Glycerol, 0.2 M DTT, 0.01% BPB], and then incubated for 5 min in 95°C.

Western blotting

To detect FLAG-FBH4 protein, the protein samples were separated by SDS-PAGE using 10% poly-acrylamide gel. In case of the evaluation of FBH4 phosphorylation

level, 50 μM Phos-tag Acrylamide (Wako) and 100 μM $MnCl_2$ was added to 7.5% poly-acrylamide gel. Then, the proteins were transferred from the gels to Immobilon-P PVDF Membranes (Millipore) in blotting buffer [25 mM Tris, 192 mM Glycine, 0.1% SDS, 10% Methanol]. The membrane was blocked for 1 h by 5% skim milk in TBS-T [10 mM Tris-HCl (pH7.5), 150 mM NaCl, 0.1% Tween-20] before antibody reactivity. Anti-FLAG M2 antibody (Sigma) was used as the primary antibody, and anti-mouse IgG HRP-Linked Whole Ab Sheep (GE Healthcare) was used as the secondary antibody. FLAG-tagged proteins were detected by the chemiluminescent using Immobilon Western Chemiluminescent HRP Substrate (Millipore).

Identification of phosphorylation sites on FBH4 by MS analysis

FLAG-FBH4 protein was enriched by immunoprecipitation from *FLAG-FBH4* overexpressing Arabidopsis as upper described. The samples were separated by SDS-PAGE using 10% polyacrylamide gel. The gel was excised after staining by SYPRO Ruby (Lonza, Switzerland) as described in the manufacture's protocol. Then, the peptides materials were prepared for liquid chromatography-tandem mass spectrometry (LC-MS/MS) analysis after in-gel digestion using sequencing grade modified trypsin as described previously (Lu et al., 2016). LC-MS/MS analysis was performed using an EASY-nLC 1000 liquid chromatograph coupled to an Orbitrap Elite Mass Spectrometer (Thermo Scientific, USA). The peptides materials were separated on a nano-capillary column (NTCC-360/75-3-125; Nikkyo Technos, Japan). Protein identification was performed by SEQUEST algorithm embedded in Proteome Discoverer 1.4 software (Thermo Scientific, USA) against TAIR10 (http://www.arabidopsis.org/index.jsp). The detailed parameters were set as described

previously (Lu et al., 2016).

Results

Low N stress induces early flowering

To examine the effect of low N stress for flowering, Growth analysis under different nitrogen (N) conditions was performed using Arabidopsis Col-0 plants. All plants were sown on modified MS medium plates containing 10 mM glucose and 30 mM N and grown for 10 days in long days (16 h light/ 8 h dark) in order to avoid inhibiting the post-germination growth by low N stress. 10-day-old plants were transferred on the rock-wool with N modified liquid 1/5×MS medium, including 3 mM N (normal N) or 0.3 mM N (low N), respectively. As a result, flowering was observed at around 9.4 days after transplanting (total 19.4 days) under low N condition, and at around 14.7 days after transplanting (total 24.7 days) under normal N condition (Figure 1A, B). In addition, rosette leaf number when 1 cm bolting was observed, the general index to measure flowering time, was approximately 11.4 under low N condition and approximately 14.2 under normal N condition (Figure 1C). These results indicate that flowering is induced earlier under low N condition compared to normal N condition.

The phosphorylation level of FBH4 protein is increased by low N stress

FLOWERING BHLH 4 (FBH4) was detected as a candidate of novel carbon and/or nitrogen responsive protein by our phosphoproteome analysis which is carried out to understand the molecular mechanism of the response to carbon/nitrogen nutrient availability focusing on protein phosphorylation. The level of phosphorylated peptides in Col-0 plants were measured and compared with control condition (100 mM glucose

and 30 mM N) and high C/low N stress condition (200 mM glucose and 0.3 mM N) (Figure 2A). Phosphorylated peptides were purified and enriched, and then identified by LC-MS/MS analysis (Figure 2A). As a result of normalized by total peptides amount in each sample, 15 peptides were increased over 2-fold at their phosphorylated level under high C/low N stress condition compared to the normal C/N condition. FBH4 was the one of them. The amount of phosphorylated peptide of FBH4; FRSAPSSVLAAFVDDDK (20-36 amino acids) was up-regulated approximately 2-fold under high C/low N condition compared to the normal C/N condition (Figure 2B).

FBH4 directly binds to *CONSTANS (CO)* promoter and positively regulate *CO* expression (Ito et al., 2012). Therefore, we examined whether *CO* expression was affected or not by high C and low N nutrient condition using transient C/N response assay. Col-0 plants were grown on normal C/N medium containing 10 mM glucose and 30 mM N for 2 weeks and then transferred to each C/N modified MS liquid medium containing 0 mM glucose and 30 mM N (low C/high N), 0 mM glucose and 0.3 mM N (low C/low N), 100 mM glucose and 30 mM N (high C/high N), or 100 mM glucose and 0.3 mM N (high C/low N) in long days. Plants were grown in each C/N modified medium for 72 hours and collected at Zeitgeber time 16 (ZT16). The expression level of *CO* was 1.9-fold in high C/low N compared to low C/high N condition and seemed to be also up-regulated (1.7-fold) in low C/low N conditions although there was no significant difference, whereas no change in high C/high N condition (Figure 3A). By the additional analysis, it was confirmed that *CO* expression level was significantly higher (2.3-fold) in low N condition than high N condition without sugar treatment (Figure 3B). Furthermore, *FLOWERING LOCUS T (FT)*, a very important flowering gene which is positively regulated by CO, was also significantly higher (4.7-fold) under

low N condition than high N condition without sugar treatment (Figure 3C). These results suggest that *CO* and *FT* expressions are induced by low N stress only rather than high C/low N stress.

Since the expression level of *CO* was increased by low N stress, we confirmed the phosphorylation status of FBH4 protein in the same condition. *FLAG-FBH4* overexpressing Arabidopsis plants (*FBH4* OX) were grown and assayed similarly to Col-0 and were collected at 0, 1, or 24 hours after beginning of assay. FLAG-FBH4 protein was purified by immunoprecipitation from the extract, and detected by western blotting with or without 50 mM phos-tag in SDS-PAGE gels (Figure 4A). When phos-tag is contained in the gel, the flow speed of phosphorylated proteins by electrophoresis becomes slower, that is, the band of higher phosphorylated protein was detected in upper position of the gel compared to low phosphorylated ones. In this experiment, all the samples were detected in the same size by normal western blotting (42.8 kDa) whereas the bands of the sample grown in low N stress condition for 24 hours was detected in upper area of the phos-tag contained gel compared to non-treatment one (0 h) (Figure 4A). This result demonstrates that the FBH4 protein is phosphorylated by low N stress.

fbh1/2/3/4 quadruple mutant showed late flowering even under low N condition

To understand further the importance of FBH4 for flowering, phenotypic analysis was carried out focusing on low N-responsive early flowering. FBH transcriptional factors consist of 4 genes (*FBH1, FBH2, FBH3,* and *FBH4*), which are suggested to be functional redundant. Therefore, single knockout mutants of them were not observed any difference about flowering compared to wild-type (Ito et al., 2012). Whereas

fbh1/2/3/4 quadruple mutant [*35S:amiRFBH1-2, fbh2-1, fbh3-1* and *35S:amiRFBH4-3*] (*fbh quadruple*) showed late flowering and over 50% reduction of *CO* expression in dark periods compared to wild-type (Ito et al., 2012). *fbh quadruple* plants were grown by the transplanting hydroponic culture method similarly to Col-0, and evaluated flowering time under normal or low N conditions. Flowering was observed at around 18.2 days after transplanting (total 28.2 days) under 0.3 mM N condition, and at around 20.4 days after transplanting (total 30.4 days) under 3 mM N condition (Figure 1A, B). Rosette leaf number was approximately 14.8 under 0.3 mM N condition and approximately 18.8 under 3 mM N condition (Figure 1C). All of these results showed late flowering compared to Col-0 (Figure 1). These data indicate that late flowering phenotype of *fbh quadruple* was not disappeared even under low N condition although low N sensitivity remains in *fbh quadruple*.

_CO_ and _FT_ expressions are promoted in the evening by low N stress

The diurnal expression patterns of *CO* and its down-stream gene *FT* show the oscillation (Shim et al., 2017; Song et al., 2013). In the morning, both *CO* and *FT* expression levels are low because of being suppressed by negative factors such as CDF proteins whereas relatively higher in the evening and night (Fornara et al., 2009; Song et al., 2013). Even in *FBHs* overexpressing plants, such oscillation pattern was maintained (Ito et al., 2012). We investigated the diurnal expression patterns of *CO* and *FT* under both normal N and low N conditions using Col-0 plants. As a result, the diurnal expression patterns of *CO* and *FT* were maintained even in low N condition (Figure 5A, B). Neither *CO* nor *FT* expressions were increased in low N condition in the morning at ZT4 and ZT8 (Figure 5A, B). In contrast, *CO* and *FT* expressions were

significantly increased in the evening at ZT12 and ZT16 under low N condition compared to normal N condition (*CO* was 2-fold at ZT12 and ZT16, *FT* was 1.5-fold at ZT12 and 5-fold at ZT16) (Figure 5A, B). *CO* expression was also increased but *FT* expression was not increased at ZT0 and ZT20 under low N condition (Figure 5A, B). These results indicate that the highly *CO* and *FT* expressions in the evenings are important for early flower induction under low N condition.

CO and *FT* expressions are further promoted by low N stress in *FBH4* OX

To clarify the contribution of FBH4 to the increase in *CO* expression under low N condition, we examined the expression levels of *CO* and *FT* at ZT16 in long days under both normal and low N conditions using *FBH4* OX. By the effect of *FBH4* overexpression, both *CO* and *FT* expressions were increased approximately 2.2- and 7-fold, respectively, compared to Col-0 under normal N condition, and which were near to that of Col-0 under low N condition (Figure 4B, C). Then, *CO* and *FT* expressions in *FBH4* OX were dramatically increased approximately 2.5- and 3-fold, respectively, under low N condition compared to normal condition (Figure 4B, C). The amount of *FBH4* transcripts was not significantly increased under low N condition (Figure 4D).

Besides *FBH4* OX, the increases in *CO* and *FT* expressions under low N condition remained in *fbh quadruple* (Figure 5C, D), suggesting FBH4 might be kept activity in this mutant because *FBH4* was not loss-of-function but decreased to half by knock down using RNAi (Ito et al., 2012). Whereas, the expression level of *CO* in *fbh quadruple* was significantly decreased approximately 0.6- or 0.75-fold compared to Col-0 under each N condition, respectively (Figure. 5C). These results suggest that post-transcriptional regulation of FBH4, in particular protein phosphorylation might be

important to activate *CO* and *FT* expressions under low N stress condition.

_FT_ expression is not promoted under low N condition when CO is defective

CO is a positive transcriptional regulator of *FT* and has very strong influence on the activation of *FT* expression particularly in long days. However, *FT* expression is controlled by a lot of factors both positively and negatively. Thus, it could not be concluded that the increase in *FT* expressions depend on only the increase in *CO* expression under low N stress condition. Therefore, we investigated *FT* expression in *co-101*, a *co* defective mutant, under low N condition. As a result, the expression level of *FT* at ZT16 under long days was dramatically decreased less than 0.01-fold regardless of N availability (Figure 5D).

CO protein was degraded by COP1-SPAs complex in the dark (Jang et al., 2008; Liu et al., 2008; Sarid-Krebs et al., 2015). Thus, even if *CO* expression is high in the dark period, *FT* expression should not be increased depending on CO inactivity. In practice, *CO* expression was increased but *FT* expression was not increased under low N condition compared to normal N condition at ZT0 and ZT20 (Figure 5A, B). This result also supports that the increase in *FT* expression by low N stress may depend on increased CO activity. Together, these results demonstrate that CO activity is very important for the increase in *FT* expression under low N stress condition.

Early flowering is not induced under low N condition when CO is defective

CO can act as positive regulator of *FT* only in long days because *CO* expression is induced after noon but CO protein is degraded in the dark (Shim et al., 2017; Song et al., 2013). As a result of the growth analysis by hydroponic method in short days, flowering

time was not different between under normal N and low N conditions (Figure 6A). On the other hand, rosette leaf number at flowering was much less under low N condition than normal N condition (Figure 6B). However, leaf number might not be an appropriate index because growth speed and limit should be much different between normal and low N conditions in such long term growth. In addition to abolishing the promotion of *FT* expression by low N stress, flowering time of *co-101* mutant showed any difference between low N and normal N conditions even in long days although over 30 days later than Col-0 (Figure 7A). Whereas, *ft* defective mutant *ft-2* showed early flowering under low N condition, suggesting that some factors may have redundant function as *FT*. For instance, *TWIN SISTER OF FT (TSF)* is known as a flowering activator redundantly with *FT* (Yamaguchi et al., 2005). However, the flowering time *of ft-2* was more than 3 weeks later than Col-0 even under low N stress condition (Figure 7A). Rosette leaf numbers of *co-101* and *ft-2* were much higher approximately 4- and 2-fold compared to Col-0 under normal N and low N conditions, respectively (Figure 7B, C), which are consistent with bolting days. Similarly to short days experiment, however, rosette leaf number might not be an appropriate index of flowering time to compare between normal and low N conditions because of different growth speed and limit (Figure 8). Together with the results of *FT* expressions in CO defective conditions, these results indicate that the CO activity is essential for early flowering induction under low N condition.

Several sites in FBH4 protein are phosphorylated by low N stress

Suggesting from our results, FBH4 protein phosphorylation and the increase in its down-stream gene *CO* expression were induced by low N stress. The remaining issue is

functional significance of the protein phosphorylation of FBH4. FBH4 was detected by phosphoproteome analysis as the amount of its phosphorylated peptide; FRSAPSSVLAAFVDDDK (20-36 amino acids) was increased by high C/low N stress treatment (Figure 2). However, several bands were detected in the result of western blotting with phos-tag contained SDS-PAGE when phosphorylation status of FLAG-FBH4 protein confirmed using *FBH4* OX with low N stress treatment for 24 h (Figure 4A). This implies that several sites may be phosphorylated in FBH4 protein. In order to clarify further phosphorylation sites in FBH4, we carried out IP-MS analysis using *FLAG-FBH4* overexpressing plants. Immunoprecipitated FLAG-FBH4 protein samples were prepared by the same conditions and methods as phosphorylation check by western blotting (Figure 4A). After confirming of the phosphorylation by low N stress condition, the samples were prepared for LC-MS/MS analysis with in gel trypsin digestion. LC-MS/MS analysis was performed using an EASY-nLC 1000 liquid chromatograph coupled to an Orbitrap Elite Mass Spectrometer (Thermo Scientific, USA) and analyzed by SEQUEST algorithm embedded in Proteome Discoverer 1.4 software (Thermo Scientific, USA) against TAIR10. Then, several phosphorylated peptides were detected although full length of peptides was not covered, unfortunately (Figure 9). Only S251 was detected as phosphorylation site in all conditions (Figure 9). S22 and S60 were detected in 1 h and 24 h, whereas not detected in 0 h (Figure 9). S257 was detected only in 24 h (Figure 9). These phosphorylation sites are candidates which might be important for FBH4 function in low N stress condition.

Discussion

CO-FT pathway is essential for early flowering induction by low N stress

It has been well known that nitrogen availability affect flowering time in many plants at places of agriculture. In this study, we established the hydroponic growth condition using Arabidopsis to investigate flowering in response to nitrogen availability, that is, the growth condition that early flowering was observed under low N condition compared to normal N condition in Col-0 plant (Figure 1). In addition to early flowering phenotype, *CO* and *FT* expressions were increased under low N condition compared to normal N condition in the evening in long days. (Figure 5A, B). *CO* and *FT* are key genes of photoperiod pathway which plays central role in flowering induction in response to long days in Arabidopsis (Shim et al., 2017; Song et al., 2013). This pathway cannot induce flowering in short days. Then, low N-responsive early flowering was also not observed in short days (Figure 6A).

We identified that protein phosphorylation level of FBH4 was increased by high C/low N stress using phosphoproteome analysis (Figure 2). FBH4 belongs to FBH transcription factors which positively regulate *CO* expression via direct binding to *CO* promoter (Ito et al., 2012). Although the increase in FBH4 phosphorylation was first detected by high C/low N stress assay, further analysis revealed that low N stress exclusively promotes FBH4 phosphorylation and *CO* and *FT* expressions (Figures 3 and 4A). These results suggest that phosphorylation of FBH4 might be a trigger for the increase in *CO* expression, and which might also influence on the increase in *FT* expression under low N stress condition.

Although the both *CO* and *FT* expressions were increased under low N stress condition, it might not be true that the increased CO activity only causes the increase in

FT expression. Actually, CO positively regulates the expression of *FT* directly with strong contribution (Shim et al., 2017; Song et al., 2013). However, the *FT* is the most important central factor of flowering induction, and a lot of factors are involved in the regulation of *FT* expression (Shim and Imaizumi, 2015; Song et al., 2013; Turck et al., 2008). The CO induces the *FT* expression only in the evening in long days when wild-type plants grown in preferable environment condition, because *CO* expression is inhibited in the morning and early afternoon and CO protein is degraded in the morning and night (Shim and Imaizumi, 2015; Song et al., 2013). Our expression analysis using Col-0 plants showed that the expression level of *CO* was increased at ZT0, ZT12, ZT16, and ZT20, whereas the expression level of *FT* was increased at ZT12 and ZT16 but not increased at ZT0 and ZT20 under low N condition compared to normal N condition in long days (Figure 5A, B). Contrary to the increase in *CO* expression, the amount of CO protein might not be increased at ZT0 and ZT20 because of its protein instability in the dark. This may be the reason why *FT* expression level was not increased at ZT0 and ZT20 even under low N condition. These results imply that *FT* expression was not changed by N availability in CO defective condition.

Furthermore, hydroponic culture experiment using *co* defective mutant, *co-101*, showed that neither the increase in *FT* expression nor early flowering were observed in c*o-101* grown under low N condition in long days (Figures 5D and 7A). Taken together, our results indicate that CO plays an essential role in the increase in *FT* expression and induction of low N-responsive early flowering.

Contrary to *co-101*, *ft* defective mutant, *ft-2*, showed early flowering grown under low N condition compared to normal N condition, although it was much later than Col-0 (Figure 7). This suggest that redundant factors such as *TSF*, the closest homolog of *FT*

and also regulated by CO, remained and might play a role in the mutant (Yamaguchi et al., 2005).

FBH4 functions in early flowering induction by low N stress

The increase in *CO* expression is a key phenomenon for early flowering induction by low N stress. Besides our results, the increase in *CO* expression by growing under limited N condition was also reported from other studies (Liu et al., 2013; Yuan et al., 2016). However, the molecular mechanism of how *CO* expression is increased by low N stress remains unknown. We clarified that FBH4, a positive regulator of *CO* expression, was phosphorylated by low N stress (Figures 2 and 4A), and suggested that the FBH4 plays a critical role in the increase in *CO* expression by low N stress. Therefore, we analyzed using *fbh quadruple* and *FBH4* OX plants to verify the hypothesis. *fbh quadruple* showed later flowering compared to Col-0 both under normal N and low N condition (Figure 1A). In addition, the expression level of *CO* in *fbh quadruple* is lower compared to that in Col-0 under both N condition (Figure 5C). Whereas early flowering induction and the increase in *CO* expression by low N remained in the mutant (Figures 1 and 5C), suggesting that post-transcriptional effect such as protein phosphorylation should remained because *FBH4* expression was not loss-of-function but decreased (knock down) in *fbh quadruple*. However, these results demonstrate that low N-responsive early flowering phenotype was partially suppressed in *fbh quadruple* at least. *CO* and *FT* expressions were much higher in *FBH4* OX plants than in Col-0 and those amounts under normal N were similar to Col-0 under low N at ZT16 on 18th day in long days (Figures 4B, C). Moreover, *CO* and *FT* expressions in *FBH4* OX were further promoted under low N condition without the increase in *FBH4* transcripts

(Figures 4B-D). These results imply that post-transcriptional regulation of FBH4 might be important for the increase in *CO* expression. The post-transcriptional regulation might be phosphorylation of FBH4 protein. Taken together, our data suggest that phosphorylation of FBH4 might be important for the modulation of *CO* expression and flowering regulation in response to N availability.

The physiological meaning of FBH4 phosphorylation

It is important to elucidate the meaning of FBH4 phosphorylation by low N stress. Our western blotting analysis with phos-tag contained SDS-PAGE indicated that several sites of FBH4 protein are phosphorylated by low N stress (Figure 4A). To identify phosphorylation sites in FBH4 protein, we carried out IP-MS analysis using *FLAG-FBH4* overexpressing Arabidopsis. As a result, several phosphorylated peptides were detected. S251 was detected in all samples regardless of N condition (Figures 9). S22, S60, and S257 were detected in the samples exposed low N condition, whereas not detected in non N treatment sample (Figures 9). Although these phosphorylated sites of FBH4 were identified, the meaning of them was not clarified. Recently, it was reported that FBH3 (AKS1), the nearest homolog of FBH4, was inhibited binding to DNA and activation of *KAT1* expression in guard cell caused by owns phosphorylation (Takahashi et al., 2016). The one of the phosphorylation site in FBH3 corresponds with S251 of FBH4 sequence, and the phosphorylation of this site contributes to inhibit dimerization of FBH3 and its activity (Takahashi et al., 2016). Although S251 phosphorylation was also detected in our experiment, it may not conflict because this site was not specific in samples exposed low N condition. Since S22, S60, and S257 are specific in samples exposed low N condition, they might be more important candidates

to modulate FBH4 activity. In addition, it is possible that further phosphorylated sites might exist in non-detected area of FBH4 protein in our experiment.

Recently, TCP transcription factors and PFT1 were identified as positive regulator of *CO* expression (Kubota et al., 2017, Liu et al., 2017). Moreover, these directly interact with FBHs and co-activate *CO* expression (Liu et al., 2017). Thus, it is important to clarify the detailed relationship among FBHs, TCPs, and PFT1. Furthermore, the phosphorylations of FBH1, FBH2, and FBH3 have not been evaluated although they act redundant to regulate *CO* expression and FBH3 is known the importance of its phosphorylation (Takahashi et al., 2016). Besides FBH4, it should be also analyzed that whether other FBHs induced phosphorylation by low N stress or not.

References

Castro Marín, I., Loef, I., Bartetzko, L., Searle, I., Coupland, G., Stitt, M., et al. (2011) Nitrate regulates floral induction in Arabidopsis, acting independently of light, gibberellin and autonomous pathways. *Planta*. 233: 539–52.

Choudhary, M.K., Nomura, Y., Wang, L., Nakagami, H., and Somers, D.E. (2015) Quantitative Circadian Phosphoproteomic Analysis of Arabidopsis Reveals Extensive Clock Control of Key Components in Physiological, Metabolic, and Signaling Pathways. *Mol Cell Proteomics*. 14: 2243–2260.

Clough, S.J., and Bent, A.F. (1998) Floral dip: A simplified method for Agrobacterium-mediated transformation of Arabidopsis thaliana. *Plant J*. 16: 735–743.

Earley, K.W., Haag, J.R., Pontes, O., Opper, K., Juehne, T., Song, K., et al. (2006) Gateway-compatible vectors for plant functional genomics and proteomics. *Plant J*.

45: 616–629.

Fornara, F., Panigrahi, K.C.S., Gissot, L., Sauerbrunn, N., Rühl, M., Jarillo, J. a, et al. (2009) Arabidopsis DOF transcription factors act redundantly to reduce CONSTANS expression and are essential for a photoperiodic flowering response. *Dev Cell*. 17: 75–86.

Hiraoka, K., Yamaguchi, A., Abe, M., and Araki, T. (2013) The florigen genes FT and TSF modulate lateral shoot outgrowth in arabidopsis thaliana. *Plant Cell Physiol*. 54: 352–368.

Imaizumi, T. (2005) FKF1 F-Box Protein Mediates Cyclic Degradation of a Repressor of CONSTANS in Arabidopsis. *Science (80-).* 309: 293–297.

Ito, S., Song, Y.H., Josephson-Day, a. R., Miller, R.J., Breton, G., Olmstead, R.G., et al. (2012) FLOWERING BHLH transcriptional activators control expression of the photoperiodic flowering regulator CONSTANS in Arabidopsis. *Proc Natl Acad Sci*. 109: 3582–3587.

Jang, S., Marchal, V., Panigrahi, K.C.S., Wenkel, S., Soppe, W., Deng, X.W., et al. (2008) Arabidopsis COP1 shapes the temporal pattern of CO accumulation conferring a photoperiodic flowering response. *EMBO J*. 27: 1277–1288.

Kant, S., Peng, M., and Rothstein, S.J. (2011) Genetic regulation by NLA and microRNA827 for maintaining nitrate-dependent phosphate homeostasis in arabidopsis. *PLoS Genet*. 7: e1002021.

Kubota, A., Ito, S., Shim, J.S., Johnson, R.S., Song, Y.H., Breton, G., et al. (2017) TCP4-dependent induction of CONSTANS transcription requires GIGANTEA in photoperiodic flowering in Arabidopsis, PLoS Genetics.

Lazaro, A., Mouriz, A., Piñeiro, M., and Jarillo, J.A. (2015) Red Light-Mediated

Degradation of CONSTANS by the E3 Ubiquitin Ligase HOS1 Regulates Photoperiodic Flowering in Arabidopsis. *Plant Cell*. 27: 2437–2454.

Liu, J., Cheng, X., Liu, P., Li, D., Chen, T., Gu, X., et al. (2017) MicroRNA319-regulated TCPs interact with FBHs and PFT1 to activate CO transcription and control flowering time in Arabidopsis. *PLoS Genet*. 13: 1–22.

Liu, L.-J., Zhang, Y.-C., Li, Q.-H., Sang, Y., Mao, J., Lian, H.-L., et al. (2008) COP1-Mediated Ubiquitination of CONSTANS Is Implicated in Cryptochrome Regulation of Flowering in Arabidopsis. *Plant Cell Online*. 20: 292–306.

Liu, T., Li, Y., Ren, J., Qian, Y., Yang, X., Duan, W., et al. (2013) Nitrate or NaCl regulates floral induction in Arabidopsis thaliana. *Biologia (Bratisl)*. 68.

Lu, Y., Yasuda, S., Li, X., Fukao, Y., Tohge, T., Fernie, A.R., et al. (2016) Characterization of ubiquitin ligase SlATL31 and proteomic analysis of 14-3-3 targets in tomato fruit tissue (Solanum lycopersicum L.). *J Proteomics*. 143: 254–264.

Sarid-Krebs, L., Panigrahi, K.C.S., Fornara, F., Takahashi, Y., Hayama, R., Jang, S., et al. (2015) Phosphorylation of CONSTANS and its COP1-dependent degradation during photoperiodic flowering of Arabidopsis. *Plant J*. 84: 451–463.

Sawa, M., Nusinow, D. a, Kay, S. a, and Imaizumi, T. (2007) FKF1 and GIGANTEA complex formation is required for day-length measurement in Arabidopsis. *Science*. 318: 261–5.

Shim, J.S., and Imaizumi, T. (2015) Circadian clock and photoperiodic response in arabidopsis: From seasonal flowering to redox homeostasis. *Biochemistry*. 54: 157–170.

Shim, J.S., Kubota, A., and Imaizumi, T. (2017) Circadian Clock and Photoperiodic

Flowering in Arabidopsis: CONSTANS Is a Hub for Signal Integration. *Plant Physiol*. 173: 5–15.

Song, Y.H., Estrada, D.A., Johnson, R.S., Kim, S.K., Lee, S.Y., MacCoss, M.J., et al. (2014) Distinct roles of FKF1, GIGANTEA, and ZEITLUPE proteins in the regulation of CONSTANS stability in *Arabidopsis* photoperiodic flowering. *Proc Natl Acad Sci*. 111: 17672–17677.

Song, Y.H., Ito, S., and Imaizumi, T. (2013) Flowering time regulation: Photoperiod- and temperature-sensing in leaves. *Trends Plant Sci*. 18: 575–583.

Song, Y.H., Smith, R.W., To, B.J., Millar, A.J., and Imaizumi, T. (2012) FKF1 conveys timing information for CONSTANS stabilization in photoperiodic flowering. *Science*. 336: 1045–9.

Srikanth, A., and Schmid, M. (2011) Regulation of flowering time: all roads lead to Rome. *Cell Mol Life Sci*. 68: 2013–37.

Takada, S., and Goto, K. (2003) Terminal flower2, an Arabidopsis homolog of heterochromatin protein1, counteracts the activation of flowering locus T by constans in the vascular tissues of leaves to regulate flowering time. *Plant Cell*. 15: 2856–65.

Takahashi, Y., Kinoshita, T., Matsumoto, M., and Shimazaki, K.I. (2016) Inhibition of the Arabidopsis bHLH transcription factor by monomerization through abscisic acid-induced phosphorylation. *Plant J*. 87: 559–567.

Turck, F., Fornara, F., and Coupland, G. (2008) Regulation and Identity of Florigen: FLOWERING LOCUS T Moves Center Stage. *Annu Rev Plant Biol*. 59: 573–594.

Valverde, F. (2004) Photoreceptor Regulation of CONSTANS Protein in Photoperiodic Flowering. *Science (80-)*. 303: 1003–1006.

Vidal, E.A., Moyano, T.C., Canales, J., and Gutiérrez, R.A. (2014) Nitrogen control of developmental phase transitions in Arabidopsis thaliana. *J Exp Bot*. 65: 5611–5618.

Wang, Y.-Y., Hsu, P.-K., and Tsay, Y.-F. (2012) Uptake, allocation and signaling of nitrate. *Trends Plant Sci*. 17: 458–67.

Wellmer, F., and Riechmann, J.L. (2010) Gene networks controlling the initiation of flower development. *Trends Genet*. 26: 519–27.

Yamaguchi, A., Kobayashi, Y., Goto, K., Abe, M., and Araki, T. (2005) TWIN SISTER of FT (TSF) acts as a floral pathway integrator redundantly with FT. *Plant Cell Physiol*. 46: 1175–1189.

Yuan, S., Zhang, Z.-W., Zheng, C., Zhao, Z.-Y., Wang, Y., Feng, L.-Y., et al. (2016) *Arabidopsis* cryptochrome 1 functions in nitrogen regulation of flowering. *Proc Natl Acad Sci*. 113: 7661–7666.

Table and Figures

Table 1. List of primers used for PCR.

Gene	Sequence (5'→3')
Gene expression analysis	
18S rRNA	CGGCTACCACATCCAAGGAA
	GCTGGAATTACCGCGGCT
IPP2	CATGGTTCAGATTGGTGGTG
	GATGTTCAGAGTTTGTGGATGG
CO	CTACAACGACAATGGTTCCATTAAC
	CAGGGTCAGGTTGTTGC
FT	CTGGAACAACCTTTGGCAAT
	TACACTGTTTGCCTGCCAAG
FBH4	ATCCTCACTTAAAAGAGAAGCCGAG
	TGTAGCTGAAGATACTTATCCACTG
Construction of plasmid	
FBH4 full length of CDS	CACCATGGATTCAAATAATCATCTCTAC
	CTATATTGACTTCTTCTCCTTGTTCATA

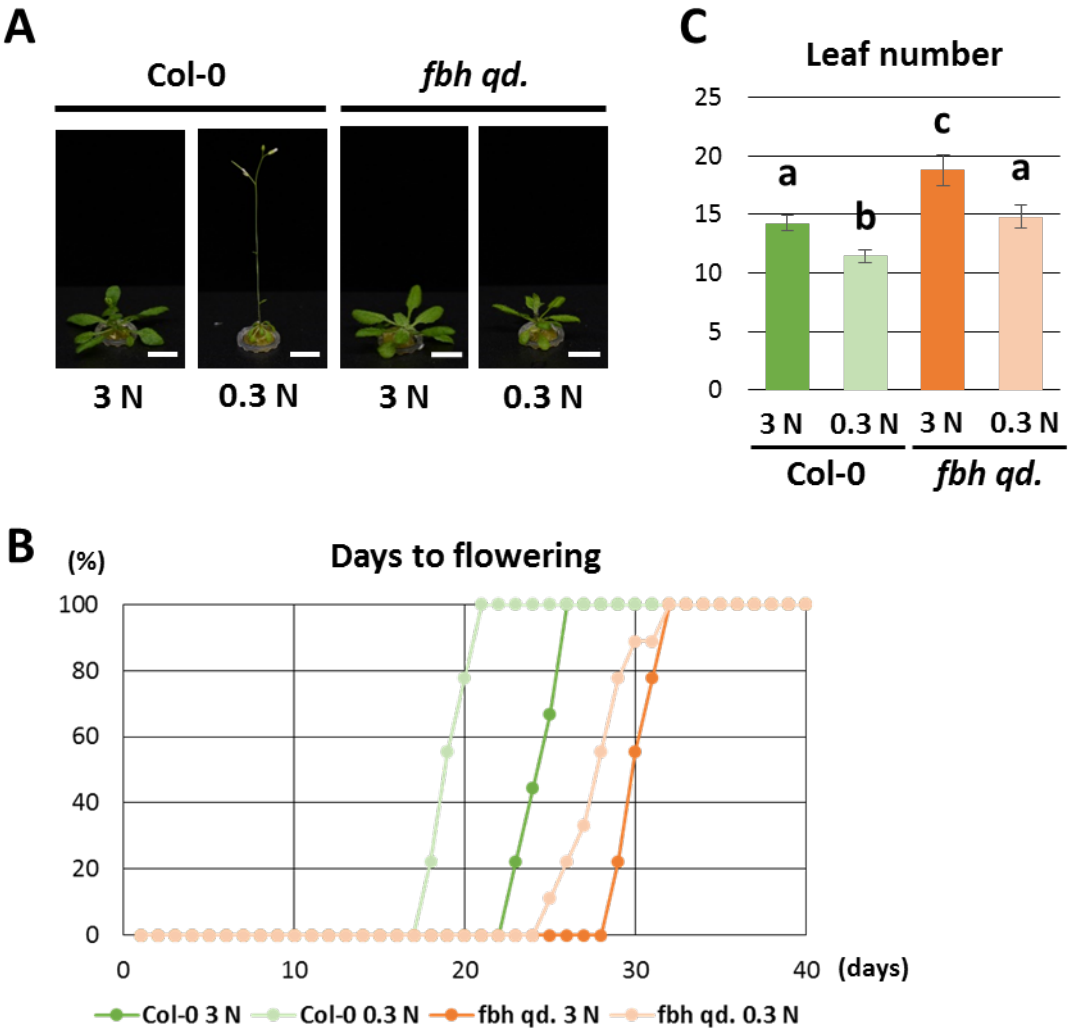

Figure 1. Low nitrogen condition induced early flowering in long days.

Wild-type Arabidopsis (Col-0) and *fbh1/2/3/4 quadruple* mutant (*fbh qd.*) were grown by hydroponic culture system including 3 mM nitrogen (3 N) or 0.3 mM nitrogen (0.3 N) under long days (16 h light/8 h dark). (A) Pictures of 25 day-old plants. Bars indicate 1 cm (B) Days to flowering was shown by the rates of over 1 cm bolting at each day. (C) Rosette leaf number at 1 cm bolting time. n = 9; error bars indicate SD with the same letter are not significantly different from one another (ANOVA + Tukey HSD, $P < 0.05$).

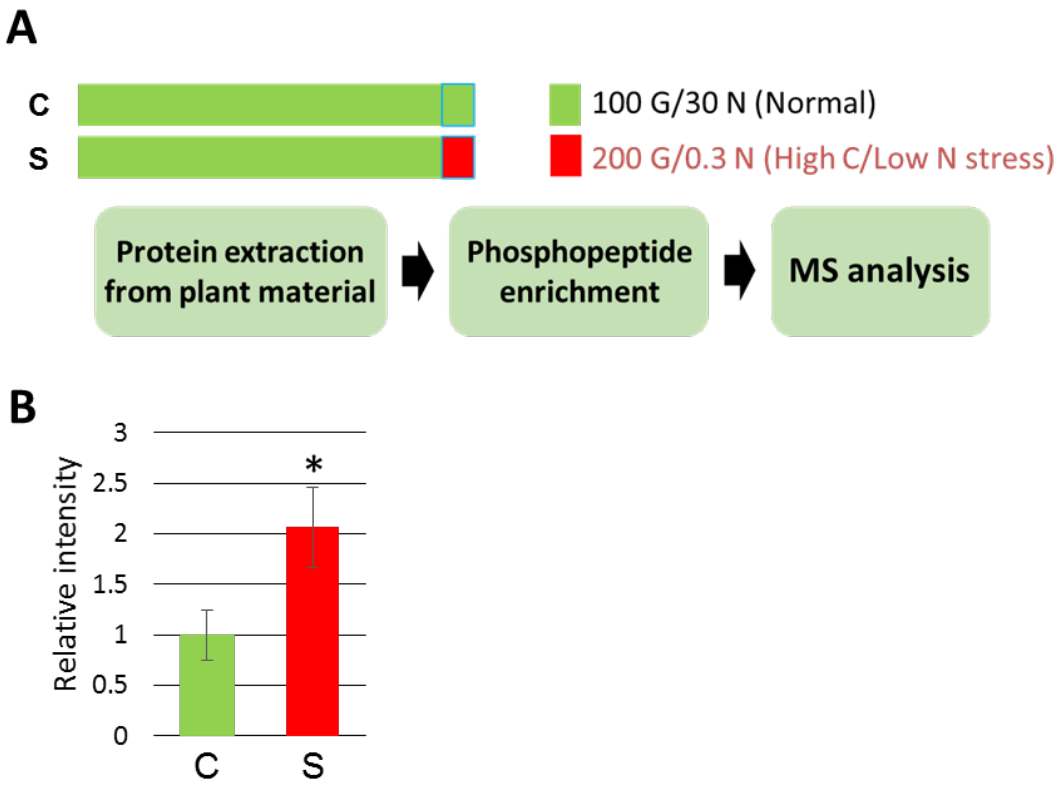

Figure 2. FBH4 was detected as a C/N responsive protein by phosphoproteome.

(A) The scheme of phosphoproteome analysis to identify C/N responsive protein. Col-0 plants were grown in 1/2×modified MS liquid medium containing 100 mM glucose (G) and 30 mM nitrogen (N) for 1 week under constant light, and then transferred to control (C; 100 mM glucose and 30 mM nitrogen, light green) or stress (S; 200 mM glucose and 0.3 mM nitrogen, red) conditions and grown additional 30 min before collection. Phosphorylated proteins were identified by LC-MS/MS analysis after enrichment of phosphopeptides from crude extract. (B) Relative intensity of the detected phosphorylated peptide of FBH4 by LC-MS/MS analysis. Relative intensity was produced by normalization using total peptides amount. C and S mean control and stress conditions, respectively. Means±SD of four independent experiments are shown An asterisk indicates significant difference. *$p < 0.05$ by Student's *t*-test.

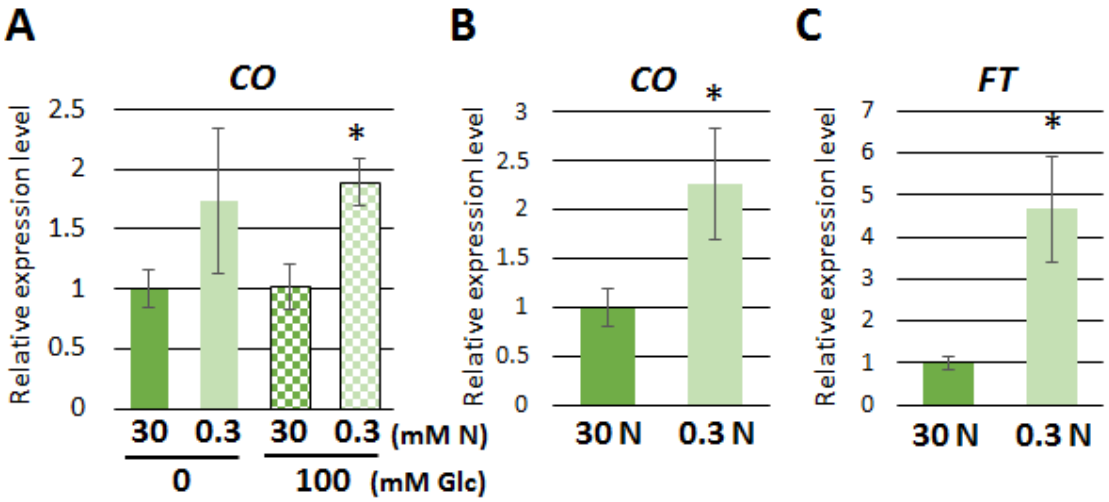

Figure 3. *CO* and *FT* expressions in response to glucose and nitrogen.

Relative expression levels of *CO* and *FT* in Col-0 plants were analyzed by qRT-PCR. Plants were assayed by modified MS liquid medium containing 0 or 100 mM glucose (Glc) and 0.3 or 30 mM nitrogen (N). 17-day-old plants were harvested at ZT16 after 3 days beginning of transfer to each liquid medium. (A) Relative expression level of *CO* under four C/N conditions. (B), (C) Relative expression levels of *CO* and *FT* under two N conditions without glucose (0 mM Glc). Relative expression level was produced from $\Delta\Delta$ Ct. by normalization using *18S rRNA*. Means $\pm$ SD of three independent experiments are shown An asterisk indicates significant difference. *p < 0.05, by Dunnet *t*-test (A), Student's *t*-test (B) and (C).

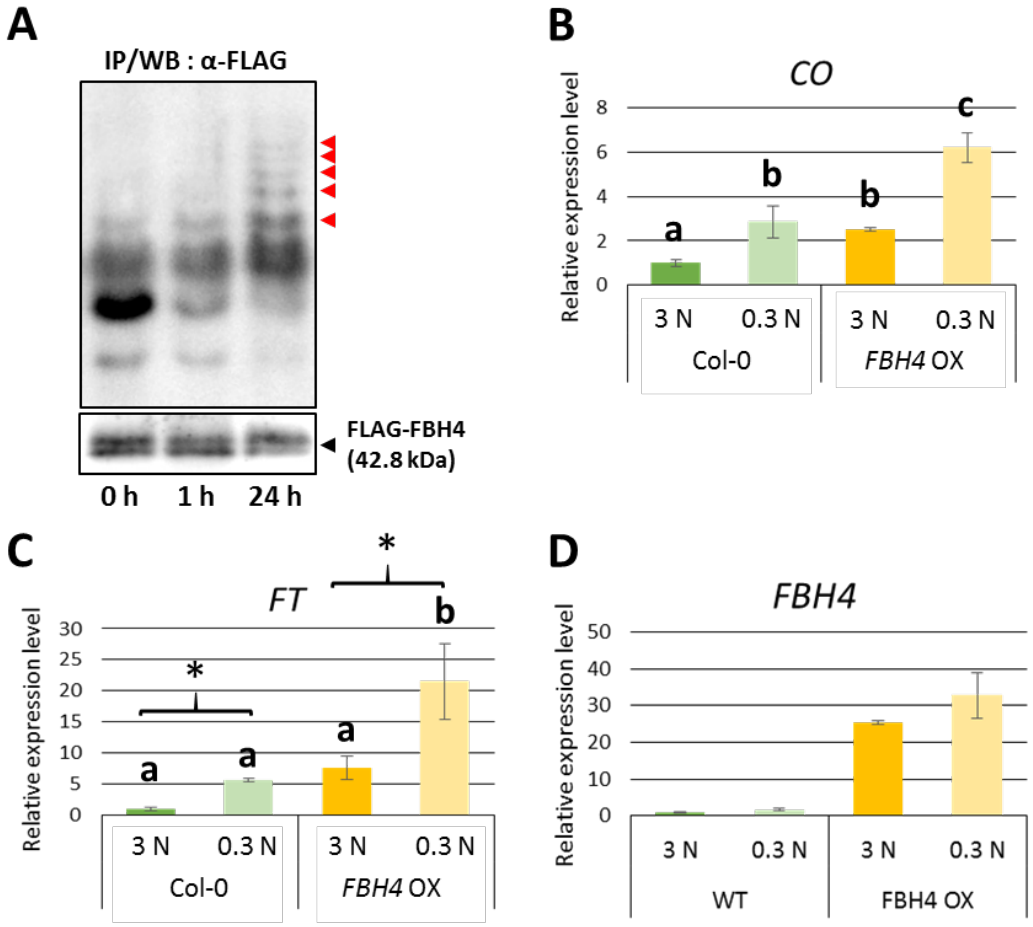

Figure 4. FBH4 phosphorylation level was increased by low nitrogen stress.

(A) FBH4 phosphorylation status was evaluated by western blotting with phos-tag contained SDS-PAGE using immunoprecipitation samples from the extract of FLAG-FBH4 overexpressed Arabidopsis. 14-day-old plants grown on MS medium in long days were transferred modified MS liquid medium containing 30 mM nitrogen (30 N) three days before collection, and then additional transfer into 0.3 mM N (0.3 N) condition at 1 or 24 h before collection, or no transfer (0 h). Plants were harvested at ZT13. Upper panel showed phos-tag contained and lower panel showed normal SDS-PAGE with western blotting results, respectively. Red-triangles indicate high level of phosphorylated FLAG-FBH4. (B-D) Relative expression levels of *CO*, *FT*, and *FBH4* in Col-0 and *FBH4* OX plants were analyzed by qRT-PCR. Plants were grown by hydroponic culture under 3 mM N (3 N) and 0.3 mM N (0.3 N) in long days. mRNA

was extracted from whole rosette of 18-day-old plants collected at ZT16. Relative expression level was produced from $\Delta\Delta$ Ct. by normalization using *IPP2*. n = 4; error bars indicate SD with the same letter are not significantly different from one another (ANOVA + Tukey HSD, $P < 0.05$). An asterisk indicates significant difference between two conditions, $*p < 0.05$ by Student's *t*-test.

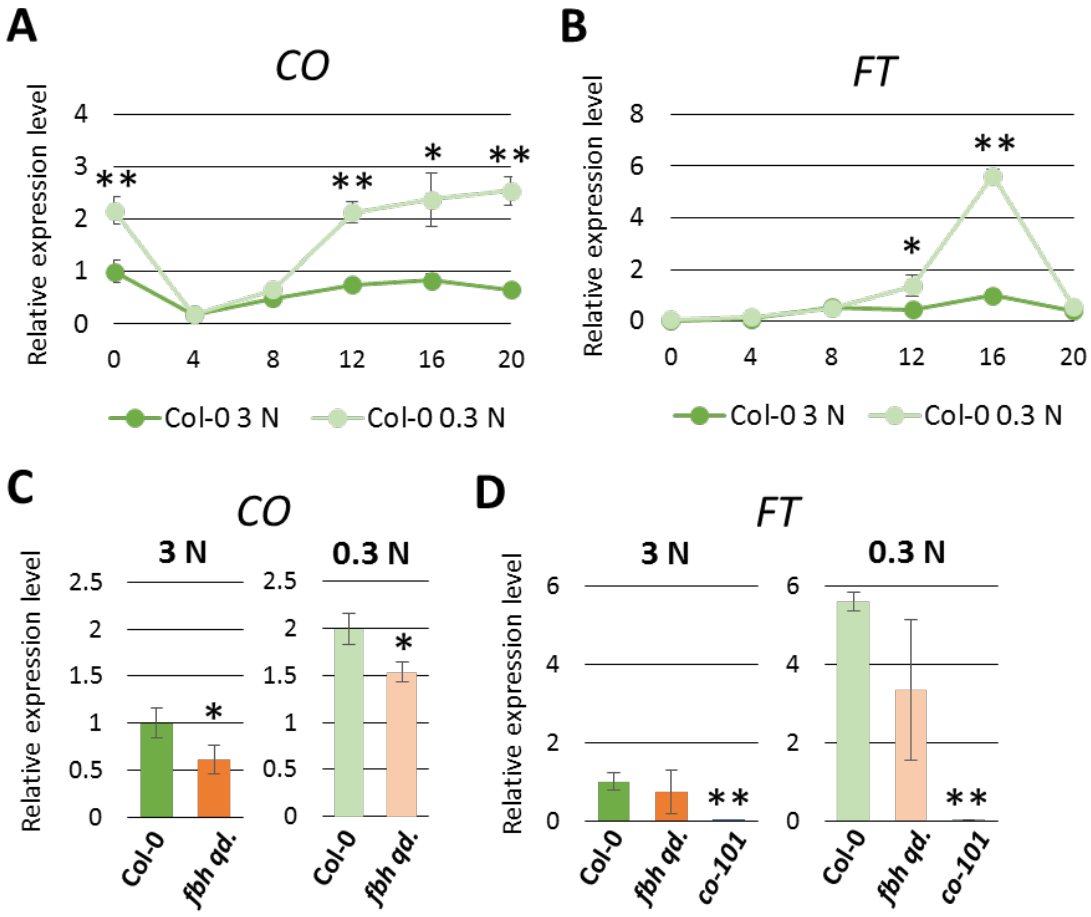

Figure 5. Diurnal rhythm of *FT* and *CO* expression under normal N and low N conditions in Col-0 and the comparison in mutants at ZT16.

Relative expression levels of *CO* and *FT* were analyzed by qRT-PCR. Plants were grown by hydroponic culture under 3 mM nitrogen (3 N) and 0.3 mM N (0.3 N) in long days. (A, B) mRNA was extracted from whole rosette of 18-day-old Col-0 plants collected at ZT0, 4, 8, 12, 16, and 20. (C, D) mRNA was extracted from whole rosette of 18-day-old Col-0, *fbh quadruple* (*fbh qd.*), and *co-101* collected at ZT16. Relative expression level was produced from $\Delta\Delta$ Ct. by normalization using *IPP2*. n = 4; error bars indicate SD. Asterisks indicate significant difference. *p < 0.05, **p < 0.01 by Student's *t*-test (A-C) , Dunnet *t*-test (D)

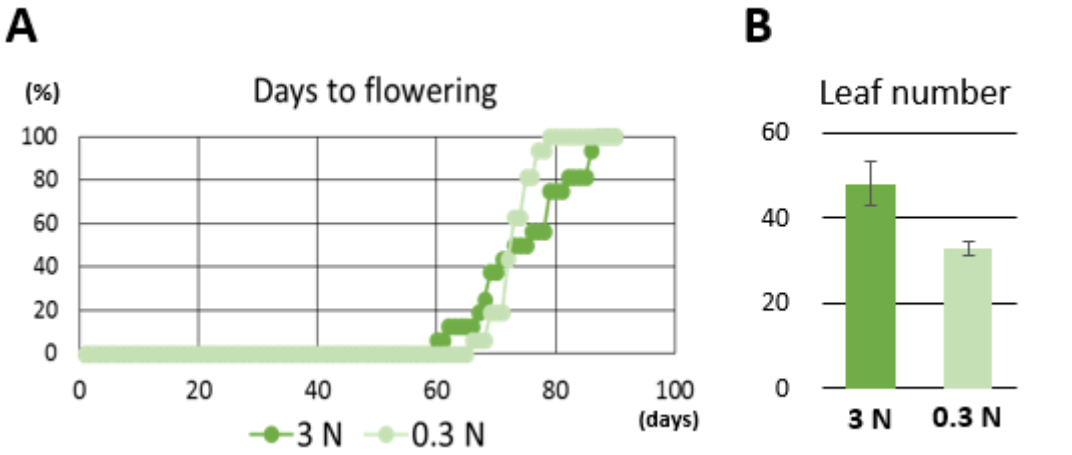

Figure 6. Low nitrogen condition did not induce early flowering in short days.
Col-0 plants were grown by hydroponic culture system including 3 mM nitrogen (3 N) or 0.3 mM nitrogen (0.3 N) under long days (16 h light/8 h dark). (A) Days to flowering was shown by the rates of over 1 cm bolting at each day. (B) Rosette leaf number at 1 cm bolting time. n = 9; error bars indicate SD.

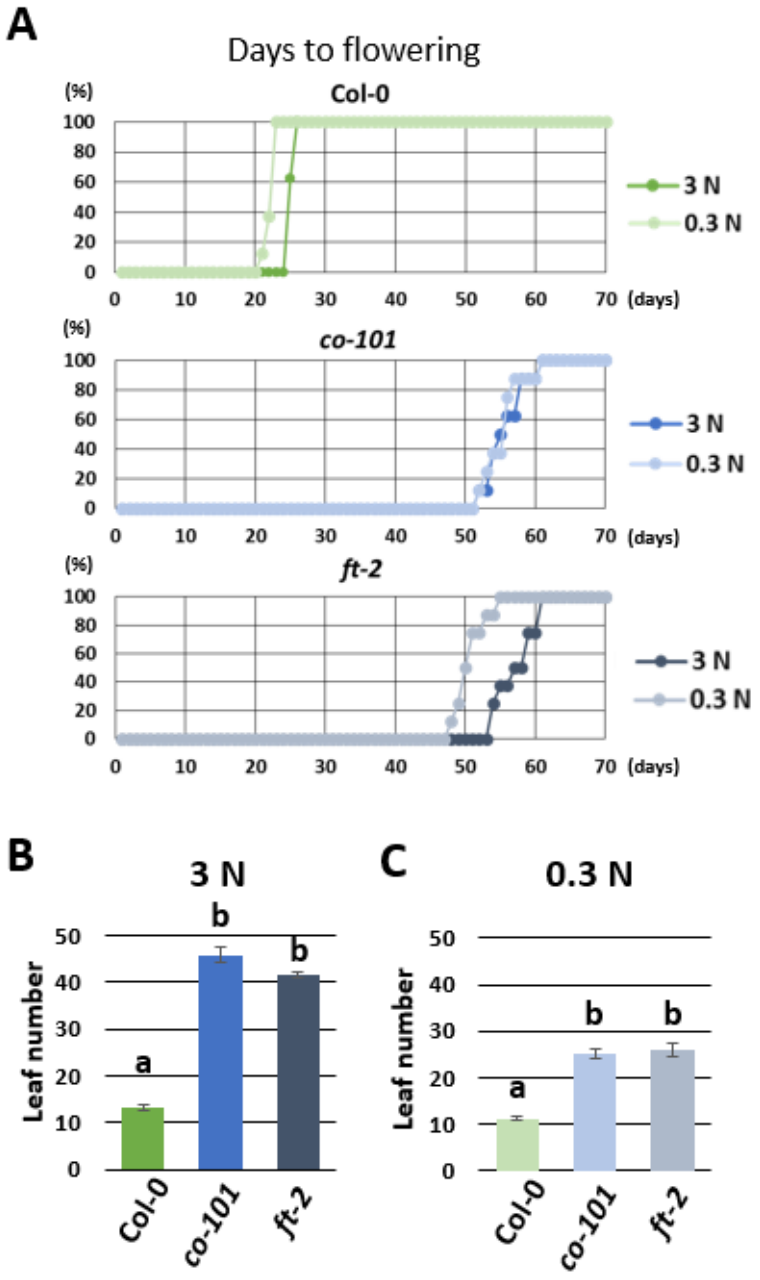

Figure 7. Low nitrogen condition did not induce early flowering in *co-101*

Col-0, *co-101*, and *ft-2* plants were grown by hydroponic culture system including 3 mM nitrogen (3 N) or 0.3 mM nitrogen (0.3 N) under long days (16 h light/8 h dark). (A) Days to flowering was shown by the rates of over 1 cm bolting at each day. (B, C) Rosette leaf number at 1 cm bolting time under 3 N (B) and 0.3 N (C). n = 9; error bars indicate SD with the same letter are not significantly different from one another (ANOVA + Tukey HSD, $P < 0.05$).

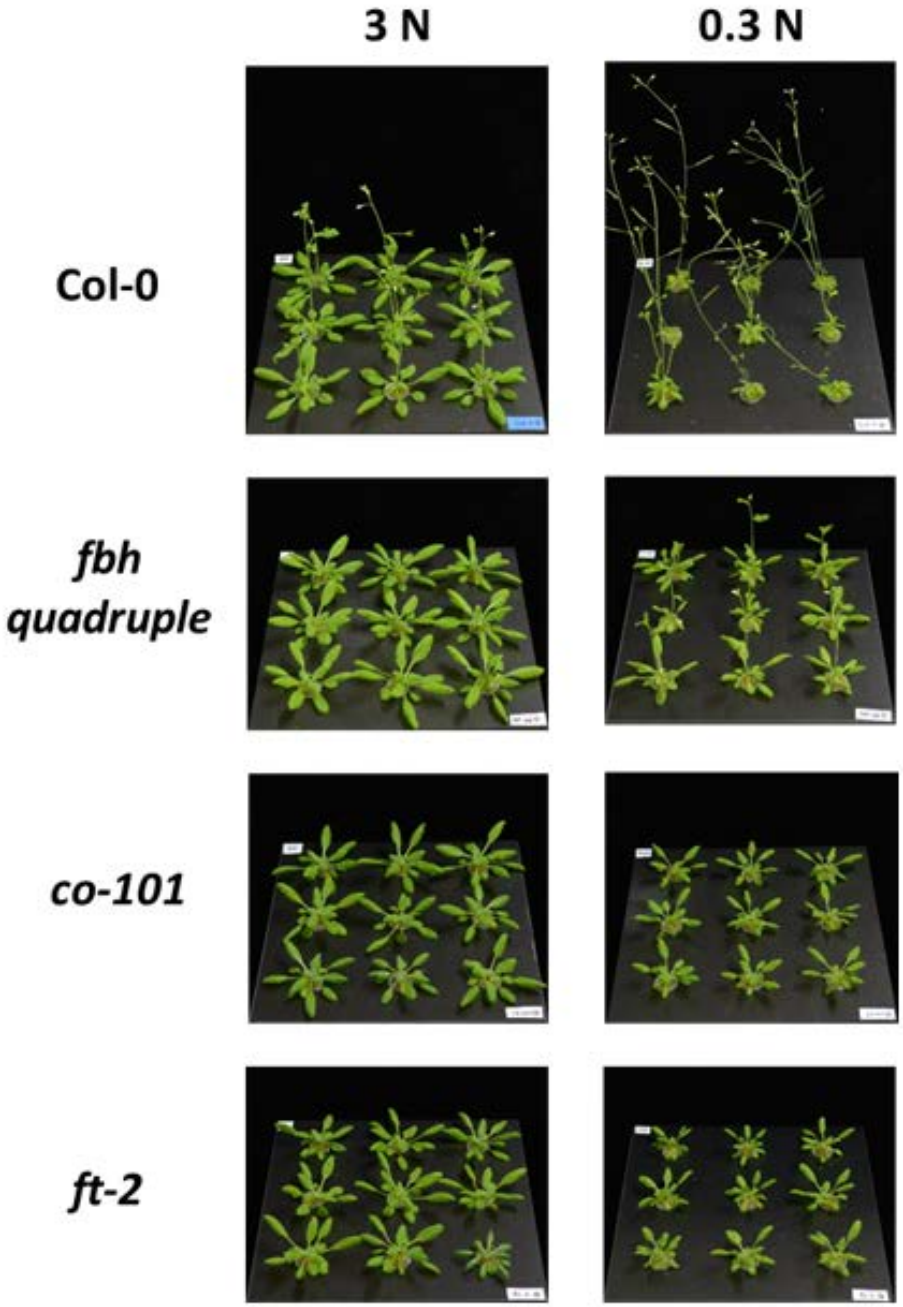

Figure 8. Low nitrogen condition did not induce early flowering in *co-101*

Col-0, *fbh quadruple*, *co-101*, and *ft-2* plants were grown by hydroponic culture system including 3 mM nitrogen (3 N) or 0.3 mM nitrogen (0.3 N) under long days (16 h light/8 h dark). 30-day-old plants grown in each condition are showed in pictures.

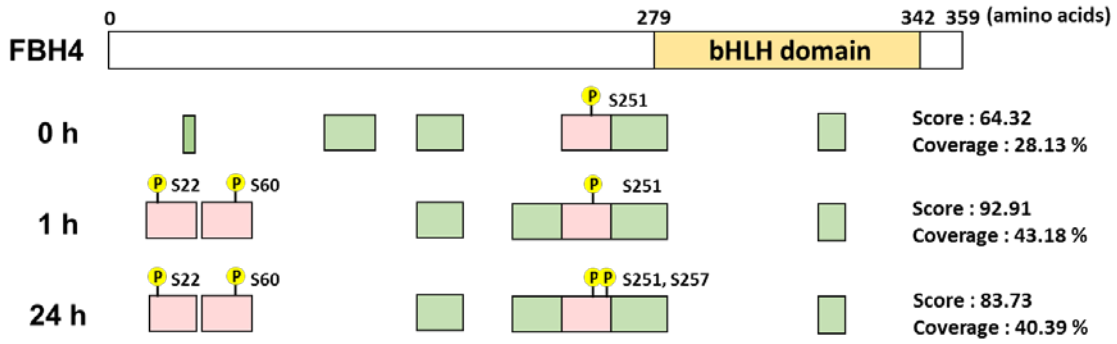

Figure 9. Detected peptides of FBH4 by IP-MS analysis

Detected peptides of FBH4 in each conditions were shown as a brief picture. Full length of FBH4 protein (359 amino acids) with bHLH domain (279-342 amino acids) are shown in upper picture. Rectangles located in right of 0 h, 1 h, and 24 h shows detected peptides by IP-MS analysis using *FLAG-FBH4* overexpressing Arabidopsis. Green rectangles indicate non-phosphorylated peptides and pink rectangles indicates phosphorylated peptides with significant score (q-value < 0.05). P in yellow circles and the numbers near to them show phosphorylated serines. Total score and coverage of FBH4 protein are shown in right area.

Chapter III

Membrane-localized ubiquitin ligase ATL15 functions in sugar-responsive growth regulation in Arabidopsis

Summary

Ubiquitin ligases play important roles in regulating various cellular processes by modulating the protein function of specific ubiquitination targets. The Arabidopsis Tóxicos en Levadura (ATL) family is a group of plant-specific RING-type ubiquitin ligases that localize to membranes via their N-terminal transmembrane-like domains. To date, 91 ATL isoforms have been identified in the Arabidopsis genome, with several ATLs reported to be involved in regulating plant responses to environmental stresses. However, the functions of most ATLs remain unknown. This study, involving transcriptome database analysis, identifies *ATL15* as a sugar responsive ATL gene in Arabidopsis. *ATL15* expression was rapidly down-regulated in the presence of sugar. The ATL15 protein showed ubiquitin ligase activity *in vitro* and localized to plasma membrane and endomembrane compartments. Further genetic analyses demonstrated that the *atl15* knockout mutants are insensitive to high glucose concentrations, whereas *ATL15* overexpression depresses plant growth. In addition, endogenous glucose and starch amounts were reciprocally affected in the *atl15* knockout mutants and the *ATL15* overexpressors. These results suggest that ATL15 protein plays a significant role as a membrane-localized ubiquitin ligase that regulates sugar-responsive plant growth in Arabidopsis.

Introduction

Protein ubiquitination is an important post-translational modification regulating many intracellular phenomena, including protein degradation by the 26S proteasome, trafficking of membrane-localized proteins and DNA-damage repair (Iwai et al., 2014; Vierstra, 2009). Protein ubiquitination is catalyzed by three enzymes, ubiquitin-activating enzyme (E1), ubiquitin-conjugating enzyme (E2), and ubiquitin ligase (E3). To date, approximately 1,400 genes encoding ubiquitin ligases have been identified in Arabidopsis plants, with differences among encoded proteins important for the recognition of specific protein targets (Callis, 2014; Vierstra, 2009). The Arabidopsis Tóxicos en Levadura (ATL) family is a family of RING-type ubiquitin ligases specific to plant species; to date, 91 ATL proteins have been identified in Arabidopsis and 119 in rice(Aguilar-Hernández et al., 2011; Guzmán, 2014). The ATL family is widely conserved in several plant species, both of monocot and eudicot species (Aguilar-Hernández et al., 2011), including fruit crops such as grapevine (96 genes) (Ariani et al., 2016) and tomato (82 gene) plants(Lu et al., 2016). All ATLs have one or two transmembrane-like hydrophobic regions at their N-termini, allowing their localization to membranes (Aguilar-Hernández et al., 2011; Guzmán, 2014). In addition, ATLs possess a RING-H2 type zinc finger domain and a GLD region, the function of which remains unknown. In contrast, their C-terminal regions are not conserved, suggesting that this region is involved in the recognition of specific target proteins. In plants, ATL proteins function in response to biotic and abiotic environmental stresses. Arabidopsis ATL1, ATL2, ATL9 and ATL55/RING1 and rice EL5 have been reported to function in plant immunity (Berrocal-Lobo et al., 2010; Lin et al., 2008; Salinas-Mondragón et al., 1999; Serrano et al., 2014). ATL78 regulates plant tolerance

to cold and drought via an abscisic acid signal transduction pathway (Kim and Kim, 2013; Suh et al., 2016). ATL proteins are also reported to play essential roles in plant responses to nutrient availability. For example, ATL14, named as IDF1, regulates iron homeostasis via the ubiquitin-dependent degradation of iron-regulated transporter1 (IRT1) proteins (Shin et al., 2013), and ATL80 is involved in phosphate mobilization (Suh and Kim, 2015). In addition, we previously reported that ATL31 and ATL6 regulate plant responses to the ratio between carbon and nitrogen nutrients, called the C/N-nutrient balance, by degrading 14-3-3 proteins, as well as being involved in plant immunity (Maekawa et al., 2012; Sato et al., 2011, 2009; Yasuda et al., 2014). To date, however, the biochemical and physiological functions of most ATLs remain unknown.

Sugar is essential in regulating plant metabolism and growth by acting both as a metabolite and a signaling molecule (Rolland et al., 2006; Smeekens et al., 2010). Hexokinase1 (HXK1) functions as an intracellular glucose sensor, regulating global gene expression, including the expression of photosynthesis- and phytohormone-related genes (León and Sheen, 2003; Moore et al., 2003). SNF-1 related kinase 1 (SnRK1) and target of rapamcyin (TOR) kinases function as central regulators that link carbon nutrients and energy status to plant development (Emanuelle et al., 2016; Smeekens et al., 2010). The plasma membrane-localized protein, regulator of G-protein signaling 1 (RGS1), is another glucose sensing protein, which modulates the activity of the heterotrimeric G-protein complex, mediating sugar signaling and cell proliferation in response to extracellular glucose concentrations (Urano et al., 2012). Sugar signaling pathways constitute a complicated molecular network and are associated with global cellular metabolism (Rolland et al., 2006). Overall sugar signaling mechanisms, especially regarding the membrane compartments that function as regions of

extracellular sugar sensing and transport, remain unclear.

To further understand the molecular mechanism underlying plant responses to sugar availability, we performed survey of transcriptome database of Arabidopsis to identify sugar responsive *ATL* genes, leading to isolation of the *ATL15* gene. Here, we assessed sugar responsive and tissue specific gene expression patterns of *ATL15*. Biochemical analysis and physiological characterization of *atl15* mutants showed the significance of ATL15 protein as a membrane-localized ubiquitin ligase regulating the sugar responsive growth of Arabidopsis plants.

Materials and Methods

Plant materials and growth conditions

Arabidopsis thaliana ecotype Columbia-0 (Col-0) were regarded as wild-type (WT) in this study. The T-DNA insertion mutant *atl15-1* (SALK_033688) was obtained from the Arabidopsis Biological Resource Center (https://abrc.osu.edu/). To generate the *ATL15-GFP* overexpressing transgenic plants, the full-length *ATL15* cording sequence in Col-0 cDNA was PCR amplified using the primers listed in Table 1. The amplified cDNA was cloned into the pENTR/D-TOPO vector (Invitrogen) and transferred to the pGWB5 binary vector (Nakagawa et al., 2007) as described by the manufacturer (Invitrogen). Constructed vectors were introduced into *Agrobacterium tumefaciens* GV3101 (pMP90) by electroporation, followed by transformation to Arabidopsis using the floral dip method (Clough and Bent, 1998). Plant growth conditions have been described (Yasuda et al., 2014).

Gene expression analysis

Gene expression was analyzed by qRT-PCR. Total RNA was extracted from Arabidopsis seedlings using Trizol-reagent (Invitrogen) and treated with RQ1 RNase-free DNase (Promega), followed by cDNA synthesis using Rever Tra Ace (TOYOBO) and oligo(dT) primer (Promega). qRT-PCR was performed using SYBR premix EX Taq (TaKaRa) with Mx3000P (Agilent Technologies) machine, according to the manufacturer's protocol. The gene specific primers are listed in Table 1.

Sugar treatment and sugar quantification

For sugar-responsive gene expression analysis, WT seedlings were grown on sugar-free 1/2 MS salt medium (Murashige and Skoog, 1962) for 7 days and transferred to 1/2 MS salt medium containing 200 mM glucose, sucrose, fructose or mannitol for 1 hour. For phenotype analysis and to measure endogenous sugar concentrations, WT, *atl15-1* mutant, *ATL15* overexpressing and complementation lines were grown on the 1/2 MS salt medium containing glucose or mannitol, and endogenous sugar concentrations were measured as previously described (Aoyama et al., 2014).

In vitro ubiquitination assay

To generate the recombinant MBP-ATL15 protein, the coding sequence of the N-terminal truncated ATL15 fragment, from Met70 to Val381, was PCR amplified using the primers listed in Table 1, and introduced into the pENTR/D-TOPO vector (Invitrogen) to generate the plasmid pENTR/D-TOPO/ΔTMATL15. This pENTR/D-TOPO/ΔTMATL15 plasmid was transferred to the pDEST-mal destination vector, followed by construction of the MBP-ATL15 expression vector using an LR

reaction (Tsunoda et al., 2005). The constructed vector was introduced into *Escherichia coli* strain BL21 (DE3) pLysS, and the recombinant protein purified from *E. coli* as described (Yasuda et al., 2014). *In vitro* ubiquitination reactions were performed as described (Yasuda et al., 2014) followed by western blotting using anti-MBP (NEB) and anti-Ubiquitin (Nippon Bio-Test Laboratories Inc.) antibodies.

Confocal laser-scanning microscopy

Subcellular localization of ATL15-GFP was analyzed by microscopy using the root tissue of *ATL15-GFP* plants. Plasma membranes were identified by staining root tissue with FM4-64 for 5 min at room temperature and examination under a Zeiss LSM510 laser scanning microscope with a C-Apochromat (x40/1.20 water immersion) objective. Excitation and emission wavelengths were 488 nm and 505-550 nm, respectively, for GFP and 561 nm and 575-615 nm, respectively, for FM4-64.

Preparation of water-soluble and membrane fractions

To extract total protein from 2-week-old *ATL15-GFP* plants, seedlings (500 mg fresh weight) were ground in 1.5 ml extraction buffer with or without Triton-X 100 and subjected to ultracentrifugation as described (Sato et al., 2009). The membrane fraction was resolved with 1% Triton-X 100, and each fraction was immunoprecipitated with anti-GFP beads (MBL). Proteins were detected by western blotting with anti-GFP (MBL) and anti-H^+-ATPase (Agrisera) antibodies.

Results

ATL15 transcription was down-regulated by sugar treatment

To identify ATL proteins particularly involved in responses to sugars, we searched the transcriptome profile of *ATL* genes with Genevestigator, an available microarray database (https://www.genevestigator.com). This search identified *ATL15* as a candidate sugar responsive *ATL* gene (Figure 1A). *ATL15* expression was down-regulated in response to exposure to sugars such as glucose. To verify that *ATL15* expression was responsive to sugars, we performed quantitative RT-PCR (qRT-PCR) analysis with Arabidopsis seedlings grown at different sugar conditions. WT Arabidopsis seedlings were grown on sugar-free medium for 8 days and transferred to medium supplemented with 200 mM (3.6%) glucose. qRT-PCR analysis showed that *ATL15* expression level was significantly reduced 1 hour after transfer to the glucose-containing medium, a pattern similar to that of the sugar repressed marker gene *BT2* (Mandadi et al., 2009) (Figures 1B and 2A), confirming the Genevestigator result. We also examined the *ATL15* transcription pattern in response to various sugars, finding that the level of *ATL15* expression was also reduced by exposure to sucrose and fructose (Figure 2A). Osmotic stress treatment with mannitol also partially down-regulated *ATL15* expression, but to a lesser extent than shown by the other sugars (Figure 2A). These findings indicate that *ATL15* in Arabidopsis plants is transcriptionally regulated by sugar availability.

Tissue-specific expression analysis showed that the ATL15 gene is broadly expressed in all plant tissues, especially in older leaves and roots, but less so in flowers and siliques (Figure 2B).

ATL15 protein exhibits ubiquitin ligase activity

ATL15 belongs to the group G ATL family, which includes the C/N-nutrient response

regulators ATL31 and ATL6 (Sato et al., 2009) and the pathogen-defense related isoform ATL9(Berrocal-Lobo et al., 2010). Similar to most other group G ATL proteins, ATL15 contains two transmembrane-like hydrophobic regions at its N-terminal and a RING-H2 type zinc finger domain at its middle part (Figures 3A and 4). The C-terminal region of group G ATL proteins varies, suggesting that this region interacts with specific ubiquitination targets or modulators. To determine the biochemical properties of ATL15, we assessed its ubiquitin ligase activity by *in vitro* ubiquitination assays. Because the N-terminal and basic regions of ATLs have been reported to inhibit sufficient expression in *E. coli* (Takai et al., 2002; Yasuda et al., 2014), these regions of ATL15 (residues Met1 through Tyr69) were deleted and the remaining residues (Met70 through Val381) were fused to MBP to generate the MBP-ATL15 fusion protein. The purified MBP-ATL15 protein was subsequently incubated with E1, E2, ubiquitin and ATP for various times and subjected to western blotting analysis with anti-ubiquitin antibody, which detected several higher molecular weight bands after 2, 5 and 10 min (Figure 3B). These bands, however, were not detected after incubation of recombinant ATL15 protein containing a serine residue in place of the third cysteine residue (MBP-ATL15C137S), which is conserved in the RING domain and required for catalytic activity (Takai et al., 2002) (Figure 3B). These results indicate ATL15 has RING-type ubiquitin ligase activity *in vitro*.

ATL15 protein localizes to membrane compartments

The N-terminal hydrophobic region of ATL proteins is thought to determine the localization to membranes (Aguilar-Hernández et al., 2011; Guzmán, 2014). ATL15 contains two N-terminal transmembrane-like hydrophobic regions (Figure 3A). To

investigate the subcellular localization of ATL15, we generated transgenic Arabidopsis plants continuously expressing ATL15 fused with green fluorescence protein (*ATL15-GFP*) (Figure 5). Confocal microscopy showed a strong fluorescent signal of ATL15-GFP around the cell surface, overlapping with the signal derived from FM4-64 stained plasma membranes (Figure 3C). We also observed dot-like ATL15-GFP structures in the cytosol, suggesting that ATL15 also localizes to the endosomal compartment (Figure 3C). To further confirm the membrane localization of ATL15, proteins were extracted from the *ATL15-GFP* seedlings using extraction buffer with or without detergent (1% Triton-X), followed by ultracentrifugation to separate soluble and insoluble fractions. After the enrichment of ATL15-GFP protein by immunoprecipitation, and in the absence of Triton X-100, ATL15-GFP was detected in the insoluble (pellet: P), but not in the soluble (supernatant: S), fraction (Figure 3D). In the presence of Triton X-100, however, most of the ATL15-GFP was detected in the soluble fraction. Together with microscope analysis, these results indicate that ATL15 localizes to both the plasma membrane and endomembrane compartments of Arabidopsis cells.

The *atl15* knockout mutants are insensitive to glucose treatment

To evaluate the physiological function of ATL15 in plant response to sugars, we tested the growth phenotype of the *atl15* loss-of function mutants in response to sugar treatment. High sugar concentrations have been shown to inhibit the post-germinative growth of Arabidopsis, including cotyledon greening (Moore et al., 2003). We identified a null mutant line of *ATL15* in a T-DNA insertion Arabidopsis population (Figure 5). At normal sugar concentrations (1% glucose) and under conditions of osmotic stress (6% mannitol), almost all WT and the *atl15* mutant (*atl15-1*) Arabidopsis seedlings showed

expansion of green-colored cotyledons (Figure 6A and 6B). At a high sugar concentration (6% glucose), the greening ratio of WT seedlings was decreased to 10%, whereas green cotyledons were present in more than 30% of the *atl15* mutant seedlings. We also tested the greening phenotype of transgenic Arabidopsis plants continuously expressing *ATL15-GFP* under the 35S promoter in WT (*ATL15-GFP*) or in the *atl15* mutant (*ATL15-GFP* in *atl15-1*) backgrounds, respectively (Figure 5). We found that the sugar-insensitive phenotype of the *atl15* mutants became sugar-sensitive following continuous expression of exogenous *ATL15*, similar to that of WT plants (Figure 6A and 6B). We further examined the physiological significance of ATL15 in sugar-responsive plant growth under normal (1% glucose) and moderate sugar (5% glucose) stress conditions. In the presence of 5% glucose, almost all seedlings of both genotypes showed green-colored cotyledons and continued to grow. At 15 days, WT and the *atl15* mutants showed similar growth phenotype in the presence of 1% glucose. At 5% glucose, however, the biomass of the *atl15* mutants was greater than that of WT plants (Figure 7A and 7B). In contrast, the growth of *ATL15-GFP* plants was lower than that of WT growth in the presence of both 1% and 5% glucose. The insensitive phenotype of the *atl15* mutants was recovered by continuous expression of exogenous *ATL15* (*ATL15-GFP in atl15-1*), confirming that *ATL15* is the cause of this phenotype.

Endogenous glucose amounts were reciprocally affected in the *atl15* mutants and the *ATL15* overexpressors

To further understand the function of ATL15 in plant responses to sugar, we compared the amounts of endogenous glucose in the *atl15* mutants and the overexpressors. The amount of endogenous glucose was about 4-times higher in WT

plants grown in the presence of 5% than 1% glucose amounts (Figure 7C). Under both conditions, *atl15* mutants accumulated relatively less glucose while *ATL15-GFP* plants contains increased glucose amounts (Figure 7C). We also measured the amounts of starch, a major carbon store synthesized from glucose in plant cells. The accumulation patterns of starch were similar to those of glucose, with the *atl15* mutants and the *ATL15-GFP* plants showing reciprocal accumulation patterns of starch in the presence of 5% glucose (Figure 7D). These results suggest that ATL15 affect the amount of endogenous glucose in Arabidopsis plants and may function as a positive regulator of glucose uptake by these cells.

Discussion

Because sugar is one of the most important plant nutrients, cellular sugar concentrations and plant growth are tightly coordinated. This study showed that ATL15 protein is a sugar-related ubiquitin ligase in Arabidopsis plants. The expression of *ATL15* was rapidly repressed after exogenous sugar application, and the *atl15* loss of function mutant was insensitive to excess sugar stress, suggesting that ATL15 negatively regulates plant growth in response to sugar availability. The glucose sensor complex protein RGS1 has been localized to the plasma membrane, translocating to endosomes following glucose-induced endocytosis. This results in modulation of G-protein coupled signaling and regulates plant growth. The molecular mechanism that triggers RGS1 endocytosis remains unclear. Ubiquitin modification is a critical cellular signal regulating endocytosis of membrane proteins in eukaryotic cells. We found that ATL15 possesses RING-type ubiquitin ligase activity and localizes to membrane compartments, both of the plasma membrane and endosome. It’s worth examining

whether RGS1 endocytosis is affected in the *atl15* mutants or the overexpressor in response to glucose status. On the other hands, the amounts of endogenous glucose and starch were reciprocally affected in the *atl15* mutants and overexpressors, suggesting another possibility that ATL15 is involved in extracellular sugar uptake. In yeast, the glucose transporter HXT1 is ubiquitinated and undergoes vacuolar degradation (Roy et al., 2014) in response to glucose starvation. Trafficking of the human glucose transporter GLUT4 is also regulated by ubiquitination under the control of insulin (Lamb et al., 2010). Similarly, the ATL isoform ATL14/IDF1 was shown to ubiquitinate and modulate the stability of iron transporter IRT1, thereby regulating iron homeostasis in Arabidopsis roots (Shin et al., 2013). More detailed investigations of ATL15 function in sugar sensing and transport, and clarification of its ubiquitination target are required to further understand the molecular mechanism regulating sugar responsive plant growth by membrane compartments.

References

Aguilar-Hernández, V., Aguilar-Henonin, L., and Guzmán, P. (2011) Diversity in the architecture of ATLs, a family of plant ubiquitin-ligases, leads to recognition and targeting of substrates in different cellular environments. *PLoS One*. 6.

Aoyama, S., Huarancca Reyes, T., Guglielminetti, L., Lu, Y., Morita, Y., Sato, T., et al. (2014) Ubiquitin ligase ATL31 functions in leaf senescence in response to the balance between atmospheric CO2 and nitrogen availability in arabidopsis. *Plant Cell Physiol*. 55: 293–305.

Ariani, P., Regaiolo, A., Lovato, A., Giorgetti, A., Porceddu, A., Camiolo, S., et al. (2016) Genome-wide characterisation and expression profile of the grapevine ATL

ubiquitin ligase family reveal biotic and abiotic stress-responsive and development-related members. *Sci Rep*. 6: 38260.

Berrocal-Lobo, M., Stone, S., Yang, X., Antico, J., Callis, J., Ramonell, K.M., et al. (2010) ATL9, a RING zinc finger protein with E3 ubiquitin ligase activity implicated in chitin- and NADPH oxidase-mediated defense responses. *PLoS One*. 5.

Callis, J. (2014) The Ubiquitination Machinery of the Ubiquitin System. *Arab B*. 12: e0174.

Clough, S.J., and Bent, A.F. (1998) Floral dip: A simplified method for Agrobacterium-mediated transformation of Arabidopsis thaliana. *Plant J*. 16: 735–743.

Emanuelle, S., Doblin, M.S., Stapleton, D.I., Bacic, A., and Gooley, P.R. (2016) Molecular Insights into the Enigmatic Metabolic Regulator, SnRK1. *Trends Plant Sci*. 21: 341–353.

Guzmán, P. (2014) ATLs and BTLs, plant-specific and general eukaryotic structurally-related E3 ubiquitin ligases. *Plant Sci*. 215–216: 69–75.

Iwai, K., Fujita, H., and Sasaki, Y. (2014) Linear ubiquitin chains: NF-κB signalling, cell death and beyond. *Nat Rev Mol Cell Biol*. 15: 503–508.

Kim, S.J., and Kim, W.T. (2013) Suppression of Arabidopsis RING E3 ubiquitin ligase AtATL78 increases tolerance to cold stress and decreases tolerance to drought stress. *FEBS Lett*. 587: 2584–2590.

Lamb, C.A., McCann, R.K., Stöckli, J., James, D.E., and Bryant, N.J. (2010) Insulin-regulated trafficking of GLUT4 requires ubiquitination. *Traffic*. 11: 1445–1454.

León, P., and Sheen, J. (2003) Sugar and hormone connections. *Trends Plant Sci*. 8: 110–116.

Lin, S.S., Martin, R., Mongrand, S., Vandenabeele, S., Chen, K.C., Jang, I.C., et al. (2008) RING1 E3 ligase localizes to plasma membrane lipid rafts to trigger FB1-induced programmed cell death in Arabidopsis. *Plant J*. 56: 550–561.

Lu, Y., Yasuda, S., Li, X., Fukao, Y., Tohge, T., Fernie, A.R., et al. (2016) Characterization of ubiquitin ligase SlATL31 and proteomic analysis of 14-3-3 targets in tomato fruit tissue (Solanum lycopersicum L.). *J Proteomics*. 143: 254–264.

Maekawa, S., Sato, T., Asada, Y., Yasuda, S., Yoshida, M., Chiba, Y., et al. (2012) The Arabidopsis ubiquitin ligases ATL31 and ATL6 control the defense response as well as the carbon/nitrogen response. *Plant Mol Biol*. 79: 217–27.

Mandadi, K.K., Misra, A., Ren, S., and McKnight, T.D. (2009) BT2, a BTB Protein, Mediates Multiple Responses to Nutrients, Stresses, and Hormones in Arabidopsis. *Plant Physiol*. 150: 1930–1939.

Moore, B., Zhou, L., Rolland, F., Hall, Q., Cheng, W.-H., Liu, Y.-X., et al. (2003) . Science.

Murashige, T., and Skoog, F. (1962) A revised medium for rapid growth and bio assays with tobacco tissue cultures. *Physiol Plant*. 15: 473–497.

Nakagawa, T., Kurose, T., Hino, T., Tanaka, K., Kawamukai, M., Niwa, Y., et al. (2007) Development of series of gateway binary vectors, pGWBs, for realizing efficient construction of fusion genes for plant transformation. *J Biosci Bioeng*. 104: 34–41.

Rolland, F., Baena-Gonzalez, E., and Sheen, J. (2006) . Annu. Rev. Plant Biol.

Roy, A., Kim, Y.B., Cho, K.H., and Kim, J.H. (2014) Glucose starvation-induced turnover of the yeast glucose transporter Hxt1. *Biochim Biophys Acta - Gen Subj*. 1840: 2878–2885.

Salinas-Mondragón, R.E., Garcidueñas-Piña, C., and Guzmán, P. (1999) Early elicitor induction in members of a novel multigene family coding for highly related RING-H2 proteins in Arabidopsis thaliana. *Plant Mol Biol*. 40: 579–90.

Sato, T., Maekawa, S., Yasuda, S., Domeki, Y., Sueyoshi, K., Fujiwara, M., et al. (2011) Identification of 14-3-3 proteins as a target of ATL31 ubiquitin ligase, a regulator of the C/N response in Arabidopsis. *Plant J*. 68: 137–46.

Sato, T., Maekawa, S., Yasuda, S., Sonoda, Y., Katoh, E., Ichikawa, T., et al. (2009) CNI1/ATL31, a RING-type ubiquitin ligase that functions in the carbon/nitrogen response for growth phase transition in Arabidopsis seedlings. *Plant J*. 60: 852–64.

Serrano, I., Gu, Y., Qi, D., Dubiella, U., and Innes, R.W. (2014) The Arabidopsis EDR1 protein kinase negatively regulates the ATL1 E3 ubiquitin ligase to suppress cell death. *Plant Cell*. 26: 4532–46.

Shin, L.-J., Lo, J.-C., Chen, G.-H., Callis, J., Fu, H., and Yeh, K.-C. (2013) IRT1 DEGRADATION FACTOR1, a RING E3 Ubiquitin Ligase, Regulates the Degradation of IRON-REGULATED TRANSPORTER1 in Arabidopsis. *Plant Cell*. 25: 3039–3051.

Smeekens, S., Ma, J., Hanson, J., and Rolland, F. (2010) Sugar signals and molecular networks controlling plant growth. *Curr Opin Plant Biol*. 13: 274–279.

Suh, J.Y., Kim, S.J., Oh, T.R., Cho, S.K., Yang, S.W., and Kim, W.T. (2016) Arabidopsis T??xicos en Levadura 78 (AtATL78) mediates ABA-dependent ROS signaling in response to drought stress. *Biochem Biophys Res Commun*. 469: 8–14.

Suh, J.Y., and Kim, W.T. (2015) Arabidopsis RING E3 ubiquitin ligase AtATL80 is negatively involved in phosphate mobilization and cold stress response in sufficient phosphate growth conditions. *Biochem Biophys Res Commun*. 1–7.

Takai, R., Matsuda, N., Nakano, A., Hasegawa, K., Akimoto, C., Shibuya, N., et al. (2002) EL5, a rice N-acetylchitooligosaccharide elicitor-responsive RING-H2 finger protein, is a ubiquitin ligase which functions in vitro in co-operation with an elicitor-responsive ubiquitin-conjugating enzyme, OsUBC5b. *Plant J*. 30: 447–455.

Tsunoda, Y., Sakai, N., Kikuchi, K., Katoh, S., Akagi, K., Miura-Ohnuma, J., et al. (2005) Improving expression and solubility of rice proteins produced as fusion proteins in Escherichia coli. *Protein Expr Purif*. 42: 268–277.

Urano, D., Phan, N., Jones, J.C., Yang, J., Huang, J., Grigston, J., et al. (2012) Endocytosis of the seven-transmembrane RGS1 protein activates G-protein-coupled signalling in Arabidopsis. *Nat Cell Biol*. 14: 1079–1088.

Vierstra, R.D. (2009) The ubiquitin-26S proteasome system at the nexus of plant biology. *Nat Rev Mol Cell Biol*. 10: 385–97.

Yasuda, S., Sato, T., Maekawa, S., Aoyama, S., Fukao, Y., and Yamaguchi, J. (2014) Phosphorylation of Arabidopsis Ubiquitin Ligase ATL31 Is Critical for Plant Carbon/Nitrogen Nutrient Balance Response and Controls the Stability of 14-3-3 Proteins. *J Biol Chem*. 289: 15179–15193.

Table and Figures

Table 1. List of primers used for PCR.

Gene	Sequence (5'→3')
Gene expression analysis	
ATL15	TTATCAGGATCGTGCTGGTG
	CGGATTGAAGGTACGAACG
18S rRNA	CGGCTACCACATCCAAGGAA
	GCTGGAATTACCGCGGCT
BT2	AATGGGTGAAGACACCAAGTG
	AACCCCTTGTGCTTGTTCAC
Construction of plasmids	
ATL15 CDS (1-381)	CACCATGGTGGTCATGTCAC
	GACAGGGCTCGCATCGCC
ΔTMATL15 CDS (70-381)	CACCATGGACAGCGGTGGTG
	GACAGGGCTCGCATCGCC

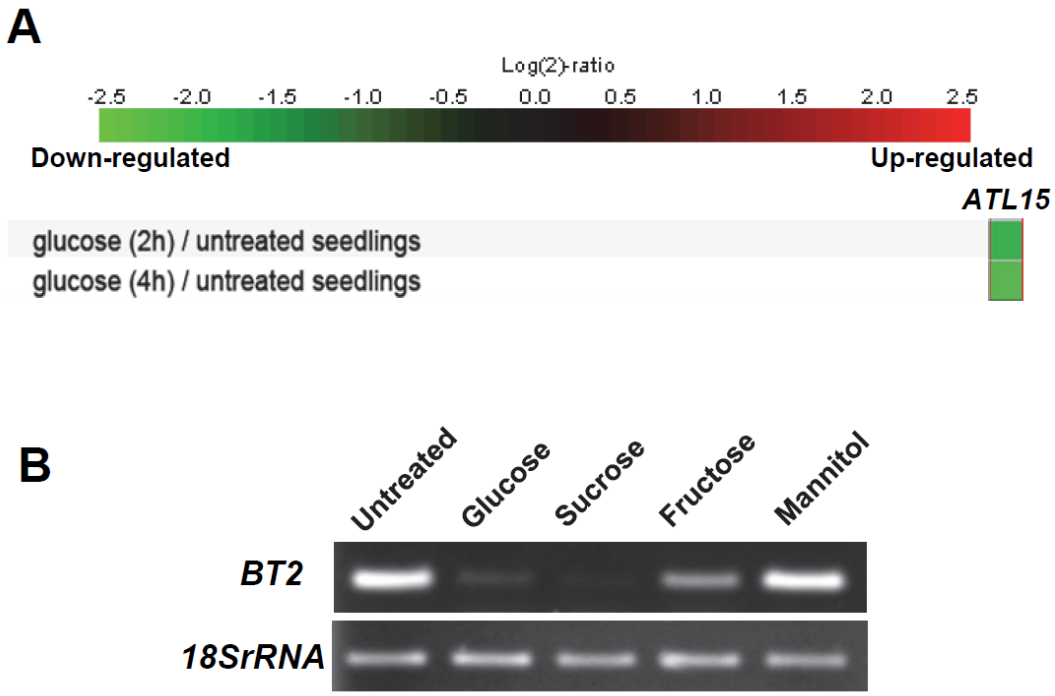

Figure 1. Analysis of sugar responsive gene expression.

(A) Transcriptome database analysis for sugar responsive *ATL* genes using Genevestigator analysis (https://www.genevestigator.com). *ATL15* was identified, and its expression found to be reduced after glucose treatment.

(B) Semi-quantitative RT-PCR analysis of sugar responsive gene expression. Total RNA was purified from 8-day-old WT plants treated with each 200 mM glucose, sucrose, fructose or mannitol for 1h. *BT2* was used as a marker of sugar repression of gene expression. *18SrRNA* was used as an internal control.

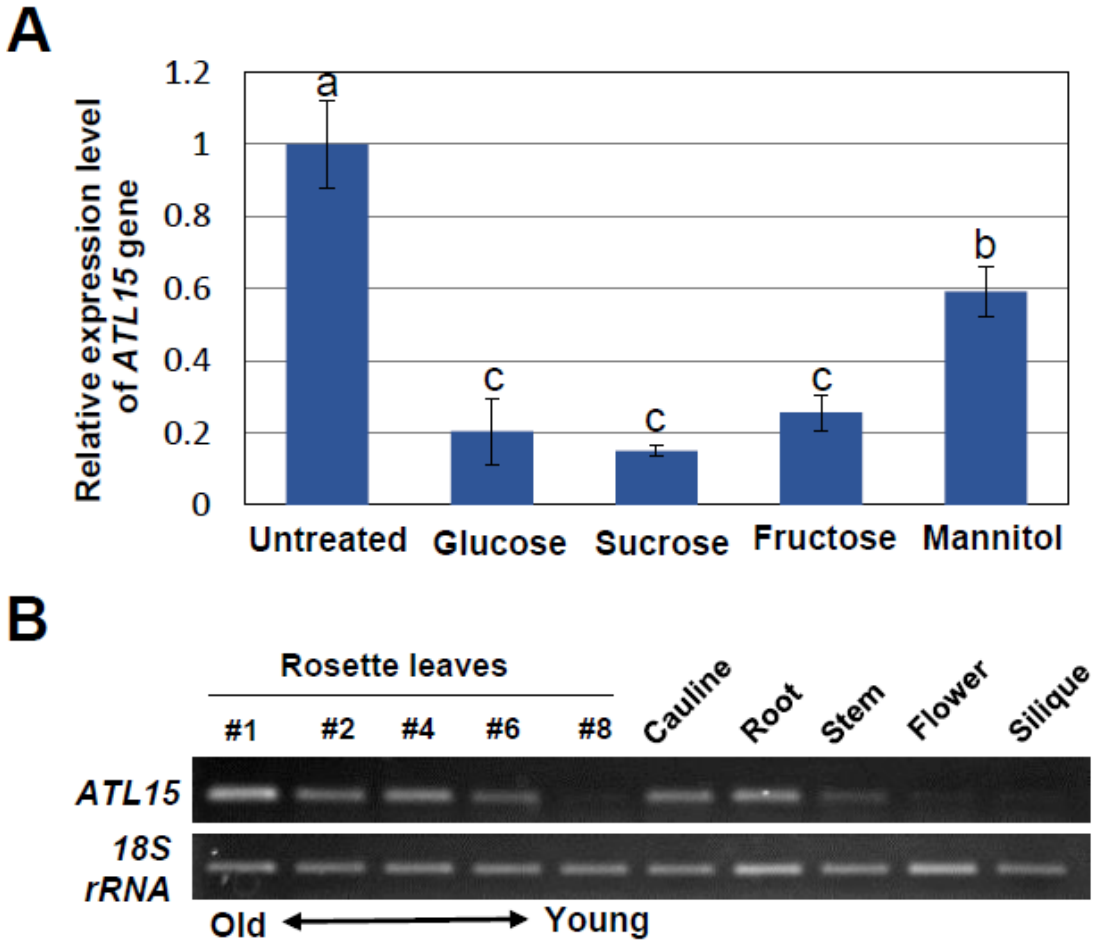

Figure 2. Expression patterns of the *ATL15* gene in response to sugars and in each plant tissue.

(A) Relative levels of *ATL15* expression in response to sugars. Total RNA was purified from 8-day-old WT plants treated with 200 mM glucose, sucrose, fructose or mannitol for 1 h, followed by qRT-PCR analysis. The level of *18S rRNA* was used as an internal control. Results are reported as means and standard deviations (SD) (*n*=3). Letters above the bars indicate significant differences, as assessed by one-way ANOVA with Turkey's *post hoc* test ($P < 0.05$). (B) Semi-quantitative PCR analysis of *ATL15* gene expression in each tissue. Total RNA was purified from 5-week-old WT plants, and *18S rRNA* was used as an internal control.

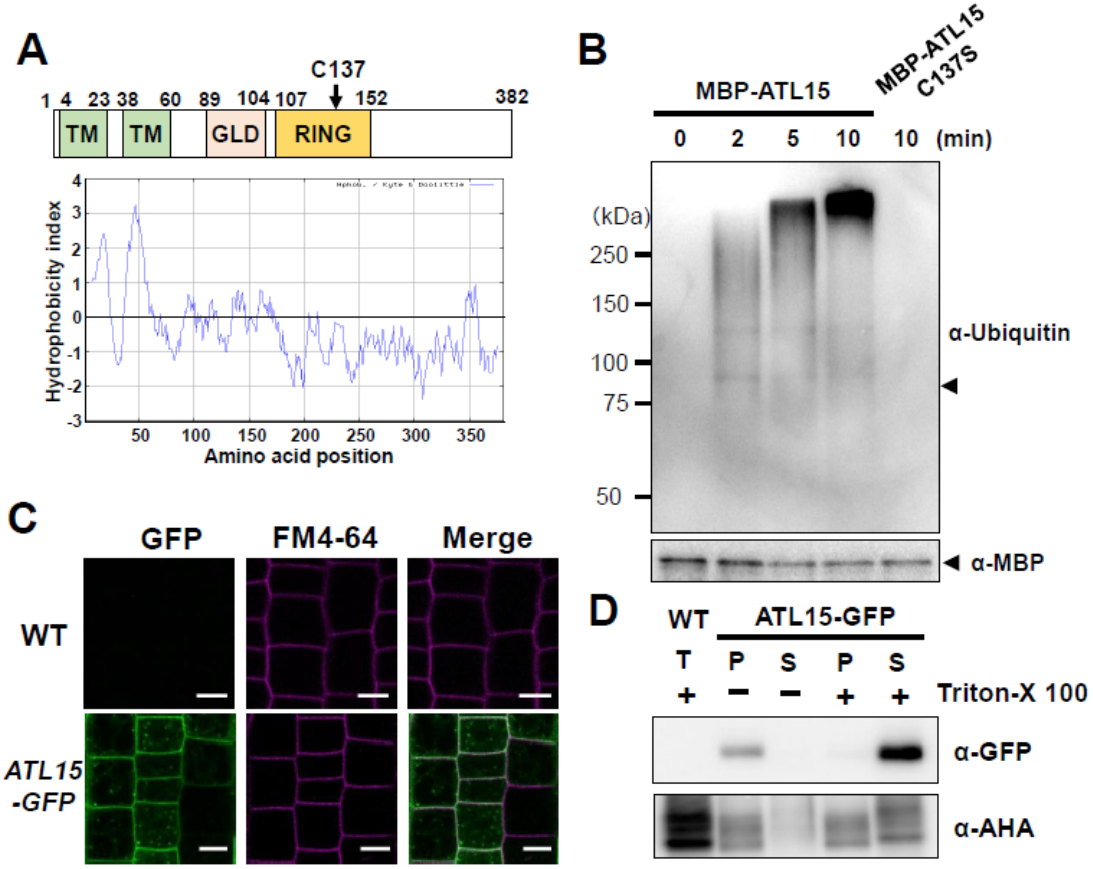

Figure 3. *In vitro* ubiquitination assay and subcellular localization of ATL15 protein.

(A) Schematic structure and hydropathy profile of ATL15 protein. Abbreviations: TM, transmembrane-like hydrophobic region; GLD, highly conserved region among ATLs including Gly-Leu-Asp residues; RING, RING-H2 zinc finger domain. The hydropathy profile was determined with ProScale software (http://web.expasy.org/protscale/). (B) *In vitro* ubiquitination assay of ATL15. Purified MBP-ATL15 protein was incubated with E1, E2, ubiquitin and ATP for 0, 2, 5 or 10 min. RING-mutated ATL15 (MBP-ATL15C137S) protein was also incubated for 10 min. Ubiquitinated proteins were detected as a heterogeneous collection of higher molecular weight band by western blotting using anti-ubiquitin antibody (upper panel). The presence of MBP-ATL15 protein was confirmed by western blotting using anti-MBP antibody (lower panel). The arrowhead indicates the position of intact MBP-ATL15 protein (86.4 kDa). (C)

Subcellular localization of ATL15-GFP protein detected by confocal laser microscopy. Root tissues of wild-type plants (upper panel) and transgenic plants expressing GFP-fused ATL15 (*ATL15-GFP*; lower panel) were subjected to FM4-64 staining followed by microscope analysis. Bar = 10 μm. (D) Western blotting analysis of water-soluble (supernatant: S) and insoluble membrane (pellet: P) fractions of Arabidopsis plants expressing ATL15-GFP fusion protein using an anti-GFP antibody. H^+-ATPase (AHA) was used as a marker for membrane-bound proteins. Extraction buffers contained no detergent (-) or 1% Triton X-100 (+). Total crude extract (T) from wild-type plants was the negative control for western blotting.

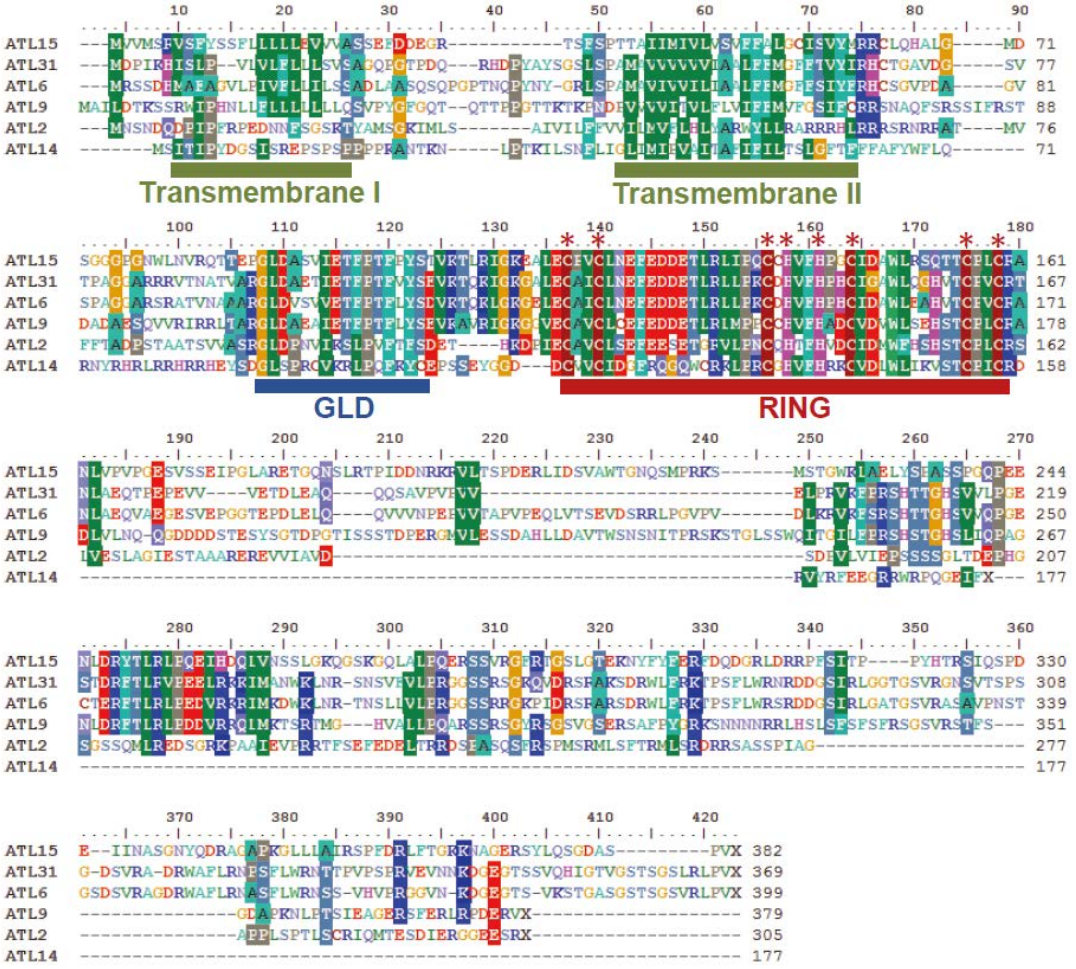

Figure 4. Amino acid sequence alignment of ATL15 and other ATL proteins.

ATL31 and ATL6, both of which have been reported to function in plant response to carbon/nitrogen nutrient balance, belong to the same subgroup as ATL15. ATL9 and ATL2 are involved in plant immunity and ATL14/IDF1 regulates iron homeostasis. Transmembrane I is present in ATL15, ATL31, ATL6 and ATL9, whereas transmembrane II, GLD and the RING domain are conserved in all ATL isoforms. The C-terminal regions vary among isoforms. Asterisks indicate conserved Cys and His residues in the RING domain.

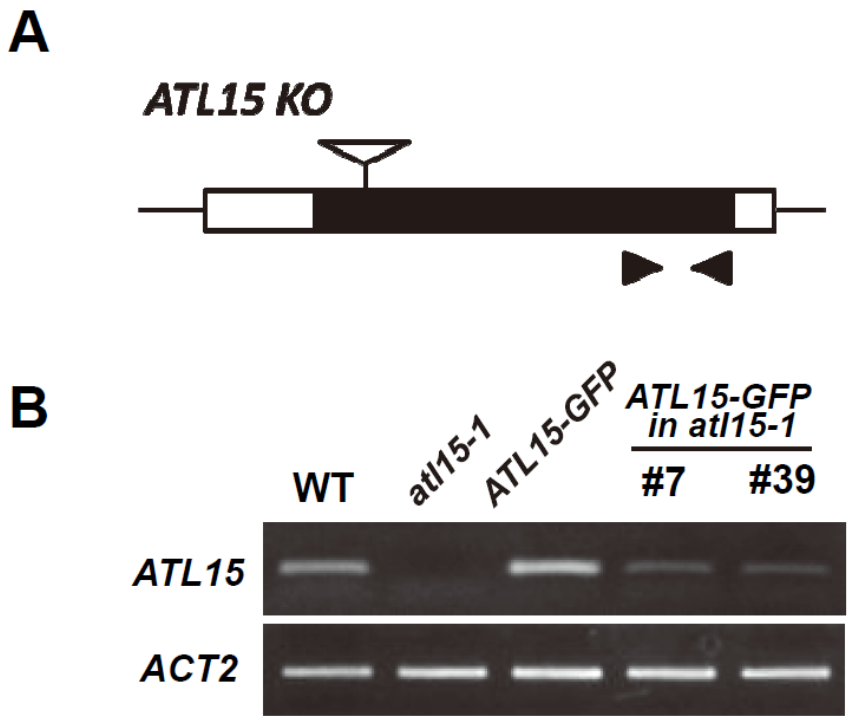

Figure. 5. Characterization of *atl15-1* mutant and transgenic plants.

(A) Gene structure of *ATL15*. The positions of T-DNA insertions are indicated by open triangles. The positions of primers used for RT-PCR in (B) are indicated by arrowheads. Black and white boxes indicate coding region and untranslated regions, respectively.

(B) RT-PCR analysis of *ATL15* mRNA in *atl15-1* mutant and *ATL15* overexpressor (*ATL15-GFP*) and complementation lines (*ATL15-GFP* in *atl15-1*). Total RNA was extracted from 7-day-old seedlings of indicated plants grown on MS medium. *Actin* (*ACT2*) was used as an internal control.

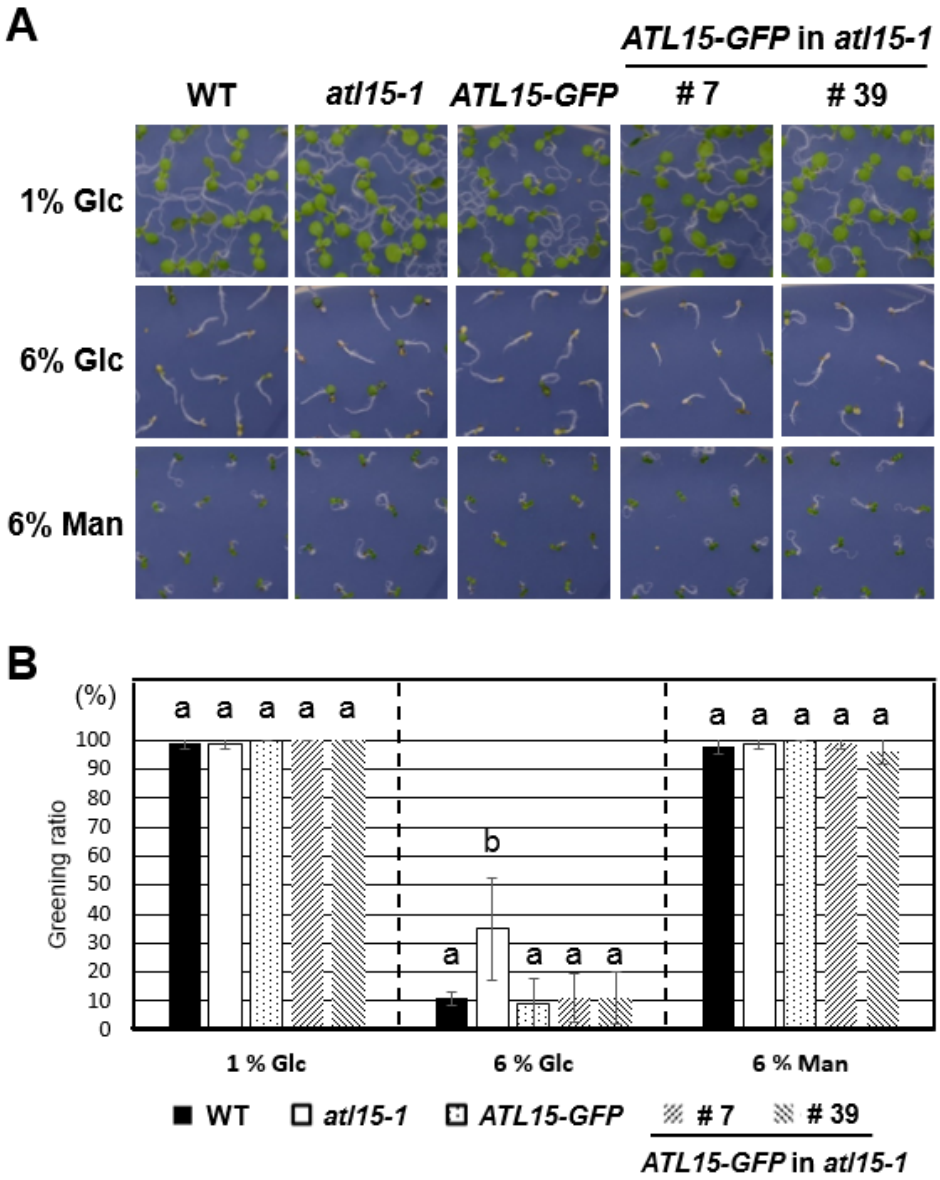

Figure 6. Effect of sugar stress on Arabidopsis greening ratio.

(A) Post-germinative growth phenotype of WT, *atl15-1* mutant, *ATL15* overexpressor (*ATL15-GFP*) and complementation lines (*ATL15-GFP* in *atl15-1*) grown on half MS medium containing 1% or 6% glucose (Glc) or 6% mannitol (Man). Images were taken 8 days after sawing (A) and greening ratio was calculated. (B) Greening ratio of each genotype. Greening ratio was calculated with 20 seedlings for each treatment and data shown are means with error bars (SD, *n*=4). Letters above the bars indicate significant differences, as assessed by one-way ANOVA with Turkey's *post hoc* test ($P < 0.05$).

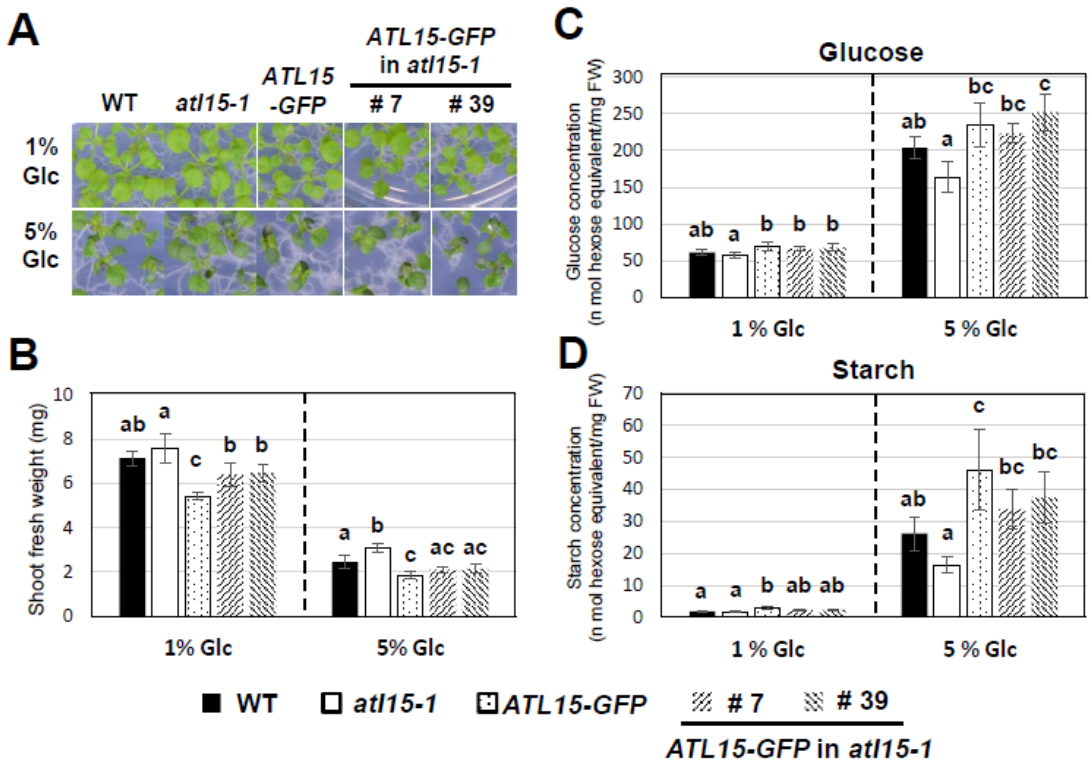

Figure 7. Effects of sugar exposure on post-germinative growth and endogenous sugar accumulation.

Post-germinative growth phenotype of WT, *atl15-1* mutant, *ATL15* overexpressor (*ATL15-GFP*) and complementation lines (*ATL15-GFP* in *atl15-1*) grown on half MS medium containing 1% or 5% glucose (Glc). (A) Images taken 15 days after sawing. (B) Shoot fresh weight and endogenous amounts of (C) glucose and (D) starch were quantitated in 5–10 seedlings per treatment. Means ± SD are shown. Letters above the bars indicate significant differences, as assessed by one-way ANOVA with Turkey's *post hoc* test ($P < 0.05$).

CONCLUDING REMARKS

In Chapter I, I demonstrated that leaf senescence is promoted in elevated atmospheric CO_2 concentration with limited N (high CO_2/low N) conditions, and then ATL31 plays an important role in the regulation process of senescence in mature Arabidopsis. In this study, I indicated that elevated atmospheric CO_2 has different affects depending on N availability. Under elevated CO_2 condition, plant growth is promoted in sufficient N application (high N), whereas it is not promoted but leaf senescence is progressed in limited N application (low N). The content of sugars and the expression levels of nitrogen starvation related genes were dramatically increased under high CO_2/low N conditions, suggesting that cellular C/N balance is disrupted (high C/low N) with such treatment. In addition, a C/N regulator ATL31 functions negatively in high CO_2/low N dependent senescence progression. However, it remains unknown how disrupted cellular C/N balance promotes leaf senescence. Elucidating of the signal transduction from C/N balance to senescence is an important issue. Moreover, the detailed function of ATL31 is also remarkable. The role of ATL31 in the post-germinative C/N response is degradation of 14-3-3 proteins (Sato et al., 2011; Yasuda et al., 2014). It should be investigated whether 14-3-3 degradation is also important or ATL31 has another ubiquitinated target for senescence progression as C/N response of mature plant.

In Chapter II, I showed that flowering time becomes earlier under limited N condition in long days, and this phenomenon is caused by accelerated signaling via photoperiod pathway. I clarified that *CO* and *FT* expressions are increased in limited N condition, which might be modulated by the increase in phosphorylation level of FBH4. However, the means of FBH4 phosphorylation remains unknown. Recently, TCP transcription

factors were identified as novel activators of *CO* expression (Kubota et al., 2017; Liu et al., 2017). Moreover, TCPs and PFT1 proteins were interact with FBHs proteins and act as co-activators of *CO* expression (Liu et al., 2017). The relationship among FBHs, TCPs, and PFT1 under limited N condition should be investigated. Photoperiod pathway strongly influences on early flowering under limited N condition suggested from that it was not observed in short days and in *co* defective mutant. However, it should be not exclude that another pathway will affect in early flowering under limited N condition. Other studies indicate that a novel pathway exists and gibberellin pathway concerns (Castro Marín et al., 2011; Liu et al., 2013). Furthermore, the effect of carbohydrate can be also important under limited N condition. Carbohydrate such as sucrose and starch are accumulated in plant cell under limited N condition (Krapp et al., 2011). It has known that carbohydrates and their source CO_2 affect flowering time (Jagadish et al., 2016; Moghaddam and Ende, 2013). Recently, trehalose-6 phosphate (T6P) which is a key metabolite reflecting on cellular sucrose status in plants regulates flowering independent pathways via FT (Wahl et al., 2013; Yadav et al., 2014). T6P is also involved in the regulation of leaf senescence (Wingler et al., 2012), which is consistent with the results in Chapter I. Although early flowering was not observed under low N stress condition if photoperiod pathway was defective in this study, it would be observed under another limited N condition such as collaboration with high atmospheric CO_2 condition.

In Chapter III, I identified ATL15 as a novel membrane localized ubiquitin ligase which is involved in sugar response. ATL15 has ubiquitin ligase activity in practice and characterized in the second as sugar responsive ATL among 91 members in Arabidopsis. Since the detailed functions are still unknown in most of ATLs, it is important to clarify

further ATL member in response to carbon and/or nitrogen nutrient availability like as ATL15 and ATL31. In addition, further analysis of ATL15 function is also an important issue. Since ATL15 has ubiquitin ligase activity, identification of an ubiquitinated target protein will be a next step to reveal a role of ATL15. The subcellular localization to membrane compartment is also an interesting point. It should have an important mean in ATL15 function.

Castro Marín, I., Loef, I., Bartetzko, L., Searle, I., Coupland, G., Stitt, M., et al. (2011) Nitrate regulates floral induction in Arabidopsis, acting independently of light, gibberellin and autonomous pathways. *Planta*. 233: 539–52.

Jagadish, S.V.K., Bahuguna, R.N., Djanaguiraman, M., Gamuyao, R., Prasad, P.V.V., and Craufurd, P.Q. (2016) Implications of High Temperature and Elevated CO2 on Flowering Time in Plants. *Front Plant Sci*. 7: 1–11.

Krapp, A., Berthome, R., Orsel, M., Mercey-Boutet, S., Yu, A., Castaings, L., et al. (2011) Arabidopsis Roots and Shoots Show Distinct Temporal Adaptation Patterns toward Nitrogen Starvation. *Plant Physiol*. 157: 1255–1282.

Kubota, A., Ito, S., Shim, J.S., Johnson, R.S., Song, Y.H., Breton, G., et al. (2017) TCP4-dependent induction of CONSTANS transcription requires GIGANTEA in photoperiodic flowering in Arabidopsis, PLoS Genetics.

Liu, J., Cheng, X., Liu, P., Li, D., Chen, T., Gu, X., et al. (2017) MicroRNA319-regulated TCPs interact with FBHs and PFT1 to activate CO transcription and control flowering time in Arabidopsis. *PLoS Genet*. 13: 1–22.

Liu, T., Li, Y., Ren, J., Qian, Y., Yang, X., Duan, W., et al. (2013) Nitrate or NaCl regulates floral induction in Arabidopsis thaliana. *Biologia (Bratisl)*. 68.

Moghaddam, M.R.B., and Ende, W. Van den (2013) Sugars, the clock and transition to flowering. *Front Plant Sci*. 4: 1–6.

Sato, T., Maekawa, S., Yasuda, S., Domeki, Y., Sueyoshi, K., Fujiwara, M., et al. (2011) Identification of 14-3-3 proteins as a target of ATL31 ubiquitin ligase, a regulator of the C/N response in Arabidopsis. *Plant J*. 68: 137–46.

Wahl, V., Ponnu, J., Schlereth, A., Arrivault, S., Langenecker, T., Franke, A., et al. (2013) Regulation of flowering by trehalose-6-phosphate signaling in Arabidopsis thaliana. *Science*. 339: 704–7.

Wingler, a, Delatte, T., O'Hara, L., Primavesi, L., Jhurreea, D., Paul, M., et al. (2012) Trehalose 6-phosphate is required for the onset of leaf senescence associated with high carbon availability. 158: 1241–1251.

Yadav, U.P., Ivakov, A., Feil, R., Duan, G.Y., Walther, D., Giavalisco, P., et al. (2014) The sucrose-trehalose 6-phosphate (Tre6P) nexus: specificity and mechanisms of sucrose signalling by Tre6P. *J Exp Bot*. 65: 1051–68.

Yasuda, S., Sato, T., Maekawa, S., Aoyama, S., Fukao, Y., and Yamaguchi, J. (2014) Phosphorylation of Arabidopsis Ubiquitin Ligase ATL31 Is Critical for Plant Carbon/Nitrogen Nutrient Balance Response and Controls the Stability of 14-3-3 Proteins. *J Biol Chem*. 289: 15179–15193.

PUBLICATION LIST

1. **Shoki Aoyama**, Thais Huarancca Reyes, Lorenzo Guglielminetti, Yu Lu, Yoshie Morita, Takeo Sato and Junji Yamaguchi (2014) C/N regulator ATL31 controls leaf senescence under elevated CO_2 and limited nitrogen condition. ***Plant Cell & Physiology*** 55(2): 293-305.

2. **Shoki Aoyama**, Yu Lu, Junji Yamaguchi and Takeo Sato (2014) Regulation of senescence under elevated atmospheric CO_2 via ubiquitin modification. ***Plant Signaling & Behavior*** e28839.

3. **Shoki Aoyama**, Saki Terada, Miho Sanagi, Yoko Hasegawa, Yu Lu, Yoshie Morita, Yukako Chiba, Takeo Sato and Junji Yamaguchi (2017) Membrane-localized ubiquitin ligase ATL15 functions in sugar-responsive growth regulation in Arabidopsis. ***Biochemical and Biophysical Research Communications*** 491(1): 33-39.

PUBLICATION LIST (APPENDIX)

1. Shigetaka Yasuda, Takeo Sato, Shugo Maekawa, **Shoki Aoyama**, Yoichiro Fukao and Junji Yamaguchi (2014) Phosphorylation of Arabidopsis ubiquitin ligase ATL31 is critical for plant C/N-nutrient response under control of 14-3-3 stability. ***Journal of Biological Chemistry*** 289(22): 15179-93.

2. Shigetaka Yasuda, **Shoki Aoyama**, Yoko Hasegawa, Takeo Sato and Junji Yamaguchi (2017) Arabidopsis CBL-Interacting Protein Kinases Regulate Carbon/Nitrogen-Nutrient Response by Phosphorylating Ubiquitin Ligase ATL31. ***Molecular Plant*** 10(4): 605-618.